Cognitive and Affective Deficits after Chronic Stress: Role of Inhibitory Circuits

By ©Derek L. Wan-Yan-Chan

A Thesis submitted

to the School of Graduate Studies in partial fulfillment of the

requirements for the degree of

Master of Science, Department of Psychology, Faculty of Science

Memorial University of Newfoundland

September 2023

St. John's, Newfoundland and Labrador

Abstract

Major depressive disorder (MDD) is a debilitating neuropsychiatric disease that affects millions of people worldwide. With an increasing prevalence, it is imperative to find a cure for such disorder. Stress is a major risk factor of MDD and thus understanding the pathophysiological mechanism underlying the onset of stress-dependent depression could translate into possible future therapies. In the present study, we investigated if different stress exposure duration, short-term (ST-UCMS) and long-term stress (LT-UCMS), would result in distinct phenotypic profile in a mouse model of depression. We found that LT-UCMS resulted in increased more anhedonia-like symptoms than ST-UCMS and surprisingly, LT-UCMS exposure enhanced cognitive abilities. Both stress duration increased the expression of small-conductance calcium-dependent potassium channel subtype 3 (SK3C) mRNA within somatostatin (SST)- and parvalbumin (PV)-positive neurons. Furthermore, LT-UCMS regimen resulted in significantly higher SK3C-SST and SK3C-PV co-expression levels in the medial prefrontal cortex and nucleus accumbens, respectively. A sex- and region-specific increase in SST mRNA was reported after LT-UCMS exposure only. Notably, after LT-UCMS exposure, stressed females show a significant increase in SK3C-PV co-expression level in the NAcc, which was not observed in males. Similarly, females expressed higher level of SST mRNA in the mPFC after LT-UCMS exposure compared to males, and regarding PV mRNA, only males showed a significant decrease in NAcc, whereas for the CA1 region, only females had a decrease. Our results demonstrate that the length of stress exposure is a determinant factor in the onset of MDD and its effects could be mediated through differential transcriptomic profiles.

General Summary

In the current study, we investigated if the duration of stress exposure could lead to different effects on depression. Indeed, we found that longer stress exposure resulted in more severe depressive-like outcomes compared to a shorter duration. We also found that longer stress administration had different effects on the production of specific proteins in several brain areas, depending on sex. Thus, our results show that the length of stress exposure is a determining factor in the development of depression and that females and males are differently impacted.

Acknowledgements

First and foremost, I would like to express my most sincere gratitude to Dr. Francis R. Bambico for his invaluable mentorship, guidance, and advice. During my residency in the M.Sc. program, Dr. Bambico showed incredible leadership and mentorship abilities, coupled with an innate, genuine compassion for his students, which helped shape my skills and views as an apprentice researcher. Under his guidance, I learnt several new research techniques, was exposed to unique opportunities, and most importantly, met numerous incredible and talented people, who further helped me in my academic journey. Furthermore, Dr. Bambico always put the well-being of his students first, by fostering a welcoming, professional, and yet sincerely friendly environment, which provides room for exponential growth. As such, all my present and future academic and scientific successes are directly or indirectly attributed to Dr. Bambico's mentorship as it laid the concrete foundation for my journey as a researcher.

Moreover, I would also like to mention Mark Corrigan, fellow M.Sc. candidate, for his inestimable assistance during my M.Sc. program. Indeed, Mark helped me with conducting experiments, collecting and analyzing data, and provided ideas for my research project. With his knowledge, abilities, and genuine friendship, Mark proved to be a resourceful person in whom I can trust. Also, I would like to express my sincere gratitude to Yellow Martin, research assistant, Nageeb Hassan, PhD candidate, for their help and advice regarding my experiments, and all the other members of the TroNL Lab, including PhD, M.Sc. candidates, honours students, MUCEPs, and volunteers, for their invaluable assistance in my research.

The current research project was funded by the Canadian Institutes of Health Research (CIHR) and was conducted at Memorial University of Newfoundland.

Table of Content

Abstract ……...ii

General Summary ……..iii

Acknowledgements ……iv

List of Figures ……..viii

List of Tables ……ix

Introduction ……...10

1.1 Literature review ……10

1.2 Causes of MDD ……...11

1.3 The default mode network in MDD ……12

1.4 Small-conductance calcium-dependent channels ……...14

1.5 Research objectives ……17

1.6 Hypotheses ……..17

2.0 Materials and Methods ……18

2.1 Animals ……...18

2.2 Unpredictable Chronic Mild Stress ……18

2.3 Behavioural Testing ……19

2.3.1 Sucrose Preference Test ……...19

2.3.2 Grooming Test ……20

2.3.3 Open Field Test ……21

2.3.4 Novel Object Recognition Test ……21

2.3.5 Social Interaction Test ……22

2.3.6 Novelty-suppressed Feeding Test ……23

2.3.7 Forced Swim Test ……23

2.4 Behavioural Test Analysis ……..24

2.5 Brain Extraction and Sectioning ……24

2.6 RNAscope™ Fluorescent In-situ Hybridization ……25

2.7 Confocal Laser Microscope Imaging and Analysis ……....28

2.8 Statistical Analysis ……..29

3.0 Results ……31

3.1 LT-UCMS exposure results in more depressive-like behaviors compared to ST-UCMS exposure ……31

3.2 LT-UCMS exposure results in increased cognitive abilities compared to ST-UCMS exposure ……35

3.3 RNAscope™ procedure resulted in quantifiable and reliable images ……38

3.4 ST-UCMS increased co-expression of SK3C-SST mRNA in mPFC, NAcc, and CA3 only ……...……45

3.5 ST-UCMS increased co-expression of SK3C-PV mRNA in mPFC, NAcc, and CA3 only ……...48

3.6 ST-UCMS increased overall expression of SST mRNA in all regions of interest except the DG

……...51

3.7 ST-UCMS decreased overall expression of PV mRNA in all regions of interest except the DRN ……54

3.8 LT-UCMS significantly increased co-expression of SK3C-SST mRNA in the mPFC region but not in other brain regions ……57

3.9 LT-UCMS significantly increased co-expression of SK3C-PV mRNA in the NAcc region but not in other brain regions …….62

3.10 LT-UCMS generally increases the expression level of SST mRNA across several brain regions in a sex-dependent manner ……..67

3.11 LT-UCMS significantly decreases the expression level of PV mRNA across several brain regions ……..…….72

4.0 Discussion ……...76

4.1 LT-UCMS induced a differential behavioral phenotypic profile as compared to ST-UCMS ……...76

4.2 Both LT-UCMS and ST-UCMS resulted in increased co-expression level of SK3C-SST mRNA and SK3C-PV mRNA in the mPFC and NAcc respective ……...80

4.3 Both ST-UCMS and LT-UCMS resulted in increased SST mRNA production ……83

4.4 Both ST-UCMS and LT-UCMS resulted in a general decreased in PV mRNA ……85

4.5 Proposed mechanistic pathway through which stress exposure result in depressive outcomes ……...86

4.6 Limitations and future directions ……89

4.7 Conclusion ……..90

References …….91

Appendix …….108

Appendix 1 ……..109

Appendix 2a ……110

Appendix 2b ……111

Appendix 3 ……..112

List of Figures

Figure 1a-d LT-UCMS induced more depressive-like outcomes than ST-UCMS ……..33

Figure 1e ST-UCMS had a sex-specific effect on grooming behaviours while LT-UCMS did not……..34

Figure 2 LT-UCMS enhances cognitive abilities while ST-UCMS did not …….37

Figure 3a Representative images of the mPFC region ……..39

Figure 3b Representative images of the DRN region ……...40

Figure 3c Representative images of the NAcc region ……..41

Figure 3d Representative images of the CA1 region ……42

Figure 3e Representative images of the CA3 region ……43

Figure 3f Representative images of the DG region ……..44

Figure 4 ST-UCMS effects on the overall co-expression level of SK3C-SST …….46

Figure 5 ST-UCMS effects on overall co-expression of SK3C-SST ……...49

Figure 6 ST-UCMS effects on overall expression of SST mRNA ……...52

Figure 7 ST-UCMS effects on the overall expression of PV mRNA ……...55

Figure 8 LT-UCMS effects on overall co-expression level of SK3C-SST mRNA ……..59

Figure 9 Co-expression of SK3C-SST mRNA in the mPFC regions of LT-UCMS animals …...61

Figure 10 LT-UCMS effects on the overall co-expression level of SK3C-PV mRNA ……64

Figure 11 Co-expression of SK3C-PV mRNA in the NAcc region of LT-UCMS animals …….66

Figure 12 LT-UCMS effects on the overall expression of SST mRNA ……...70

Figure 13 LT-UCMS effects on overall expression of PV mRNA ……...74

List of Tables

Table 1 Summary table for the ST-UCMS effects on overall co-expression of SK3C-SST mRNA……47

Table 2 Summary table for the ST-UCMS effects on overall co-expression of SK3C-PV mRNA……50

Table 3 Summary table for ST-UCMS effects on overall expression of SST mRNA……53

Table 4 Summary table for ST-UCMS effects on the overall expression of PV mRNA……56

Table 5 Post-hoc Tukey test Results for Co-expression of SK3C-SST mRNA……60

Table 6 Post-hoc Tukey test Results for Co-Expression for SK3C-PV mRNA……65

Table 7 Summary of Post-hoc Tukey test for Overall Expression of SST mRNA……71

Table 8 Summary of Post-hoc Tukey test for Overall Expression of PV mRNA……75

Cognitive and Affective Deficits after Chronic Stress: Role of Inhibitory Circuits

1.0 Introduction

1.1 Review of Literature

Depression is one of the most common neuropsychiatric disorders, affecting more than 300 million people worldwide, with an alarmingly ever-increasing prevalence rate (Moreno-Agostino et al., 2021). Multiple subcategories of depression exist, namely late-life depression (Borges et al., 2021), early-onset depression (Augustinavicius et al., 2014), seasonal affective disorder (Fonte & Coutinho, 2021), major depressive disorder (Reviewed in Duman et al., 2019), and post-partum depression (Reviewed in Payne & Maguire, 2019), with each one presenting overlapping, yet clearly distinct phenotypic profiles. Among the plethora of depressive disorders, MDD deserves a particular interest as this single subtype accounts for a landslide proportion of all depressive cases, representing a serious debilitating mental health issue on both the individual and societal perspective. Indeed, suicidal ideation and suicide planning are threateningly common among MDD patients, with a prevalence of 37.7% and 15.1% respectively, constituting millions of potential lost lives (Cai et al., 2021). From an economic standpoint, MDD also represents a huge financial burden on society as advanced by Greenberg et al. (2021), who demonstrated that between the period of 2010 and 2018, cases of MDD among US adult citizens increased by 12.9%, resulting in a rise in incremental economic cost from USD 236.6 billion to USD 326.2 billion. The economic area mostly affected by this financial load was indirect workplace cost, such as absenteeism and reduced productivity, accounting for 61% of overall costs in 2018. Therefore, it is of utmost importance to find effective therapeutic alternatives to potentially treat MDD and reduce its associated detrimental effects. Unfortunately, a definitive

cure for the disorder remains elusive despite the countless research and advances made during the past decades. In fact, among all the patients suffering from depression, an estimated 30% of them will eventually develop treatment-resistant depression, preventing them from achieving remission (Kverno & Mangano, 2021). The reason for such ineffectiveness in therapeutic approaches could reside in the pathophysiological development of MDD, and by extension depression in general. In fact, the causative factors of this neuropsychiatric disorder are multimodal, giving MDD a diverse phenotypical profile, potentially rendering a treatment effective for one factor but ineffective for the others.

1.2 Causes of MDD

MDD can be induced by several elements, notably genetic (Q. S. Li et al., 2023), past traumas (Ebert et al., 2019), comorbid disorders (Avenevoli et al., 2015), and stress (Reviewed in Zajkowska et al., 2021), among a plethora of causative factors. Amid the multitude of possible depressive inductors, stress has gained a renewed interest in the past decades. The traditional and well-accepted stress-dependent depressive pathophysiological profile involves the classical hypothalamus-pituitary-adrenal axis (HPA axis) which proposes that excessive stress exposure results in a dysregulated production of corticotropic hormones, adrenocorticotropic hormones, and cortisol, all of them being prototypical stress-related hormones, alongside other molecular dysfunctionalities (Reviewed in Swaab et al., 2005). Such altered hormonal profile would then induce neurophysiological modifications, favorizing the depressive onset. Subsequently, this proposed cascade of events intertwining neurons, excessive hormones release, and other diverse neurochemicals is supported by evidence in sample analysis from MDD patients (Fiksdal et al., 2019; Mayer et al., 2018) and was also recapitulated in animal studies (Eliwa et al., 2021;

Kinlein et al., 2019), providing strong corroborations in support of the HPA axis involvement in stress-related depression. Nevertheless, the HPA axis proposal remains incomplete as it fails to account for the early, almost non-symptomatic phase of depressive onset and the gradual, time-dependent development of MDD. Moreover, HPA axis dysregulation was reported in only a portion of depressive patients (Ceruso et al., 2020), indicating that other neuro-molecular mechanisms are at play in stress-induced depression. Interestingly, during the past decades, increased attention has been given to the excitatory: inhibitory imbalance (E:I) in neuronal circuitries in the context of stress-dependent MDD outcomes (Reviewed in Godfrey et al., 2018). Since healthy brain activities are, in essence, electrochemical signals transmitted through a meticulously, well-coordinated, and specific pattern of excitation and inhibition, it is natural that the disturbance of such finely tuned neuronal patterns would result in disastrous neurophysiological consequences, akin to severe depressive episodes. In fact, using different brain recording and scanning techniques, including computational tomography scan, positron emission tomography scan, functional magnetic resonance imaging, and electroencephalogram, it was demonstrated that MDD patients experienced significant and drastic alterations in cortical activity.

1.3 The default mode network in MDD

Interestingly, abnormal activity in the default mode network (DMN), an assembly of different neuronal structures, is associated with MDD (Saris et al., 2020; Zhang et al., 2016). The DMN is composed of the medial prefrontal cortex (mPFC), the cingulate cortex, the precuneus, the hippocampus (HPC), and the angular gyrus, among other regions, and under normal conditions, is involved with the resting, non-task-oriented wakefulness period (Andrews-Hanna

et al., 2014; Buckner et al., 2008). Additionally, the DMN is also associated with self-thought, past events recollection, anticipation and preparedness for the future, and perception of others (Figueroa et al., 2017). Considering the importance of the DMN in self-cognisance, it is unsurprising that abnormal neuronal activity found in its individual components relate to MDD. However, divergent opinions and results regarding the DMN involvement in depressive outcomes exist in the literature. Indeed, the hyper- and hypoactive DMN views contradict each other, with the former proposing an increased, unregulated burst of neuronal activity, while the later advocate for a dampened, quiescent state of the DMN. For instance, a notable decrease in neuronal activity and synchronisation was observed in the right mPFC, the anterior cingulate cortex, and the left dorsal cingulate cortex, among other brain areas, of MDD patients when compared to healthy controls (Y. Song et al., 2020). In the same study, depressed participants were found to express reduced spontaneous activity levels in the precuneus, cerebellum, cingulate cortex, and mPFC regions as opposed to non-depressed participants. On the other hand, a meta-analysis conducted by Li et al. (2020) showed that MDD patients presented increased cortical volume in their DMN, and similarly, other studies demonstrated a hyper functional connectivity within the DMN components (Liang et al., 2020). Taken within the context of stress-dependent depression, such opposing results concerning the DMN involvements in MDD could be explained, in part or fully, by the intensity and duration of stress exposure. In fact, short-term compared to long-term stress could potentially have differential effects on the neuronal activity of DMN, and thus, distinct yet confluent contributions to MDD's pathogenesis. Irrespective of the stressor's duration, such effects on corticolimbic activities would be mediated through functionally and/or quantitatively altered ion channels. Indeed, the connection between dysfunctional ion channels, often referred to as channelopathies, and depressive outcomes has

been well-characterized through genetic studies, pharmacological interventions, and preclinical models (Kavuran Buran et al., 2022; Smolin et al., 2012; Subramanian et al., 2022). Therefore, stressful events could potentiate the pathological dysfunctionality of specific ion channels, promoting severe channelopathies which consequently translate into MDD.

1.4 Small-conductance calcium-dependent channels

One compelling candidate as a possible stress-related channelopathy which could cause MDD is the small-conductance calcium-dependent potassium channel family, referred to as SKC, which groups together the subtype 1 (SKC1), subtype 2 (SKC2), and subtype 3 (Reviewed in Adelman et al., 2012), and are respectively encoded by the KCNN1, KCNN2, and KCNN3 genes (Köhler et al., 1996). SKC are essential components of the medium afterhyperpolarization (mAHP) segment of the action potential and thus, are primary modulator of neuronal firing (Alix et al., 2014; Egorova et al., 2014; Etchepare et al., 2021). Characteristics of these potassium channels include: a small conductance of about 10-20 pS, high affinity to rise in intracellular calcium level ($[CA^{2+}]_{in}$), being non-voltage-gated, having an intracellular calmodulin calcium-sensing region, and being composed of six transmembrane domain which form a tetrameric structure (Brown et al., 2020). Due to their innate dependence on $[CA^{2+}]_{in}$ and their natural role as neuronal firing inhibitors, SKC are intrinsically coupled with calcium-permeable channels, such as voltage-dependent calcium channels and N-methyl-D-aspartate receptor (NMDAR) (Ballesteros-Merino et al., 2014; Jones & Stuart, 2013; Marrion & Tavalin, 1998). Interestingly, SKC were shown to suppress long-term potentiation (LTP) and depression (LTD) through inhibition of NDMAR in both cortical and hippocampal pyramidal neurons (Jones et al., 2017). Considering that LTP and LTD are essential processes in learning, memory formation, and

cognitive abilities (Diamond et al., 2005; Golitabari et al., 2022; Q.-Q. Li et al., 2022), their impairments through stress related SKC dysfunctionality could result in observable depressive phenotypes. Among the three subtypes, SK3C is a promising target for pharmacological interventions against stress-dependent MDD. Notably chronic stress exposure has been shown to cause depressive-like symptoms through the abnormal heightened modulation of SK3C (Sargin et al., 2016), and moreover, overexpression of SK3C in a transgenic SK3C-positive mouse model demonstrated that prolonged increased of the channel resulted in significant cognitive impairments, in addition to hippocampal volume loss (Martin et al., 2017), which are both hallmarks of depressive-like state. Further implicating the role of SK3C in stress-linked depression, Nashed et al. (2022) showed that using a chronic unpredictable stress paradigm induced depressive-like behaviours in rats, which were then rescued through pharmacological inhibition of the potassium channel. Hence, stress exposure possibly leads to depressive outcomes, and eventually MDD, through dysfunctional SK3C in the DMN.

Furthermore, the brunt of the pathological stress-dependent SK3C upregulation could be primarily clustered to the GABAergic inhibitory interneurons, namely parvalbumin (PV-INs)- and somatostatin (SST-INs)-expressing interneurons. Indeed, dysfunctionalities of these neuronal subtypes have been implicated in several neuropsychiatric and neurodegenerative disorders, including Schizophrenia, Alzheimer's disease, Parkinson's disease, and MDD (Fee et al., 2017; Ruden et al., 2021; Y.-H. Song et al., 2021; Woodward & Coutellier, 2021). Aside from their commonality of being GABA producers and thus, being inhibitory in nature, PV-INs and SST-INs are distinctly different from each other. For instance, PV-INs represent the majority of GABAergic interneurons, with quantification levels reported at around 50% or more, whereas SST-INs are in much fewer amount, usually neighboring 30% or less (Gonchar, 2008; Van

Brederode et al., 1990; Xu et al., 2010). Additionally, PV-INs synapse with the perisomatic region of pyramidal neurons, while SST-INs are dendrite-targeting (Schulz et al., 2018). Moreover, PV-INs display fast-spiking characteristics (Descalzo et al., 2005), producing large inhibitory postsynaptic potentials, and firing at a higher rate (Reviewed in Hu et al., 2014), whereas SST-INs demonstrate the opposite (Reviewed in Riedemann, 2019). Nevertheless, despite their marked differences, PV-INs and SST-INs work together in a synergistic manner to regulate the proper functioning of the brain. Notably, their conjoint efforts is required for the production of gamma oscillations (Antonoudiou et al., 2020), which has been associated with pro-cognitive characteristics (Yamamoto et al., 2014). In fact, disrupted, aberrant gamma waves have been observed in MDD patients and could provide a potential mechanistic explanation for the phenotypic onset of the disease (T.-Y. Liu et al., 2012; X. Liu et al., 2022). Moreover, actions from both GABAergic interneurons are essential for regularizing and monitoring the hippocampal formation activities, eventually translating into healthy and adequate memory formation and cognition (Udakis et al., 2020). Further strengthening the concept that PV-INs and SST-INs are impacted in stress-dependent MDD, several studies have demonstrated that these interneurons are negatively affected due to stress exposure (Page et al., 2019; Pesarico et al., 2022; Spijker et al., 2020; Wang et al., 2021) and that MDD patients expressed abnormal levels of GABA and glutamate (Kantrowitz et al., 2021). Linking SK3C as a potential channelopathy for stress-related MDD through the intersection of PV-INs and SST-INs, it was reported that the potassium subtype was localized on GABAergic neurons (Obermair et al., 2003). Additionally, SK3C are naturally expressed in brain regions related to the DMN, such as the hippocampal formation and the different cortical layers that compose the mPFC, but also in other neuronal structure which are reported to be affected in MDD, including the nucleus accumbens (NAcc)

and the dorsal raphe nuclei (DRN) (Sailer et al., 2004). Therefore, considering all these proposed arguments, we decided to investigate if duration of stress exposure (short-term compared to long-term) could have differential effects on SK3C density and functionality in SST-INs and PV-INs of the mPFC region of the DMN, in addition to other brain areas that have neuronal projections to the network, with the hope of providing a more detailed and holistic view on the etiology of MDD.

1.5 Research objectives

Our research objectives were two-fold: 1) to determine if stress exposure results in overexpression of SK3C mRNA in specific brain areas, and 2) if the overexpression levels of SK3C mRNA would differ between short-term and long-term stress. To this end, we used an unpredictable chronic mild stress (UCMS) paradigm in a mouse model of depression.

1.6 Hypotheses

Our hypotheses were: 1) both short-term and long-term stress exposure would result in higher expression levels of SK3C within both SST-IN and PV-IN, and 2) both short-term and long-term stress exposure would result in lower overall density of SST and PV mRNA. For confirmation, identification, and quantification of SK3C, SST-INs, and PV-INs, we used the RNAscope™ procedure, a fluorescence in-situ hybridization technique developed by Advanced Cell Diagnostic™ (ACD™). To our knowledge, the current thesis is the first to investigate SK3C expression levels in SST-INs and PV-INs in the context of stress-dependent depression.

2.0 Materials and Methods

2.1 Animals

BALB/c mice (males and females) aged approximatively three months old were obtained from Charles River Laboratory, Quebec, Canada. Upon arrival, the animals were given three to five days to habituate. During the habituation period, the mice were handled daily between two to three minutes by all experimenters. All animals were single-housed and were kept in a 12-hour dark-light cycle starting from 7:00 pm. Subjects were also given unrestricted access to food and water supply, unless otherwise required for the stress paradigm. Following the habituation period, the animals were divided into equal groups. All procedures were reviewed and approved by Memorial University Animal Care Committee and were in accordance to the Canadian Council on Animal Care guidelines.

2.2 Unpredictable Chronic Mild Stress (UCMS) paradigm

The UCMS paradigm is a well-known and reliable rodent model of depression, demonstrating generally consistent outcomes (Reviewed in Wilner, 2005). As such, we decided to employ this model adopting a protocol similar to those of Bambico et al., (2009), and Burstein & Doron (2018). Slight modifications were introduced to accommodate the specificities of our experimental design. Briefly, the animals were subjected to different mild stressors including: 1) difficult food and water access, 2) cage tilt, 3) water in cage, 4) predator odor, 5) high-frequency sound, 6) restraining and shaking, 7) stroboscopic illumination, and 8) intermittent overnight illumination. Animals were exposed to three stressors per day at different time points, and for five days a week. Two days were randomly chosen each week as rest days whereby no stressors were administered to better mirror the unpredictability aspect of stress exposure. A more detailed

schedule of stressor administration is provided in the Appendix section (Appendix 1). Stress-naïve, control counterparts were exposed to non-stressful conditions where the control animals were briefly placed in a plastic, white container with two small objects (identical to the one used in the UCMS paradigm). The UCMS paradigm was administered in two formats, namely: 1) long-term stress (LT-UCMS) and 2) short-term stress (ST-UCMS). For LT-UCMS, the duration of stress exposure was 7 to 9 weeks, whereas for the ST-UCMS, the paradigm lasted between 2 to 3 weeks. The grouping for the LT-UCMS cohort was as follows: CTR Males (n = 10), CTR Females (n = 10), LT-UCMS Males (n = 10), and LT-UCMS Females (n = 10), while for the ST-UCMS cohort it was: CTR Males (n = 9), CTR Females (n = 9), ST-UCMS Males (n = 9), and ST-UCMS Females (n = 9).

2.3 Behavioural Testing

A battery of behavioral tests was conducted to investigate the depressive-like and cognition-related deficits induced through exposure to different stress durations. Prior to each behavioral test (except for sucrose preference test), the animals were brought to the testing room 30 minutes before beginning of testing for habituation. Before and after each trial, all apparatus and working stations were cleaned and wiped with 70% alcohol. Briefly, the following tests were used:

2.3.1 Sucrose Preference Test (SPT)

The SPT is a standard procedure to determine anhedonia-like symptoms in rodent models of depression (Reviewed in Liu et al., 2018). For the present study, the animals were given two cylindrical, red plastic cups, one containing tap water, while the other was filled with a 4%

sucrose solution and were tested once every week. Upon administration of the SPT, the cups were filled with their respective solution and were weighted to obtain their initial weights. They were then placed in each cage and were maintained in position using a gray plastic holder to avoid any accidental spilling by the animals. The test lasted for 18 hours overnight and water bottles were removed for the whole procedure. The next day, the cups were re-weighted, and the amount of water consumed, and amount of sucrose solution consumed were calculated as follows:

1. *Initial cup water weight – final cup water weight = amount of water consumed*
2. *Initial cup sucrose weight – final cup sucrose weight = amount of sucrose solution consumed*

Following this, the sucrose preference (expressed in percentage) for each animal was calculated as follows:

$$\frac{Amount\ of\ sucrose\ solution\ consumed}{(Amount\ of\ water\ consumed + amount\ of\ sucrose\ solution\ consumed)}\ x\ 100$$

2.3.2 Grooming Test (GT)

For the GT, animals were sprayed with a 20% sucrose solution on their backs and were then placed in a chamber whereby they were recorded for grooming behaviors. Grooming behaviors were defined as facial, rear, and genital cleaning with clear usage of paws and/or licking actions (Kalueff et al., 2016). The testing length was five minutes and grooming duration (expressed in seconds) was used for data processing.

2.3.3 Open Field Test (OFT)

For the OFT, a similar protocol as described by Alqurashi et al. (2022) was used, with some changes added for the purpose of our experimental design. Each animal was placed in a rectangular, transparent plexiglass chamber, which was divided into three zones by two separators. The walls of the chambers and the separators were covered with opaque paper of neutral colour to avoid external visual cues. Each animal was placed in the middle zone and were left undisturbed for five minutes to habituate, after which, they were recorded for another five minutes from above.

2.3.4 Novel Object Recognition Test (NORT)

The NORT was conducted in three phases, two were habituation phases with two identical familiar objects, while the third one was the testing phase with a familiar object and a novel object (similar to Alqurashi et al., 2022). The same plexiglass chambers used for the OFT were employed in the NORT. Dividers were also used to delineate the middle zone and two peripheral zones. In the peripheral zones, identical familiar objects were placed for phase 1 and 2, while for phase 3, a similar-sized novel object was placed in one peripheral zone. All novel objects were placed on the same-sided peripheral zone. The animals were individually placed in the middle zone and upon starting the test, the dividers were removed, and recording was initiated. For each phase, the test lasted for five minutes. Duration of time spent with novel object was processed to produce an index of time spent with novel object. The calculation was as follows:

$$NORT\ index\ = \frac{Time\ spent\ with\ novel\ object}{Time\ spent\ with\ novel\ object + time\ spent\ with\ familiar\ object}$$

2.3.5 Social Interaction Test (SIT)

For the SIT, a modified protocol as the one used Dang et al. (2022) was employed for the present study. The SIT was conducted in two consecutive phases. In phase 1, a single conspecific and sex-matched animal was used and was referred to as familiar mouse, whereas in phase 2, the same familiar mouse and a novel, sex-matched conspecific, referred to as novel mouse, were both used. SIT-Phase 1 was conducted to determine the spontaneous sociability index (SSI), while SIT-Phase 2 was used to determine the social discrimination index (SDI). For SIT-Phase 1, the plexiglass chambers were divided into three zones, similar in NORT, and the familiar mouse was placed in one peripheral zone in a small cage, while in the other peripheral zone, a similar but empty cage placed. The animal was placed in the middle zone and upon starting, the dividers were removed, and recording was started. SIT-Phase 1 lasted for five minutes and after it was completed, SIT-Phase 2 immediately started. For phase 2, the animals were transported to their respective home cages, while the familiar mice remained in the chambers. The dividers were placed back, and a novel mouse was introduced in the previously empty peripheral zone. The novel mice were all placed in a similar small cage as the familiar mouse. Thereafter the animals were placed back in the middle zone and both the test and recording were started upon removal of the dividers and lasted for five minutes. SSI and SDI were calculated as follows:

$$SSI = \frac{Time\ spent\ with\ familiar\ mouse}{Time\ spent\ with\ familiar\ mouse\ + time\ spent\ with\ empty\ cage}$$

$$SDI = \frac{Time\ spent\ with\ novel\ mouse}{Time\ spent\ with\ novel\ mouse + time\ spent\ with\ familiar\ mouse}$$

2.3.6 Novel-suppressed feeding test (NSFT)

The NSFT was conducted in two phases, namely home cage and novel cage (Bambico et al., 2020). Prior to the testing day, the animals were food-deprived for a duration of 18 hours overnight. On testing day, the animals were brought to a completely novel room and were individually placed in a plexiglass chamber. A single piece of Froot Loops™ (Kellogg's) was positioned on one side of the chamber while the animal was placed on the opposite side. All Froot Loops™ were placed on the same side. The animals were then allowed to reach for the food and the latency to reach the food was recorded using manual stopwatches. An animal was considered to reach the food when it actively grabs the Froot Loops™ with its paws and starts nibbling. Upon reaching the Froot Loops™, the animals were prevented from completely eating it and were placed back in their respective cages. Pieces of used Froot Loops™ were discarded after each trial even if no animals reached them and replaced with new ones for the next trial. After completing all trials, the home cage phase was immediately started. For this phase, the animals were brought back to their resting room and the test was performed in their home cage. Similar setting and criteria were used as for the novel cage phase and the latency to reach the food was recorded. For both home and novel cage phases, the cut-off limit was five minutes. If the animals have not reached the Froot Loops™ before the cut-off limit, their scores were reported as 300 seconds. After completion of the NSFT, food deprivation was removed, and the animals had full and normal access to their foods.

2.3.7 Forced Swim Test (FST)

For the FST, the animals were individually placed in water-filled transparent cylindrical containers (Bambico et al., 2020). The test lasted for 10 minutes, and the coping behavior were recorded as immobilized time (stressed animals are expected to demonstrate greater immobilized time than their control counterparts). After completion of each trial, the animals were gently removed from the containers and were dried up before returning to their respective home cage. The water was changed between each trial and the temperature was kept at 25 $\pm$ 5 °C.

2.4 Behavioural Tests Analysis

For video analysis, the software Ethovision XT version 14.02 by Noldus (Wageningen, the Netherlands) was used. For GT analysis, the Behavioural Observation Research Interactive Software (BORIS) for Windows Setup v.8.20.3 was used (https://www.boris.unito.it/). BORIS is an open-sourced software used for coding and processing behavioral recordings (Friard & Gamba., 2016).

2.5 Brain Extraction and Sectioning

After completing the behavioral tests battery, all animals were euthanized the following day. For euthanasia, cervical dislocation without anesthesia was preferred as the use of any anesthetics could introduce possible confounds in the RNAscope™ technique. After being euthanized, the brains were rapidly extracted and placed on dry ice for approximately two minutes and were then immediately transferred and stored in a -80°C freezer. The fresh frozen brains were then processed for sectioning in a cryostat system (Leica Cryostat). Briefly, the brains were brought and placed in the cryostat system and were left undisturbed for approximately 30 minutes to equilibrate to the system's internal temperature, maintained at -

20°C. All apparatus used for the sectioning procedure were also placed in the system to equilibrate their temperatures too. Following the waiting period, the brains were mounted on the cryomold and cryo-embedding medium was used to hold them in position. Coronal sections of 20 μm thickness were collected on SuperFrost® Plus slides (Thermo Fisher Scientific, Canada) and were subsequently stored in appropriate slides boxes in a -80°C freezer. On one slide, four sections were collected, including: 1) the mPFC, 2) the nucleus accumbens (NAcc), 3) the hippocampal layers CA1 and CA3 (referred as CA1 and CA3), dentate gyrus (DG), and 4) dorsal raphe nuclei (DRN). The procedure was repeated four times for each brain, such that each slide would contain the four areas of interest. Collection was conducted in an anterior-to-posterior manner, and the mouse brain atlas for stereotaxic surgery (Paxinos & Franklin, 2019) was used to determine all the coordinates, relative to bregma.

2.6 RNAscope™ Fluorescent In-situ Hybridization

The RNAscope™ technique was developed by Advanced Cell Diagnostics™ (ACD™, Newark, USA), a bio-techne brand. We utilized the RNAscope™ Multiplex Fluorescent Reagents Kit V2 Assay, which consisted of a series of fixing, dehydration, washing, amplification, and hybridization steps. The section for fresh frozen brain of the RNAscope™ Multiplex Fluorescent Reagents Kit V2 Assay User Manual (Document number: UM 323100) was used and adapted for the current study. The following probes for mRNA detection were obtained from ACD™ (Newark, USA): 1) somatostatin (SST: Mm-Sst-C2, cat# 404631-C2), parvalbumin (PV: Mm-Pvalb-C3, cat# 421931-C3), and SK3C (Mm-Kcnn3, cat# 427961). The probes were all mixed prior to the procedure according to ACD™ recommendations and the mixed solution was covered with aluminium foil and stored between 2 to 8°C. Additionally, the

following TSA Vivid dyes were also from ACD™: 1) TSA Vivid 520 (cat# 323271), 2) TSA Vivid 570 (cat# 323272), and TSA Vivid 650 (cat# 323273). Each dye was reconstituted in 100 µL 1X dimethylsulfoxide (DMSO) provided by ACD™ and were then diluted in TSA buffer solution (cat# 322810) to be used. The diluted dyes were covered in aluminium foil and stored at a temperature between 2 to 8°C.

The RNAscope™ procedure was as follows: the sections were firstly fixed with 10% neutral buffered formalin (10% NBF, Fisher Scientific, cat# 245-684), maintained at 4°C, for one hour. Then, they were washed twice in 1X phosphate buffered saline (1X PBS) and were successively dehydrated in 50%, 70%, and 100% ethanol. The sections were dehydrated twice in 100% ethanol. Subsequently, the sections were allowed to air-dry for five minutes at room temperature (RT) and hydrophobic barriers were drawn using the ImmEdge Hydrophobic Barrier Pen (ACD, cat# 310018) and were allowed to air-dry for five minutes at RT. From here on, the amount of solution added to the sections (except for washing steps) were determined sufficient when the sections were fully covered. RNAscope hydrogen peroxide (reagent kit V2, cat# 323100) was added to each section and were left incubating for 10 minutes at RT. Following this, the sections were washed using distilled water (dH_2O) twice. Thereafter, RNAscope protease IV (reagent kit V2, cat# 323100) was added to each section and incubated for 25 minutes at RT and were washed twice using fresh dH_2O each time. The next step was probes' hybridization. The mixed probes solution was added to each section which were then placed in the HybEZ II Hybridization System oven (cat# 321711 or 321721) to incubate for two hours at 40°C. After this, the sections were washed twice in 1X wash buffer solution (prepared from RNAscope 50X wash buffer solution, reagent kit V2, cat# 323100) for two minutes each wash at RT and were then subsequently kept overnight in a 5X saline sodium citrate (5X SSC) between 2

to 8°C, covered with aluminium foil. The next day, the sections were removed from the 5X SSC and washed once with 1X wash buffer for two minutes at RT, and a series of amplification steps (reagent kit V2, cat# 323100) was applied according to ACD™ and were as follows: AMP 1 was applied and placed in the oven for 30 minutes at 40°C, AMP 2 was applied and placed in the oven for 30 minutes at 40°C, and AMP 3 was applied and placed in the oven for 15 minutes at 40°C. The sections were washed twice with fresh 1X wash buffer solution for two minutes at RT between each amplification step and after AMP 3. Thereafter, development of the horseradish peroxidase signals (HRP-C1 to HRP-C3, reagent kit V2, cat# 323100) was conducted as follows: 1) HRP-C1 was added to each section and was placed in the oven for 15 minutes at 40°C and TSA Vivid Dye 520 (1:1500, green) was subsequently added. The samples were incubated in the oven for 30 minutes at 40°C, were then remove and HRP blocker was immediately added. The sections were then incubated for 15 minutes at 40°C. 2) Following this, HRP-C2 was added to each section and was placed in the oven for 15 minutes at 40°C and TSA Vivid Dye 570 (1:3000, yellow/orange) was subsequently added. The samples were incubated in the oven for 30 minutes at 40°C, were then remove and HRP blocker was immediately added. The sections were then incubated for 15 minutes at 40°C. 3) Then, HRP-C3 was added to each section and was placed in the oven for 15 minutes at 40°C and TSA Vivid Dye 650 (1:1500, far-red) was subsequently added. The samples were incubated in the oven for 30 minutes at 40°C, were then remove and HRP blocker was immediately added. The sections were then incubated for 15 minutes at 40°C. The sections were washed twice with fresh 1X wash buffer between each incubation step and after the last one, for two minutes at RT. After this, DAPI (reagent kit V2, cat# 323100) was immediately added to each section and was incubated for 30 seconds at RT. Then ProLong™ Gold Antifade Mountant (Thermo-Fisher Scientific, cat# P36930) was added and the slides were

covered with glass coverslips (Fisher Scientific, cat# 22X50-1.5-602811G). The sections were stored overnight in complete darkness between 2 to 8°C and were imaged within 2 weeks of the RNAscope™ procedure completion.

2.7 Confocal Laser Microscope Imaging and Analysis

The processed sections were scanned using a confocal microscope (Zeiss LSM 900 with Airyscan 2, Carl Zeiss) and the following parameters were used: 1) image size was 319.5 µm by 319.5 µm, 2) pixel size was 0.12 µm, 3) frame size was 2586 pixel by 2586 pixel, 4) sampling was 1.0X, 5) frame time and pixel time were 1 minute 42 second and 1.63 µs, respectively, 6) scan speed was 5, 7) bidirectional scanning, 8) 2X averaging, 9) 16 bits per pixel. Additionally, the following filters were used: 1) FITC (green), Cy3 (yellow/orange), Cy5.5 (far-red), and DAPI (blue). The regions of interest (ROIs) for each brain structure were determined by the combined use of the coordinates from the mouse brain atlas for stereotaxic surgery (Paxinos & Franklin, 2019) and visual neuronal landmarks (e.g., the mPFC region was sampled between the anterior forceps of the corpus callosum), so that to ensure maximum standardization between the different samplings. The Zeiss Zen Lite software (https://www.zeiss.com/microscopy/en/products/software/zeiss-zen-lite.html) was used for image sampling, which was done at a magnification of 5X and 20X. The collected images were then processed and analyzed through ImageJ software (NIH, https://imagej.nih.gov/ij/download.html). The images were equally distributed among blinded experimenters for visual counting, such that each experimenter analyzed images from all treatment groups. Overall co-expression of SK3C-SST and SK3C-PV mRNA, and overall expression of SST and PV for both LT-UCMS and ST-UCMS were obtained from the image analysis and were expressed as percentage. The calculations were conducted as shown below:

$$\frac{Number\ of\ neurons\ co-expressing\ SK3C-SST}{Overall\ number\ of\ neurons\ expressing\ SST} X\ 100 = \%\ co-expression\ of\ SK3C-SST$$

$$\frac{Overall\ number\ of\ neurosn\ expressing\ SST\ mRNA}{Total\ number\ of\ neurons} x\ 100 = \%\ overall\ expression\ of\ SST$$

Similar calculations were done for PV mRNA and SK3C mRNA. A neuron was considered expressing a type of mRNA if colored dots (SK3C = green, SST = yellow/orange, PV = far-red) were observed within or in proximity of a nucleus (blue colour). Co-expression was determined if dots of different colours were observed simultaneously in close range to a nucleus or within it.

2.8 Statistical Analysis

2x2 between ANOVAs (Sex by Treatment) were conducted using the Jamovi version 2.3.21 open-sourced software (https://www.jamovi.org/download.html). The independent variables were Sex (males vs. females) and Treatment (CTR, LT-UCMS, ST-UCMS). Post-hoc Tukey tests were performed if significant main effects or a significant interaction were observed to determine which groups significantly differed from each other. Student's *t* test was conducted for the SPT data to compare ST-UCMS against LT-UCMS sucrose preference. Whenever Levene's test was significant, Welch's *t* test was performed instead of Student's *t* test. An alpha level of .05 was used and results were considered significant if *p*-value was less than .05. Results were considered marginally significant if the *p*-value was between .05 and .10 and if there was a large effect size ($\eta 2 \geq 0.14$, Cohen's $d \geq 0.8$). Outliers were determined using a z-score analysis. A z-score range of -1.50 to 1.50 was arbitrarily used and data outside of this range were considered outliers. Regarding the RNAscope™ data, two round of z-score analysis were

conducted for outliers' detection. The first one concerned the raw data from each slide, while the second round was done after averaging all the data from the same animal. All graphs were expressed as Mean $\pm$ SE and were produced through Microsoft Office™.

3.0 Results

3.1 LT-UCMS exposure results in more depressive-like behaviors compared to ST-UCMS exposure

To determine if the different UCMS paradigms used induced distinct depressive phenotypes, we conducted several behavioural tests to infer on the possible depressive-like symptomatic profiles expressed by the animals. In the SPT (Figure 1a), animals exposed to eight weeks of LT-UCMS demonstrated a significant reduction in sucrose consumption (CTR: M = 77.65%, SE = 1.38%, LT-UCMS: M = 73.07%, SE = 1.20%; Student's t test: p = .018, Cohen's d = 0.86, 95% CI [0.11, 1.58]) as compared to those exposed to two weeks of ST-UCMS (CTR: M = 63.98%, SE = 4.25%, ST-UCMS: M = 54.88%, SE = 2.83%; Welch's t test was marginally significant: p = .086, Cohen's d = 0.62, 95% CI [-0.09, 1.32]), confirming that our UCMS paradigm was successful in inducing anhedonia-like symptoms in LT-UCMS animals, but not in their ST-UCMS counterparts. The SPT was conducted through nine consecutive weeks and the data for ST-UCMS were collected at Week 2, while those for LT-UCMS were collected at Week 8, with both time points representing their respective stress duration. Data for both control and stressed animals were collected simultaneously, such that at each time point, there were a control and stressed group. For the SPT, sex effect was investigated however, no differences were observed (data not reported), therefore we decided to investigate only the effect of stress exposure for this test, combining data from males and females. The decision was two-fold: 1) stress exposure was the main variable of interest for the thesis, and 2) SPT is generally delicate test to implement, with several external factors that could affect the result, thus we decided to combine both sexes such that to increase the sample size, reducing the variability.

Furthermore, 2x2 ANOVA was conducted for the NSFT-Novel Cage (Figure 1b) and showed no significant interaction and no significant main effect of Sex, but a significant main

effect of Treatment ($F_{(1, 34)} = 19.55$, $p < .001$, $\eta^2 = 0.36$) was observed. For the ST-UCMS cohort, 2x2 ANOVA revealed no significant interaction and no significant main effects for the NSFT-Novel Cage phase. Moreover, for the NSFT-Home Cage phase (Figure 1c) within the context of LT-UCMS exposure, 2x2 ANOVA reported no significant interaction and no significant main effect of Sex, but a significant main effect of Treatment ($F_{(1, 34)} = 12.52$, $p = .001$, $\eta^2 = 0.27$) was observed. Regarding the ST-UCMS cohort, 2x2 ANOVA for the NSFT-Home Cage showed a main effect of Treatment ($F_{(1, 29)} = 6.93$, $p = .013$, $\eta^2 = 0.19$) only.

Regarding the LT-UCMS exposure, the SIT-Spontaneous Sociability phase (Figure 1d), 2x2 ANOVA reported a significant main effect of Treatment ($F_{(1, 34)} = 16.62$, $p < .001$, $\eta^2 = 0.31$) only. Then, for the ST-UCMS cohort, 2x2 ANOVA for the SIT-Spontaneous Sociability phase showed only a marginally significant main effect of Sex ($F_{(1, 28)} = 3.94$, $p = .057$, $\eta^2 = 0.12$).

For the GT (Figure 1e), no significant interaction was reported but a significant main effect of Sex was observed ($F_{(1, 26)} = 16.62$, $p = .006$, $\eta^2 = 0.25$) in the ST-UCMS group. For the LT-UCMS group, no significant interaction and no significant main effects were reported. The FST and OFT showed no significant nor marginally significant results (Appendix 2). Taken together, the current data demonstrate that LT-UCMS demonstrate more depressive-like outcomes than ST-UCMS, which corroborates with the progressive onset and pathological development of stress-related depression.

Figure 1a-d

LT-UCMS induced more depressive-like outcomes than ST-UCMS

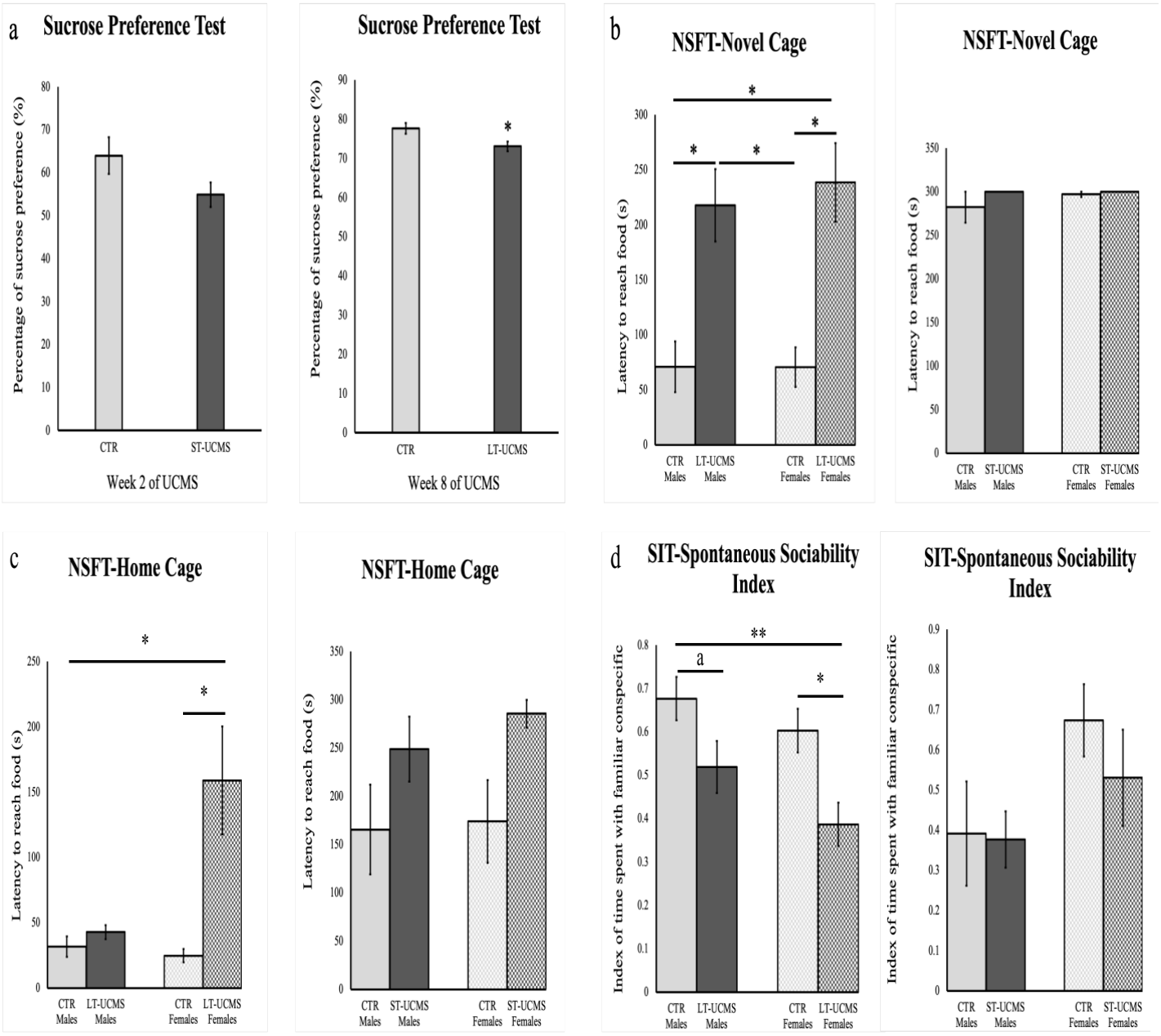

Figure 1a-d. *LT-UCMS exposure resulted in more depressive-like behaviors compared to ST-UCMS exposure.* Graphs for LT-UCMS and ST-UCMS are besides each other. a) SPT shows a significant reduction in sucrose consumption for LT-UCMS but not for ST-UCMS when compared to their respective controls. b) and c) for both phases of NSFT, the LT-UCMS groups reported a significant main effect of Treatment whereas for ST-UCMS, only the NSFT-Home cage phase showed a significant main effect of Treatment. d) In the SIT-Spontaneous sociability phase, only LT-UCMS group showed a significant main effect of Treatment, whereas the ST-UCMS group reported only a marginally significant interaction. Post-hoc Tukey: $*p < .05$, $**p < .01$, ^{a}p = marginally significant.

Figure 1e

ST-UCMS had a sex-specific effect on grooming behaviours while LT-UCMS did not

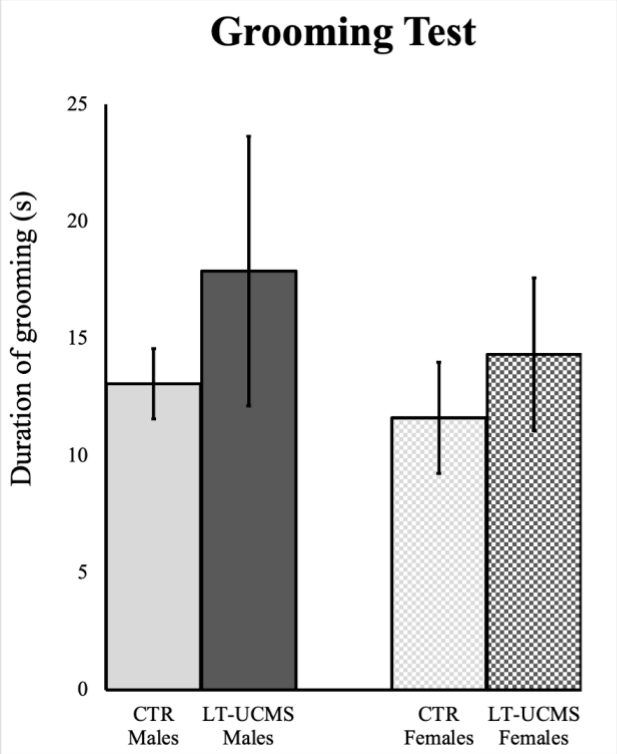

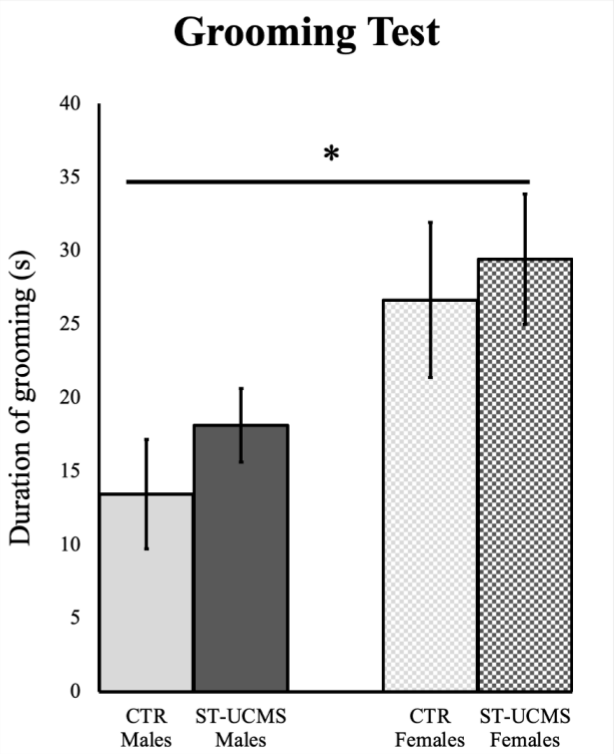

Figure 1e. *ST-UCMS but not LT-UCMS exposure resulted in sex-specific effect on grooming behaviors*. Graphs for LT-UCMS and ST-UCMS are besides each other. A significant main effect of Sex was reported in the GT for ST-UCMS but not LT-UCMS. No significant interaction nor significant main effect of Treatment were reported for the UCMS duration. ST-UCMS caused a higher grooming time in females compared to males. Post-hoc Tukey: $*p < .05$

3.2 LT-UCMS exposure results in increased cognitive abilities compared to ST-UCMS exposure

To our surprise, we found that exposure to LT-UCMS resulted in increased cognitive abilities as opposed to what is commonly reported in the literature (Høifødt et al., 2019; Thalamuthu et al., 2022; Vance & Winther, 2021). Indeed, for both the NORT and SIT-Social discrimination phase (Figure 2a and 2b respectively), the current results demonstrated that animals exposed to long-term stress presented higher cognitive capacities, while those exposed to short-term stress showed no significant changes. Regarding LT-UCMS exposure, 2x2 ANOVA showed no significant main effect of Treatment and no significant interaction in the NORT, but a significant main effect of Sex ($F_{(1, 29)} = 8.12$, $p = .008$, $\eta^2 = 0.21$) was reported. For ST-UCMS exposure, a significant interaction between Sex and Treatment was reported ($F_{(1, 30)} = 5.17$, $p = .030$, $\eta^2 = 0.14$), while post-hoc Tukey test showed a marginally significant difference ($p_{Tukey} = .074$, Cohen's $d = -1.23$, 95% CI [-2.28, -0.19]) between CTR Males ($M = 0.33$, $SE = 0.11$) and CTR Females ($M = 0.70$, $SE = 0.08$), and also between CTR Females and ST-UCMS Females ($M = 0.34$, $SE = 0.12$; $p_{Tukey} = .091$, Cohen's $d = 1.19$, 95% CI [0.15, 2.23]).

Similarly, for the SIT-Social discrimination phase, we also observed a general enhancement in cognitive abilities in the context of LT-UCMS exposure. In fact, 2x2 ANOVA reported no significant interaction, but instead, a significant main effect of Sex ($F_{(1, 32)} = 5.11$, $p = .031$, $\eta^2 = 0.12$) and a significant main effect of Treatment ($F_{(1, 32)} = 5.76$, $p = .022$, $\eta^2 = 0.13$) were found. On the other hand, in the context of ST-UCMS, 2x2 ANOVA also showed no significant main effects, but only a marginally significant interaction ($F_{(1, 27)} = 3.78$, $p = .062$, $\eta^2 = 0.12$) for the SIT-Social discrimination phase. Post-hoc Tukey test reported no significant nor marginally significant comparisons. Taken together, the current results indicate a potential

coping mechanism induced through LT-UCMS exposure which would lead to a seemingly rescuing effect on cognition.

Figure 2

LT-UCMS enhances cognitive abilities while ST-UCMS did not

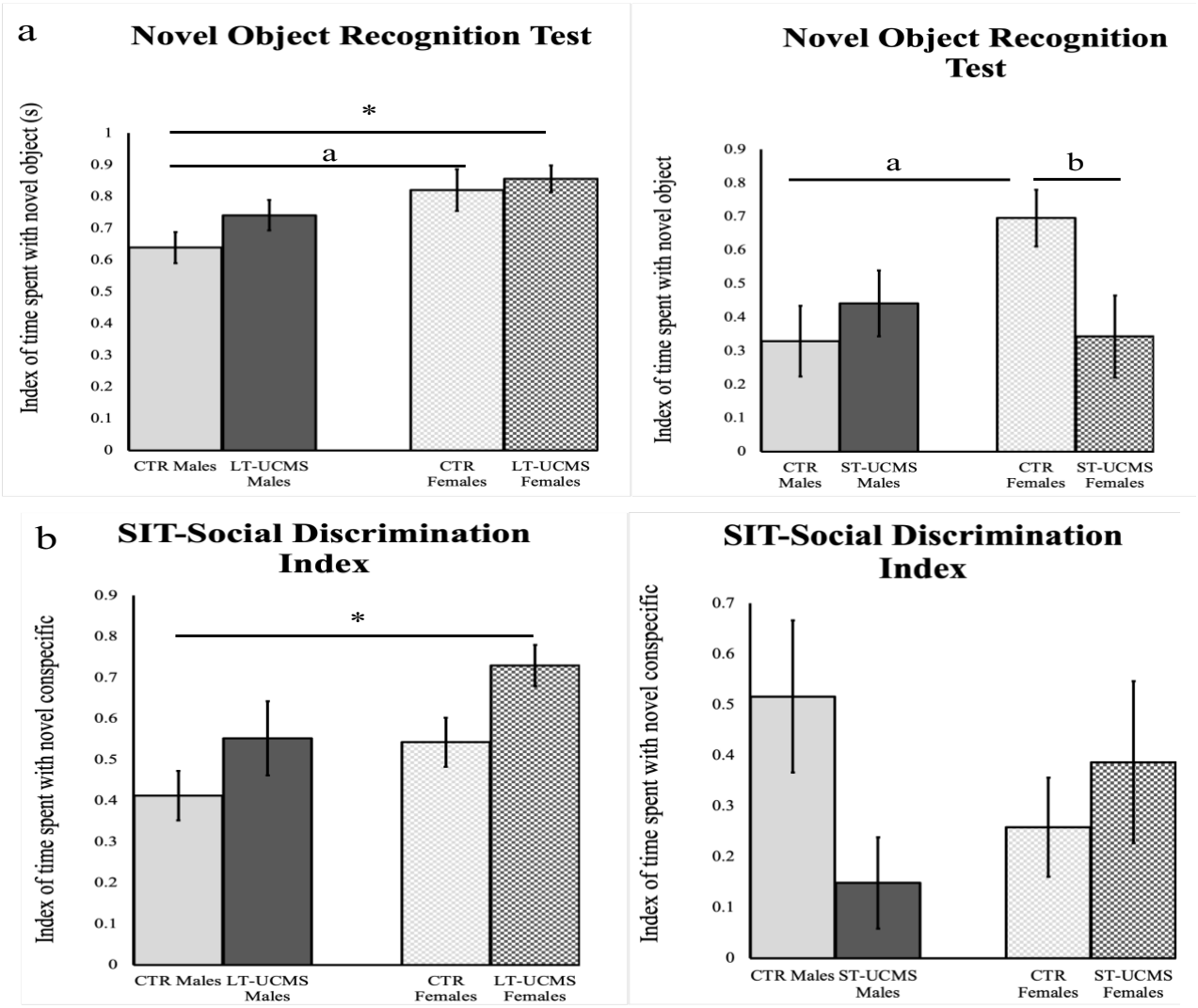

Figure 2. *LT-UCMS exposure resulted in increased cognitive abilities as compared to ST-UCMS*. Graphs for LT-UCMS and ST-UCMS are besides each other. 2 a) and b) Surprisingly, LT-UCMS appears to provide some cognitive enhancements because for both NORT and SIT-Social discrimination phase, the long-term stressed animals had a higher index than their respective controls. For the NORT, only a significant main effect of Sex was reported, while for the SIT-Social discrimination phase, both a significant main of Sex and Treatment were reported. For the ST-UCMS animals, only a significant interaction between Sex and Treatment was reported in NORT and a marginally significant interaction in SIT-Social discrimination phase. Post-hoc Tukey: $*p < .05$, $**p < .01$, $^{a,b}p$ = marginally significant.

3.3 RNAscope™ procedure resulted in quantifiable and reliable images

Our RNAscope™ technique was considered reliable since clear images for both quantitative and qualitative analyses were obtained (Figure 3a-f). Our mRNA of interest (SST, PV, and SK3C mRNA) were distinctly expressed as clear, colored puncta in proximity to or within the blue-colored nuclei. The colour association was as follows: SST mRNA was primed with yellow dye, PV mRNA was primed with far-red dye, and SK3C mRNA was primed with green dye, while the nuclei were associated with blue dye (DAPI). Clusters of colored dots were observed which could potentially indicate that the specific type of mRNA is being produced in greater amounts. For instance, several large clusters of SST mRNA (yellow) were reported in the images; however similar results were found in the literature (See Thek et al., 2019). Further confirming the success of the RNAscope™ procedure, both the positive and negative controls demonstrated the expected results (Appendix 3). It is important to note that due to time constraint and personal problems that happened during our residency period, we were unable to fully process the ST-UCMS cohort for the RNAscope™ procedure. As such, for the ST-UCMS cohort, only one brain per group was processed, and therefore no conclusive opinions were made for the effects of ST-UCMS treatment. Nevertheless, for the purpose of the current thesis, the presented data were deemed sufficient to provide, at the very least, a general idea of how the ST-UCMS condition could have potentially impacted the production of the targeted mRNA as compared to LT-UCMS treatment, while waiting for the full processing and analysis to be completed. For the LT-UCMS cohort, the number of brains per group varied between three to five, which was determined as a sufficient sample size for statistical analysis (See Ballesteros-Merino et al., 2014). Despite these unforeseen interferences, the quality of the present RNAscope™ images strengthen our confidence in their attribute and reliability for analysis.

Figure 3a

Representative images of the mPFC region

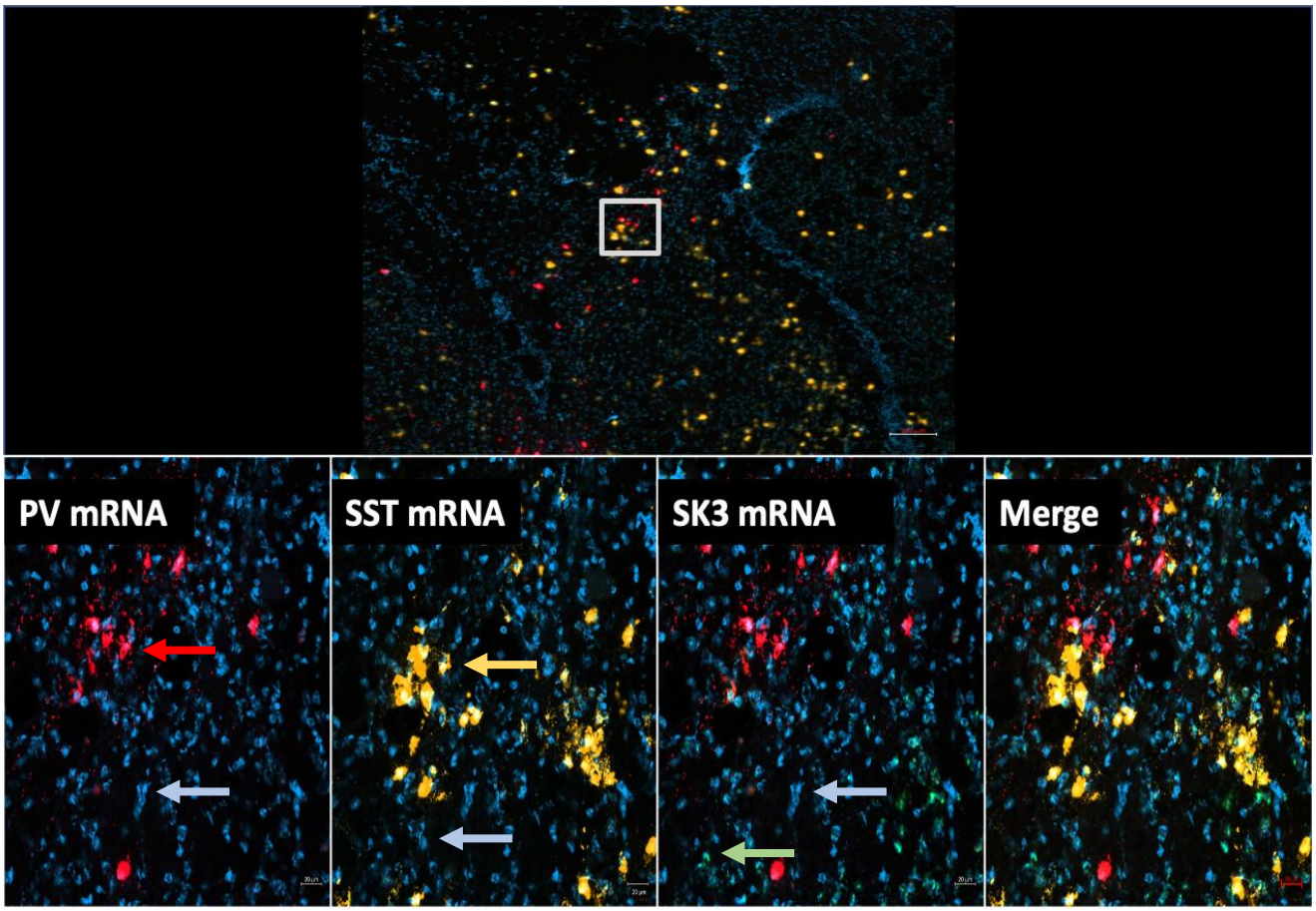

Figure 3a. *Representative image of the mPFC region*. The upper, larger image is a representation of the selected area, enclosed in a white box, at x5 magnification. Underneath it, the four images (from the left to right) are representation of PV mRNA (red arrow) with DAPI (light-blue arrow), SST mRNA (yellow arrow) with DAPI, SK3C mRNA (green arrow) with DAPI, and a merged image of all mRNAs with DAPI. The individual mRNA representative images and their merged images were all collected at x20 magnification. The colour association was as follows: SST mRNA = yellow, PV mRNA = far-red, SK3C mRNA = green, and DAPI = blue. The above images were all collected from a control animal to have a baseline, non-manipulated representation.

Figure 3b

Representative images of the DRN region

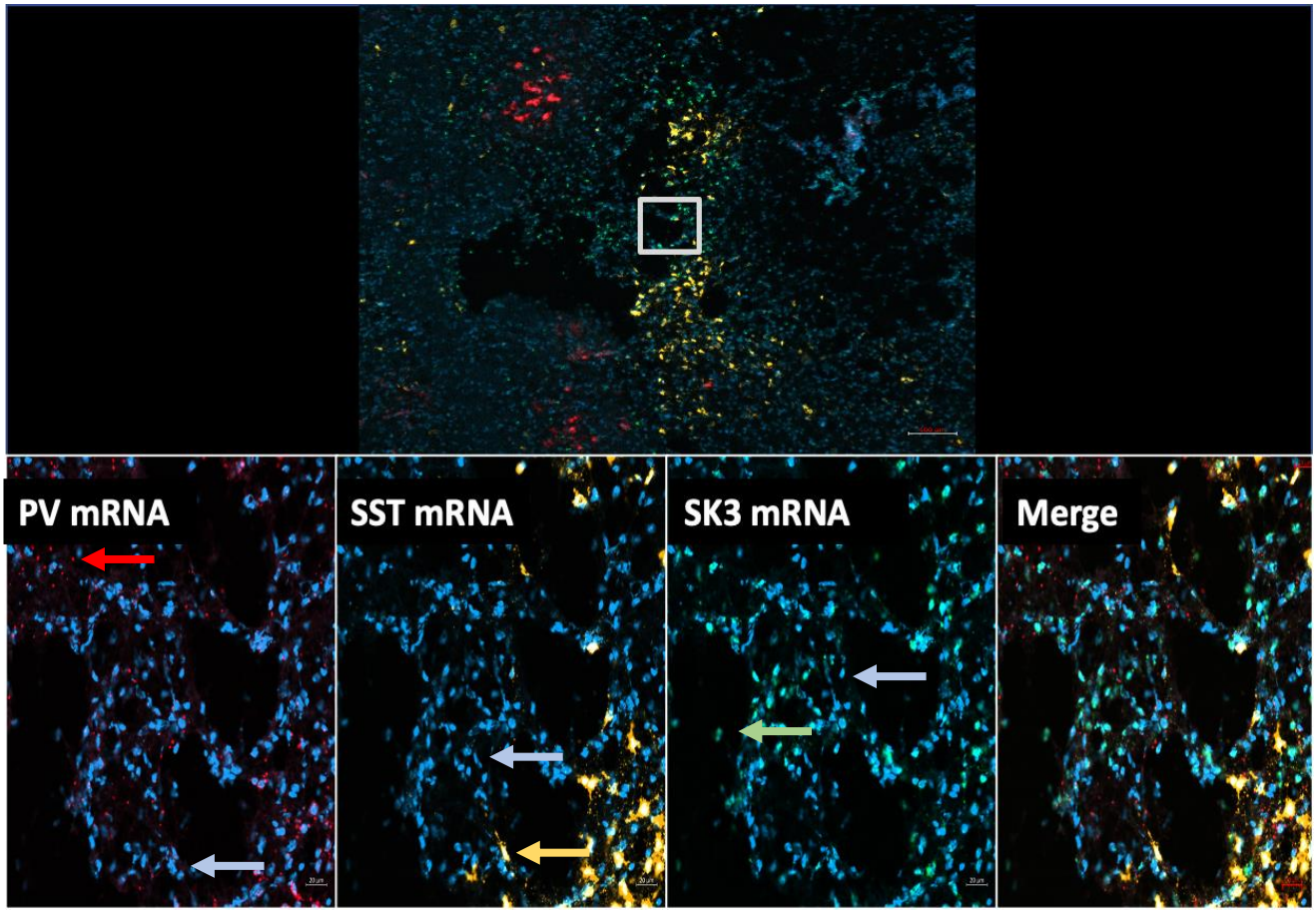

Figure 3b. *Representative image of the DRN region*. The upper, larger image is a representation of the selected area, enclosed in a white box, at x5 magnification. Underneath it, the four images (from the left to right) are representation of PV mRNA (red arrow) with DAPI (light-blue arrow), SST mRNA (yellow arrow) with DAPI, SK3C mRNA (green arrow) with DAPI, and a merged image of all mRNAs with DAPI. The individual mRNA representative images and their merged images were all collected at x20 magnification. The colour association was as follows: SST mRNA = yellow, PV mRNA = far-red, SK3C mRNA = green, and DAPI = blue. The above images were all collected from a control animal to have a baseline, non-manipulated representation.

Figure 3c

Representative images of the NAcc region

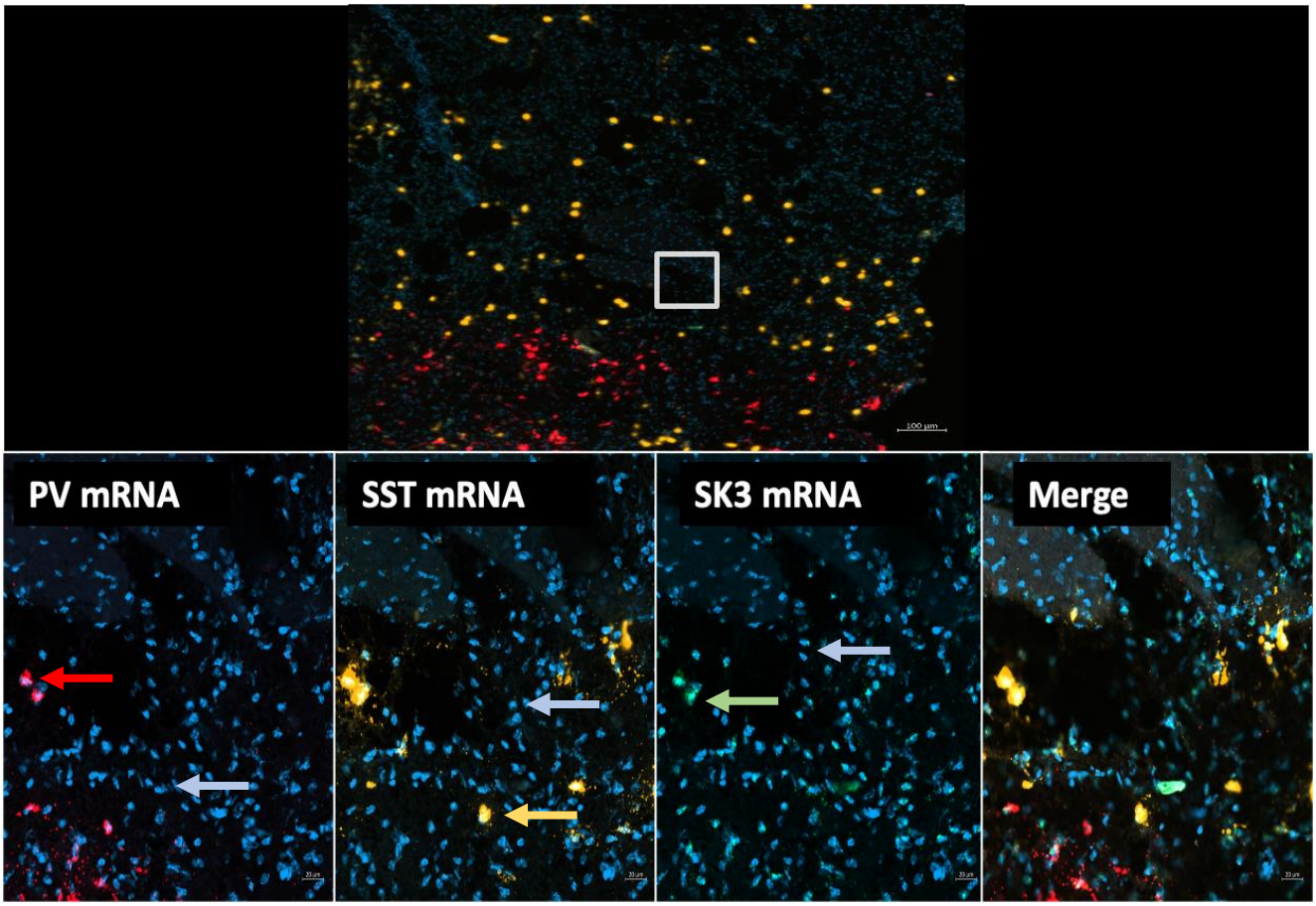

Figure 3c. *Representative image of the NAcc region*. The upper, larger image is a representation of the selected area, enclosed in a white box, at x5 magnification. Underneath it, the four images (from the left to right) are representation of PV mRNA (red arrow) with DAPI (light-blue arrow), SST mRNA (yellow arrow) with DAPI, SK3C mRNA (green arrow) with DAPI, and a merged image of all mRNAs with DAPI. The individual mRNA representative images and their merged images were all collected at x20 magnification. The colour association was as follows: SST mRNA = yellow, PV mRNA = far-red, SK3C mRNA = green, and DAPI = blue. The above images were all collected from a control animal to have a baseline, non-manipulated representation.

Figure 3d

Representative images of the CA1 region

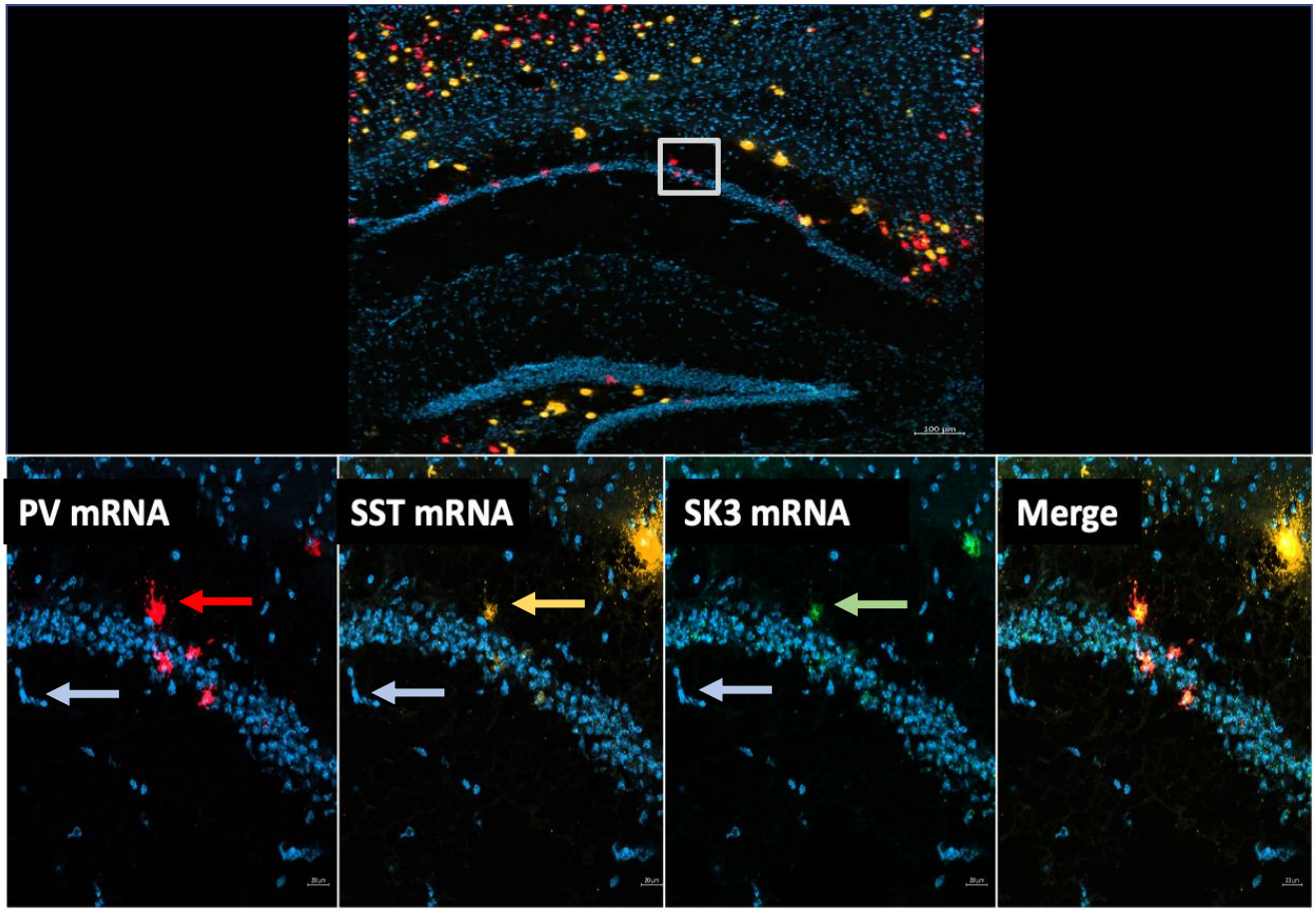

Figure 3d. *Representative image of the CA1 region*. The upper, larger image is a representation of the selected area, enclosed in a white box, at x5 magnification. Underneath it, the four images (from the left to right) are representation of PV mRNA (red arrow) with DAPI (light-blue arrow), SST mRNA (yellow arrow) with DAPI, SK3C mRNA (green arrow) with DAPI, and a merged image of all mRNAs with DAPI. The individual mRNA representative images and their merged images were all collected at x20 magnification. The colour association was as follows: SST mRNA = yellow, PV mRNA = far-red, SK3C mRNA = green, and DAPI = blue. The above images were all collected from a control animal to have a baseline, non-manipulated representation.

Figure 3e

Representative images of the CA3 region

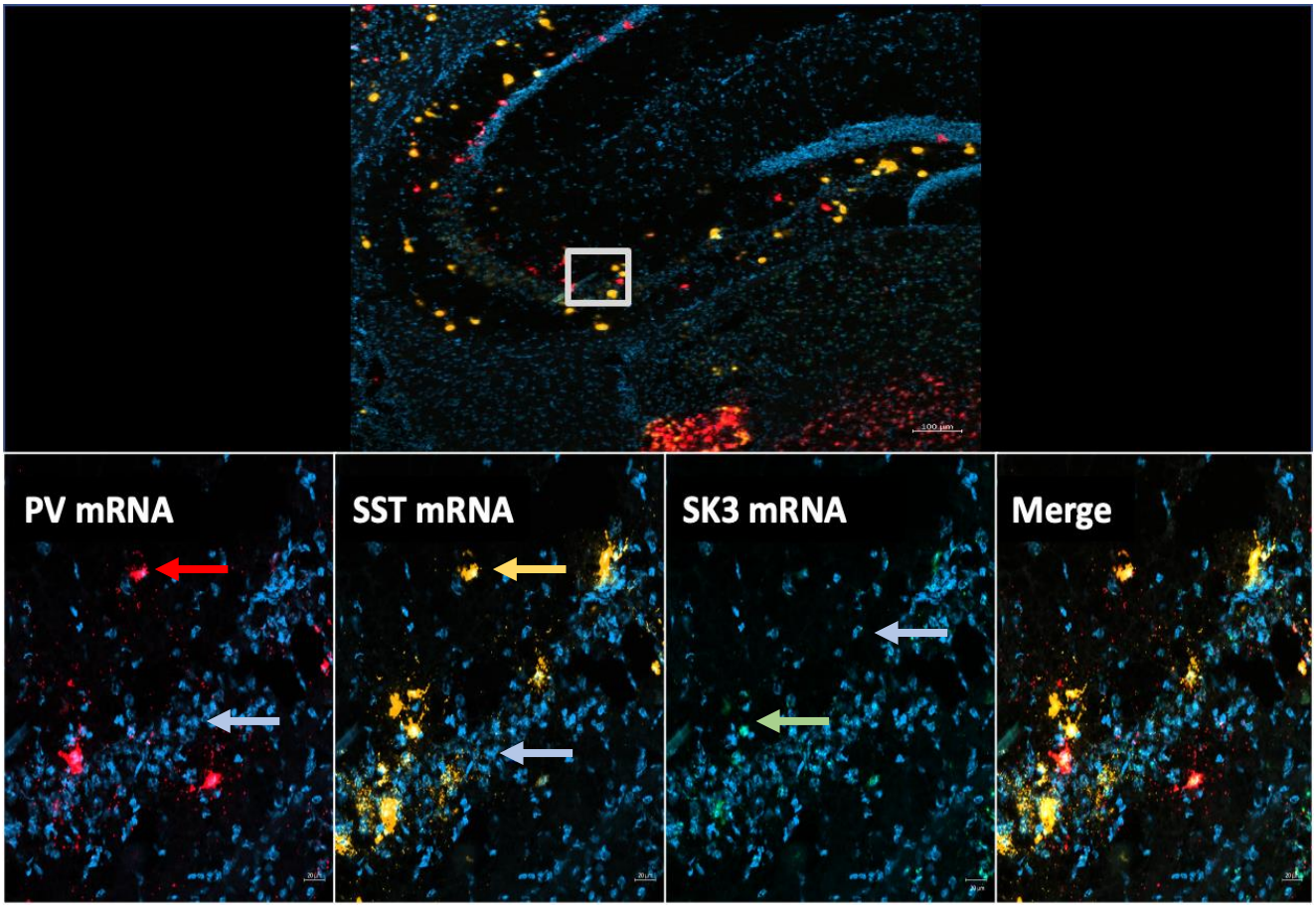

Figure 3e. *Representative image of the CA3 region*. The upper, larger image is a representation of the selected area, enclosed in a white box, at x5 magnification. Underneath it, the four images (from the left to right) are representation of PV mRNA (red arrow) with DAPI (light-blue arrow), SST mRNA (yellow arrow) with DAPI, SK3C mRNA (green arrow) with DAPI, and a merged image of all mRNAs with DAPI. The individual mRNA representative images and their merged images were all collected at x20 magnification. The colour association was as follows: SST mRNA = yellow, PV mRNA = far-red, SK3C mRNA = green, and DAPI = blue. The above images were all collected from a control animal to have a baseline, non-manipulated representation.

Figure 3f

Representative images of the DG region

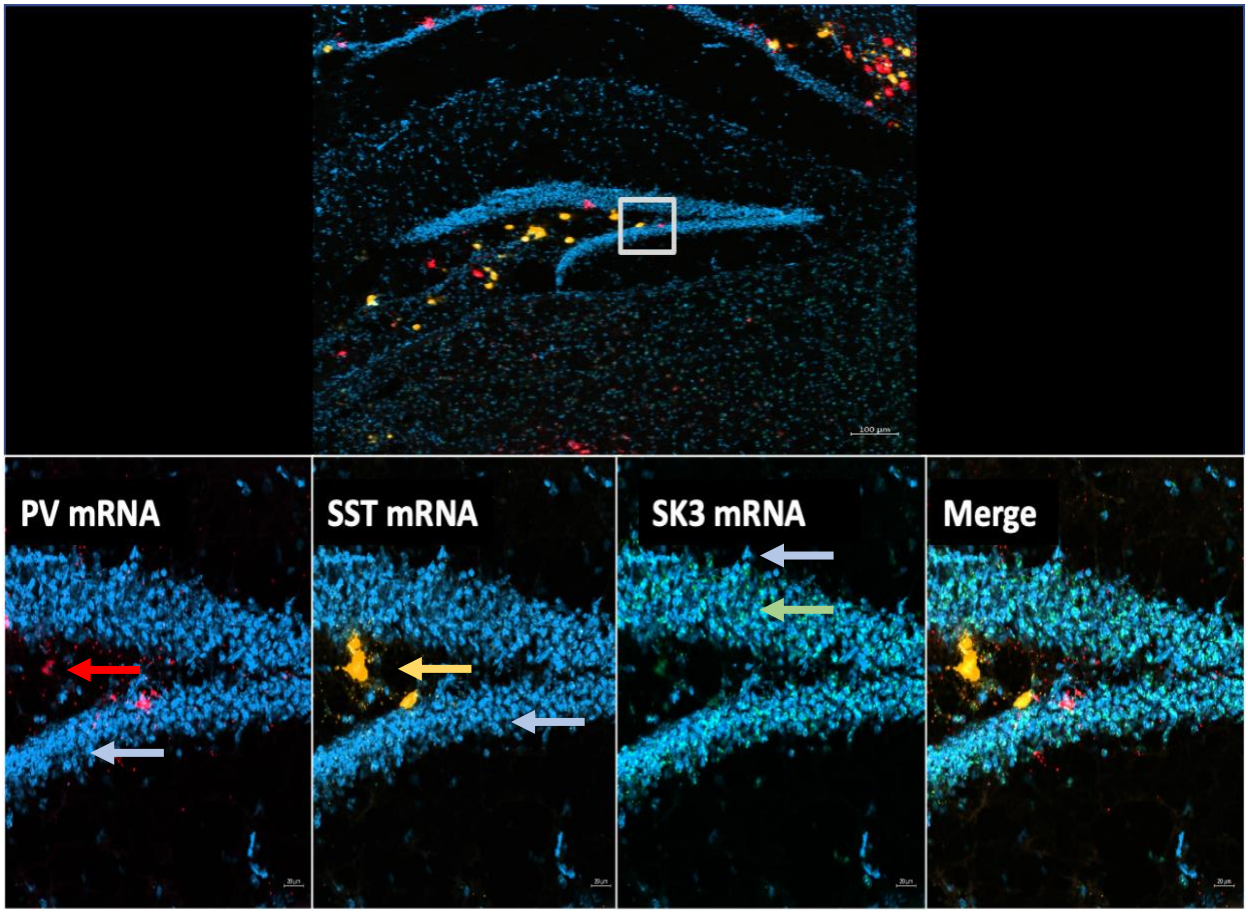

Figure 3f. *Representative image of the DG region*. The upper, larger image is a representation of the selected area, enclosed in a white box, at x5 magnification. Underneath it, the four images (from the left to right) are representation of PV mRNA (red arrow) with DAPI (light-blue arrow), SST mRNA (yellow arrow) with DAPI, SK3C mRNA (green arrow) with DAPI, and a merged image of all mRNAs with DAPI. The individual mRNA representative images and their merged images were all collected at x20 magnification. The colour association was as follows: SST mRNA = yellow, PV mRNA = far-red, SK3C mRNA = green, and DAPI = blue. The above images were all collected from a control animal to have a baseline, non-manipulated representation.

3.4 ST-UCMS increased co-expression of SK3C-SST mRNA in mPFC, NAcc, and CA3 only

It is interesting to observe that ST-UCMS treatment caused an increase the co-expression level of SK3C-SST mRNA in the mPFC (CTR: *M* = 19.43%; ST-UCMS: *M* = 34.61%), NAcc (CTR: *M* = 30.65%; ST-UCMS: *M* = 37.06%), and CA3 (CTR: *M* = 16.36%; ST-UCMS: *M* = 26.73%) regions, whereas the DRN (CTR: *M* = 51.25%; ST-UCMS: *M* = 19.42%), CA1 (CTR: *M* = 30.18%; ST-UCMS: *M* = 24.76%), and DG (CTR: *M* = 74.04%; ST-UCMS: *M* = 55.50%) regions demonstrated the opposite (Figure 4).

Furthermore, when investigating Sex effect, the following observations were made: 1) for the mPFC and CA3 regions, both ST-UCMS Males and ST-UCMS Females experienced an increase in co-expression density of SK3C-SST mRNA, but a decrease in co-expression level was reported for the DRN, and 2) for the NAcc and CA1 regions, sex-dependent effects of ST-UCMS exposure was observed. No comparisons were inferred for DG since data for the CTR Males are being processed. All data are summarized in Table 1. Therefore, the current data could imply a synergistic effect of Sex and ST-UCMS on the co-expression level of SK3C-SST mRNA, related to specific brain regions, indicating that the production of SK3C protein in SST-IN is dependent on the brain areas, sex, and on the level of stress exposure.

Figure 4

ST-UCMS effects on the overall co-expression level of SK3C-SST

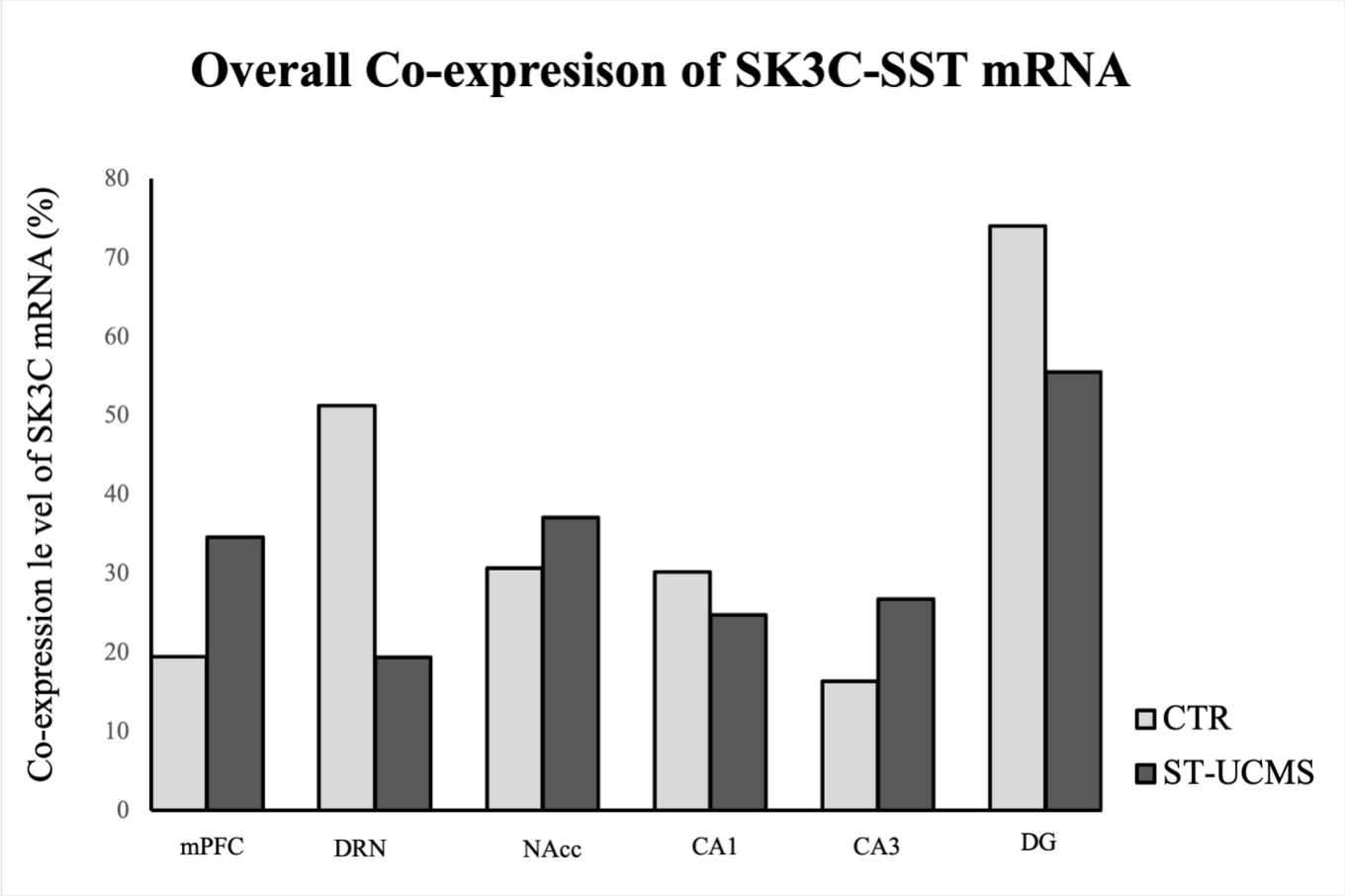

Figure 4. *Overall co-expression level of SK3C-SST mRNA after ST-UCMS exposure.* The figure compares the difference in SK3C-SST co-expression density in ST-UCMS animals with their respective controls. It can be observed that there is a general increase in co-expression levels for the mPFC, NAcc, and CA3, but for the DRN, CA1, and DG, the opposite was reported. All data were sex pooled. No statistical analysis was conducted due to limited sample size (n =1 brain per group)

Table 1

Summary table for the ST-UCMS effects on overall co-expression of SK3C-SST mRNA

ROI	♂		♀	
	CTR	ST-UCMS	CTR	ST-UCMS
mPFC	19.04%	33.51%	19.82%	35.71%
DRN	53.85%	29.63%	48.65%	9.21%
NAcc	22.73%	18.18%	38.58%	55.94%
CA1	0%	15.15%	60.36%	34.38%
CA3	0%	3.57%	32.72%	49.88%
DG	N/A	33.61%	74.04%	77.38%

Table 1. *Summary of the co-expression level of SK3C-SST mRNA after ST-UCMS exposure, separated by sex*. The current data show the difference between CTR Males, ST-UCMS Males, CTR Females, and ST-UCMS Females for the co-expression level of SK3C-SST mRNA across different brain regions (n = 1 brain per group). An expression level of 0% indicate that no neurons expressed SK3C mRNA in this ROI, whereas an expression level of 100% indicate that all neurons expressed SK3C mRNA. The p_{Tukey} value was not reported due to limited sample size. N/A = Data for CTR Males in the DG are still under processed.

3.5 ST-UCMS increased co-expression of SK3C-PV mRNA in mPFC, NAcc, and CA3 only

Similar to the SK3C-SST co-expression results reported, ST-UCMS increased the co-expression of SK3C-PV mRNA (Figure 5) in the mPFC (CTR: M = 25.83%; ST-UCMS: M = 34.96%), NAcc (CTR: M = 27.44%; ST-UCMS: M = 47.71%), and CA3 (CTR: M = 30.59%; ST-UCMS: M = 33.45%), and a decrease in the DRN (CTR: M = 34.09%; ST-UCMS: M = 15.53%), CA1 (CTR: M = 39.24%; ST-UCMS: M = 33.70%), and DG (CTR: M = 71.06%; ST-UCMS: M = 55.95%).

Moreover, when investigating at the effect of Sex, it is interesting to note the opposite effect of ST-UCMS on SK3C-PV co-expression density depending on sex. For instance, in the mPFC, ST-UCMS Males experienced a large increase in co-expression density compared to CTR Males, while the ST-UCMS Females demonstrate only a slight increase. On the other hand, for the DRN, NAcc, CA1, and CA3, ST-UCMS Males an increase in SK3C-PV mRNA co-expression compared to their controls, whereas the opposite was reported for ST-UCMS Females when compared to their controls. No comparisons were inferred for DG since data for the CTR Males are being processed. All data are summarized in Table 2. The obtained results could imply a potential combined effect of Sex and ST-UCMS exposure on the co-expression tendency of SK3C-PV mRNA, indicating that the production SK3C protein in the PV-IN is dependent on sex and stressful events, like SST-IN.

Figure 5

ST-UCMS effects on overall co-expression of SK3C-SST

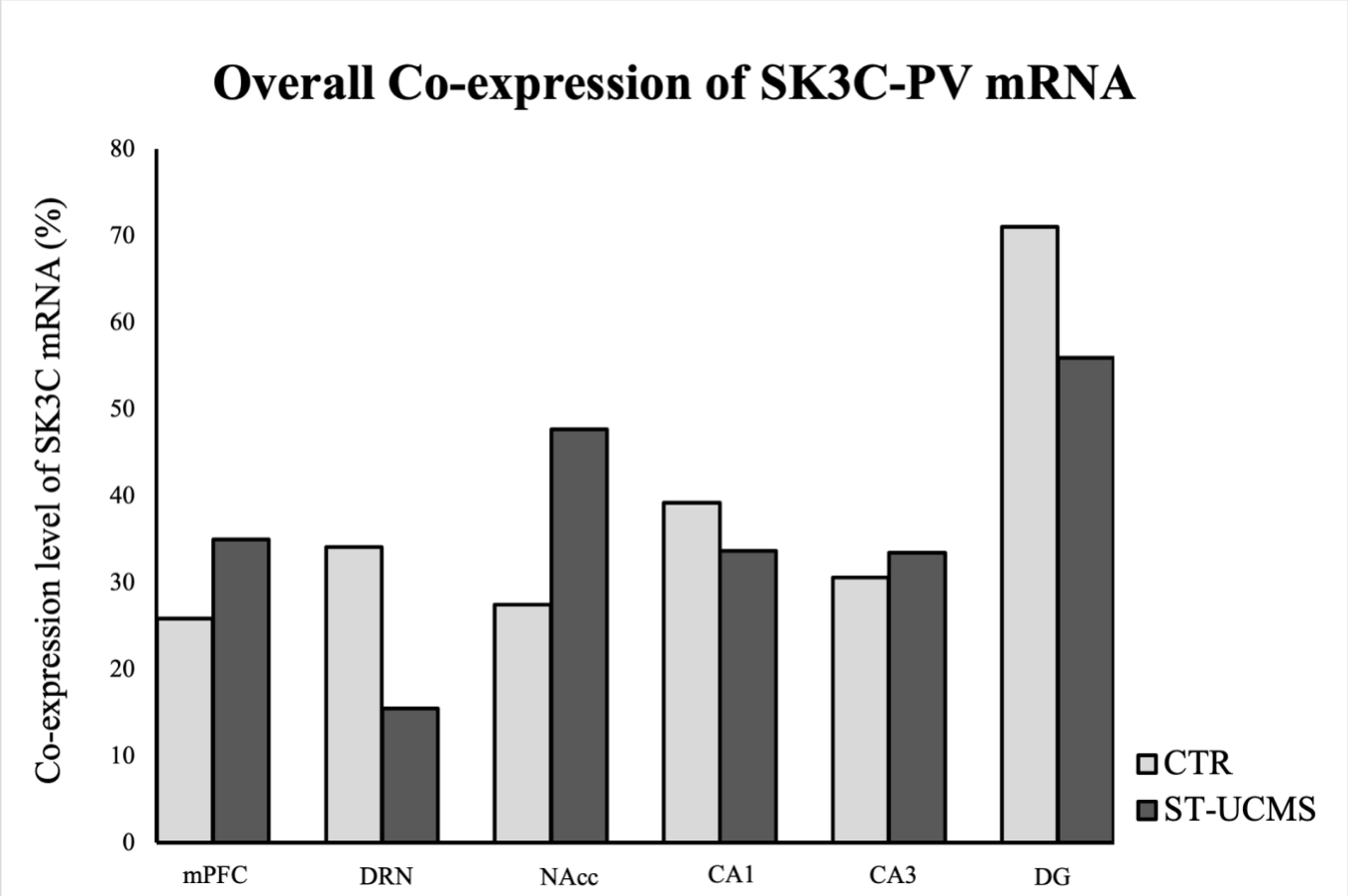

Figure 5. *Overall co-expression level of SK3C-PV mRNA after ST-UCMS exposure.* The figure compares the difference in SK3C-PV co-expression density in ST-UCMS animals with their respective controls. It can be observed that there is a general increase in co-expression levels for the mPFC, NAcc, and CA3, but for the DRN, CA1, and DG, the opposite was reported. All data were sex pooled. No statistical analysis was conducted due to limited sample size (n =1 brain per group)

Table 2

Summary table for the ST-UCMS effects on overall co-expression of SK3C-PV

ROI	♂		♀	
	CTR	ST-UCMS	CTR	ST-UCMS
mPFC	9.50%	25.13%	42.15%	44.79%
DRN	23.53%	30.05%	44.66%	1.01%
NAcc	0%	57.50%	54.87%	37.92%
CA1	11.11%	33.70%	67.36%	14.81%
CA3	17.39%	27.62%	43.79%	39.29%
DG	N/A	37.08%	71.06%	74.83%

Table 2. *Summary of the co-expression level of SK3C-PV mRNA after ST-UCMS exposure, separated by sex*. The current data show the difference between CTR Males, ST-UCMS Males, CTR Females, and ST-UCMS Females for the co-expression level of SK3C-PV mRNA across different brain regions (n = 1 brain per group). An expression level of 0% indicate that no neurons expressed SK3C mRNA in this ROI, whereas an expression level of 100% indicate that all neurons expressed SK3C mRNA. The p_{Tukey} value was not reported due to limited sample size. N/A = data for CTR Males in the DG are still under processed.

3.6 ST-UCMS increased overall expression of SST mRNA in all regions of interest except the DG

Surprisingly, we observed an increase in overall SST mRNA density across all the ROIs, except for the DG region (Figure 6). Indeed, for the mPFC (CTR: M = 24.83%; ST-UCMS: M = 31.00%), DRN (CTR: M = 29.85%; ST-UCMS: M = 34.54%), NAcc (CTR: M = 13.33%; ST-UCMS: M = 15.64%), CA1 (CTR: M = 29.63%; ST-UCMS: M = 40.02%), and CA3 (CTR: M = 21.77%; ST-UCMS: M = 32.75%) region, the SST mRNA density increased after ST-UCMS exposure as compared to their controls, whereas for the DG region, the opposite was reported (CTR: M = 29.44%; ST-UCMS: M = 18.47%).

Interestingly, when separated by Sex, it can be clearly observed that at baseline, CTR Females have higher level of SST mRNA compared to their male counterparts. Moreover, the increase in SST mRNA density following ST-UCMS exposure was more pronounced in ST-UCMS Males as opposed to ST-UCMS Females, when compared to their respective controls. Only the DRN region reported a decrease in SST mRNA density for ST-UCMS Males compared to their controls. Nevertheless, for all brain regions, ST-UCMS Females distinctively expressed higher level of SST mRNA compared to the ST-UCMS Males. No comparisons were inferred for DG since data for the CTR Males are being processed. All data are summarized in Table 3. Taken together, the current results could indicate that females have an innate neurobiological mechanism that is protective against stress exposure, at least in the context of SST mRNA synthesis and ultimately, SST protein production and release.

Figure 6

ST-UCMS effects on overall expression of SST mRNA

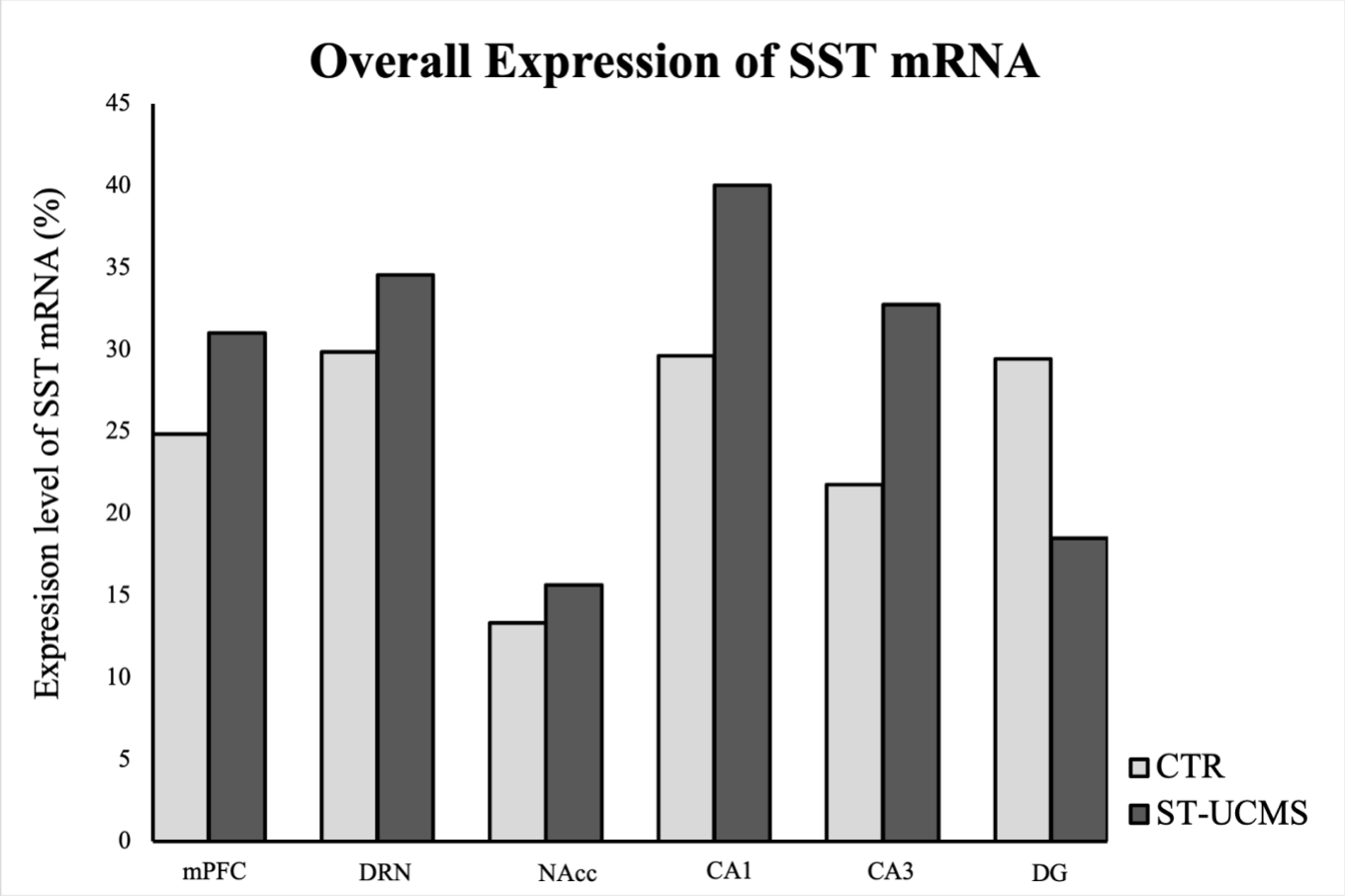

Figure 6. *Overall expression level of SST mRNA after ST-UCMS exposure.* The figure compares the difference in SST mRNA density in ST-UCMS animals with their respective controls. It can be observed that there is a general increase in expression levels for the mPFC, DRN, NAcc, CA1, and CA3, but for the DG, the opposite was reported. All data were sex pooled. No statistical analysis was conducted due to limited sample size (n = 1 brain per group)

Table 3

Summary table for ST-UCMS effects on overall expression of SST mRNA

ROI	♂		♀	
	CTR	ST-UCMS	CTR	ST-UCMS
mPFC	10.58%	17.41%	39.08%	44.59%
DRN	27.66%	7.30%	32.03%	61.79%
NAcc	2.45%	5.62%	24.18%	25.66%
CA1	2.47%	22.90%	56.79%	57.14%
CA3	4.32%	18.18%	39.23%	47.31%
DG	N/A	9.03%	29.44%	27.91%

Table 3. *Summary of the overall expression level of SST mRNA after ST-UCMS exposure, separated by sex*. The current data show the difference between CTR Males, ST-UCMS Males, CTR Females, and ST-UCMS Females for the expression level of SST mRNA across different brain regions (n =1 brain per group). An expression level of 0% indicate that no neurons expressed SST mRNA in this ROI, whereas an expression level of 100% indicate that all neurons expressed SST mRNA. The p_{Tukey} value was not reported due to limited sample size. N/A = data for CTR Males in the DG are still under processed.

3.7 ST-UCMS decreased overall expression of PV mRNA in all regions of interest except the DRN

After investigating the overall expression level of SST mRNA, we next sought to determine if ST-UCMS would have any impacts on the overall density of PV mRNA across the different ROIs (Figure 7). As expected, ST-UCMS exposure decreased PV mRNA density in the mPFC (CTR: $M = 26.09\%$; ST-UCMS: $M = 18.13\%$), NAcc (CTR: $M = 12.41\%$; ST-UCMS: $M = 10.33\%$), CA1 (CTR: $M = 28.03\%$; ST-UCMS: $M = 14.74\%$), CA3 (CTR: $M = 33.93\%$; ST-UCMS: $M = 20.73\%$), and DG (CTR: $M = 34.73\%$; ST-UCMS: $M = 13.14\%$) regions, but a sharp increase in PV mRNA was reported for the DRN region (CTR: $M = 30.50\%$; ST-UCMS: $M = 86.79\%$).

When investigating the effect of Sex, it can be observed that at baseline, CTR Females had higher level of PV mRNA as compared to their male counterparts, similar to the reported results for SST mRNA. Interestingly, only the CA1 regions showed that a decrease in PV mRNA density for both ST-UCMS Males and ST-UCMS Females, whereas for the mPFC, NAcc, and CA3 regions, ST-UCMS Males experienced an increase in PV mRNA density, while ST-UCMS Females experienced a decrease. For the DRN showed that both males and females experienced a sharp increase in PV mRNA density following ST-UCMS exposure, although ST-UCMS Females had a larger increase. No comparisons were inferred for DG since data for the CTR Males are being processed. All data are summarized in Table 4. Taken together, the current results could indicate a sex-dependent mechanism through which stress exposure affects the density of PV mRNA and hence, the production and release of PV protein.

Figure 7

ST-UCMS effects on the overall expression of PV mRNA

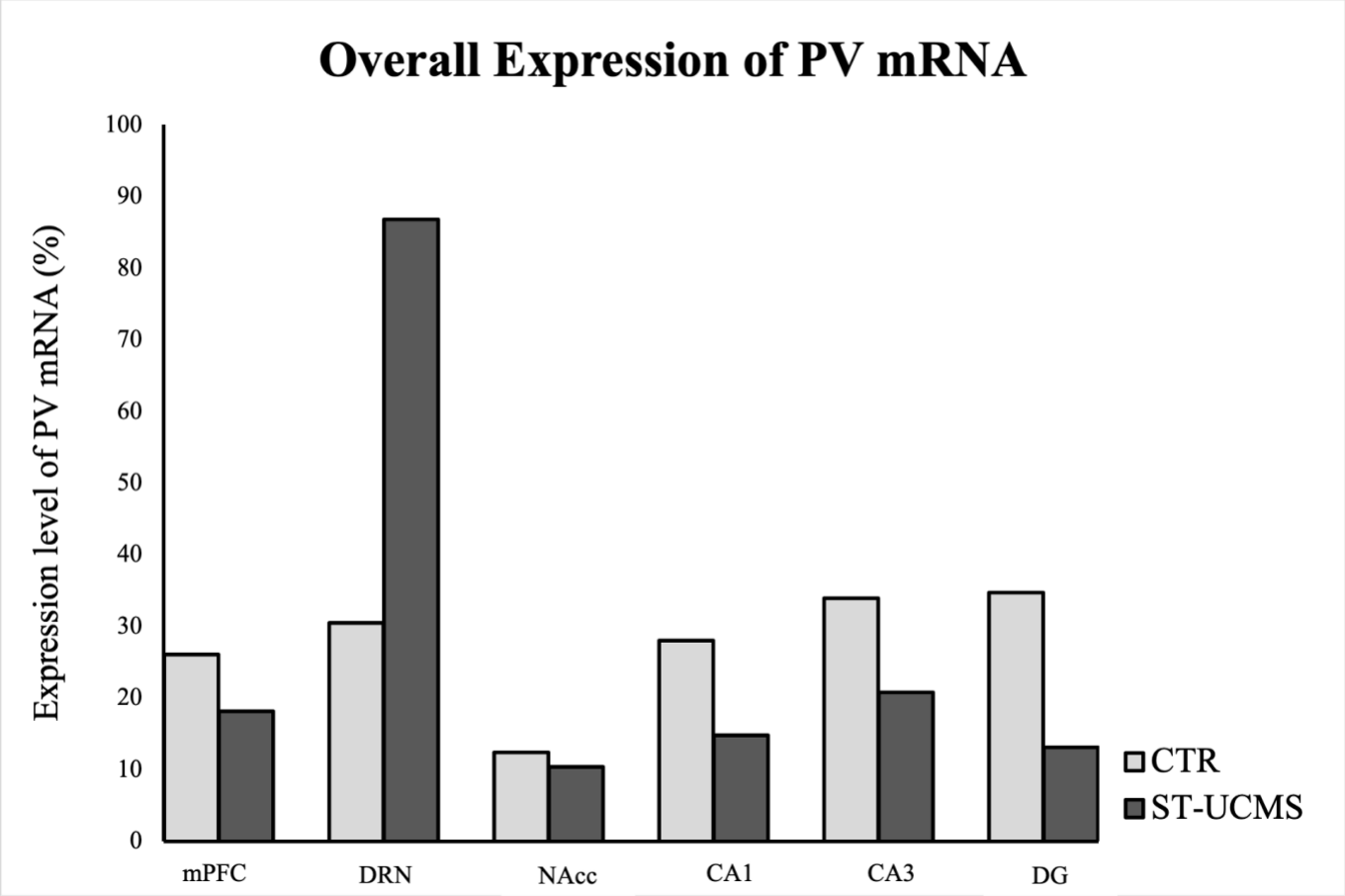

Figure 7. *Overall expression level of PV mRNA after ST-UCMS exposure.* The figure compares the difference in PV mRNA density in ST-UCMS animals with their respective controls. It can be observed that there is a general decrease in expression levels for the mPFC, NAcc, CA1, CA3, and DR, but for the DRN region, the opposite was reported. All data were sex pooled. No statistical analysis was conducted due to limited sample size (n = 1 brain per group).

Table 4

Summary table for ST-UCMS effects on the overall expression of PV mRNA

ROI	♂		♀	
	CTR	ST-UCMS	CTR	ST-UCMS
mPFC	16.48%	21.47%	35.69%	14.78%
DRN	18.09%	76.03%	42.92%	97.55%
NAcc	0%	3.68%	24.83%	16.98%
CA1	19.78%	14.94%	36.27%	14.54%
CA3	16.91%	21.09%	50.95%	20.44%
DG	N/A	6.35%	34.73%	19.93%

Table 4. *Summary of the overall expression level of PV mRNA after ST-UCMS exposure, separated by sex*. The current data show the difference between CTR Males, ST-UCMS Males, CTR Females, and ST-UCMS Females for the expression level of PV mRNA across different brain regions (n = 1 brain per group). An expression level of 0% indicate that no neurons expressed PV mRNA in this ROI, whereas an expression level of 100% indicate that all neurons expressed PV mRNA. The p_{Tukey} value was not reported due to limited sample size. N/A = data for CTR Males in the DG are still under processed.

3.8 LT-UCMS significantly increased co-expression of SK3C-SST mRNA in the mPFC region but not in other brain regions

Considering that SST-IN are important components of the overall inhibitory mechanism of the brain (Schulz et al., 2018), we decided to investigate the effects of LT-UCMS on the co-expression of SK3C mRNA with SST mRNA across several neuronal regions, and the potential underlying dysfunctionality impacting this type of interneuron. The current results demonstrated no significant interaction and no significant main effect of Sex, but a significant main effect of Treatment ($F_{(1,13)} = 6.75$, $p = .022$, $\eta^2 = 0.30$) on co-expression level of SK3C-SST mRNA in the mPFC region was reported. Interestingly, for the CA1 region, only a significant main effect of Sex ($F_{(1,13)} = 5.96$, $p = .030$, $\eta^2 = 0.30$), and for the NAcc, a marginal interaction was reported ($F_{(1,13)} = 3.86$, $p = .072$, $\eta^2 = 0.19$) and a marginal main effect of Treatment ($F_{(1,13)} = 3.26$, $p = .094$, $\eta^2 = 0.16$). However, for the DRN, CA3, and DG regions, no significant interaction and no significant main effects were observed.

Independent samples *t* tests were conducted to determine if a significant difference was present between CTR and LT-UCMS animals (sex-pooled data) across the areas of interest (Figure 8). Regarding the mPFC, a significant difference was observed (Student's *t* test, $p = .013$, Cohen's $d = -1.38$, 95% CI [-2.53, -0.16]) between CTR ($M = 33.93\%$, $SE = 3.28\%$) and LT-UCMS ($M = 48.45$, $SE = 3.75$) animals. No significant difference was observed for the other brain regions; however, it is interesting to note that a marginal significant increase was reported between the CTR ($M = 22.34\%$, $SE = 2.59\%$) and LT-UCMS ($M = 29.76\%$, $SE = 2.68\%$) animals for the CA3 region (Student's *t* test, $p = .069$, Cohen's $d = -1.03$, 95% CI [-2.14, 0.14]). Similar result was observed for the DG region (Student's *t* test, $p = .080$, Cohen's $d = 0.94$, 95% CI [-0.18, 2.01]), but for this area, LT-UCMS animals (M = 36.43, SE = 6.18) had a lower co-

expression level of SK3C-SST mRNA compared to their CTR counterparts (M = 49.03, SE = 2.51).

A summary of the post-hoc Tukey results is reported in Table 5. Regarding the mPFC region (Figure 9), a marginal significant difference was observed (p_{Tukey} = .072, Cohen's d = -2.09, 95% CI [-3.96, -0.21]) between CTR Males (M = 28.27%, SE = 5.56%) and LT-UCMS Males (M = 53.00%, SE =6.08%). For the DRN, NAcc, CA1, CA3, and DG regions, no significant difference and no marginally significant differences were observed.

Figure 8

LT-UCMS effects on overall co-expression level of SK3C-SST mRNA

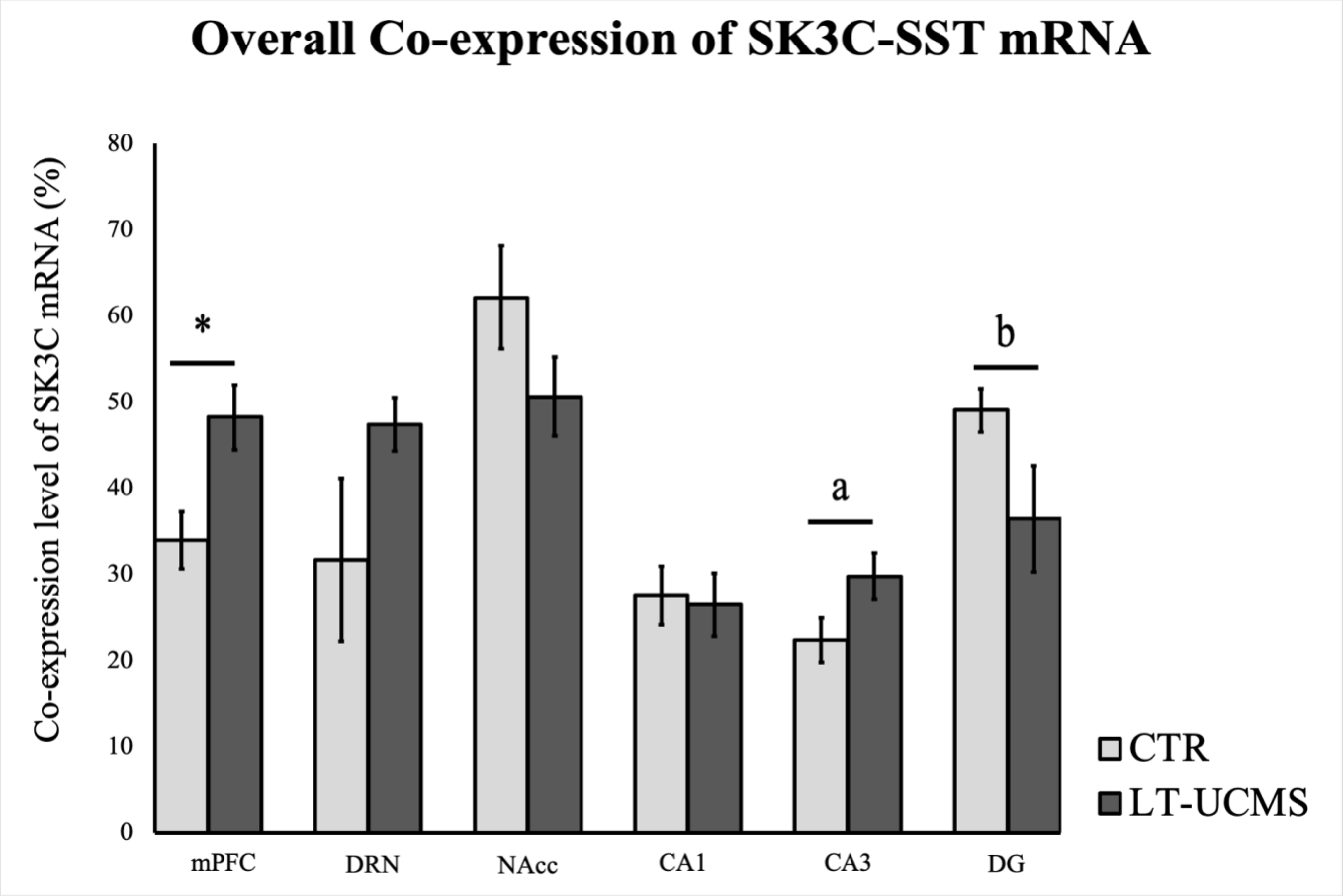

Figure 8. *Overall co-expression of SK3C-SST mRNA across different brain regions after LT-UCMS exposure*. The figure compares the difference in co-expression of SK3C-SST mRNA in the mPFC (CTR: n = 8; LT-UCMS: n = 9), DRN (CTR: n = 7; LT-UCMS: n = 8), NAcc (CTR: n = 7; LT-UCMS: n = 8), CA1 (CTR: n = 8; LT-UCMS: n = 8), CA3 (CTR: n = 9; LT-UCMS: n = 7), and DG (CTR: n = 8; LT-UCMS: n = 8) between controls and long-term stressed animals. LT-UCMS significantly increases co-expression of SK3C-SST mRNA in the mPFC area compared to stress-naïve animals. Differences in the CA3 and DG regions were marginally significant. Data were sex pooled. Student's *t* test: $*p = .038$, $^{a}p = .069$, $^{b}p = .80$.

Table 5

Post-hoc Tukey test Results for Co-expression of SK3C-SST mRNA

ROI	CTR ♂	LT-UCMS ♂	p_{Tukey}-value
mPFC	28.27±5.56%	53.00±6.08%	.072

Table 5. *Summary of post-hoc Tukey test for the overall co-expression level of SK3C-SST mRNA after LT-UCMS exposure*. Only the mPFC reported a marginal significant difference between CTR Males (n = 3) and LT-UCMS Males (n = 4). An expression level of 0% indicate that no neurons expressed SK3C mRNA in this ROI, whereas an expression level of 100% indicate that all neurons expressed SK3C mRNA. The p_{Tukey} value of the comparison is reported in the right-end column titled "p_{Tukey}". Only comparisons which are significant or marginally significant are shown.

Figure 9

Co-expression of SK3C-SST mRNA in the mPFC regions of LT-UCMS animals

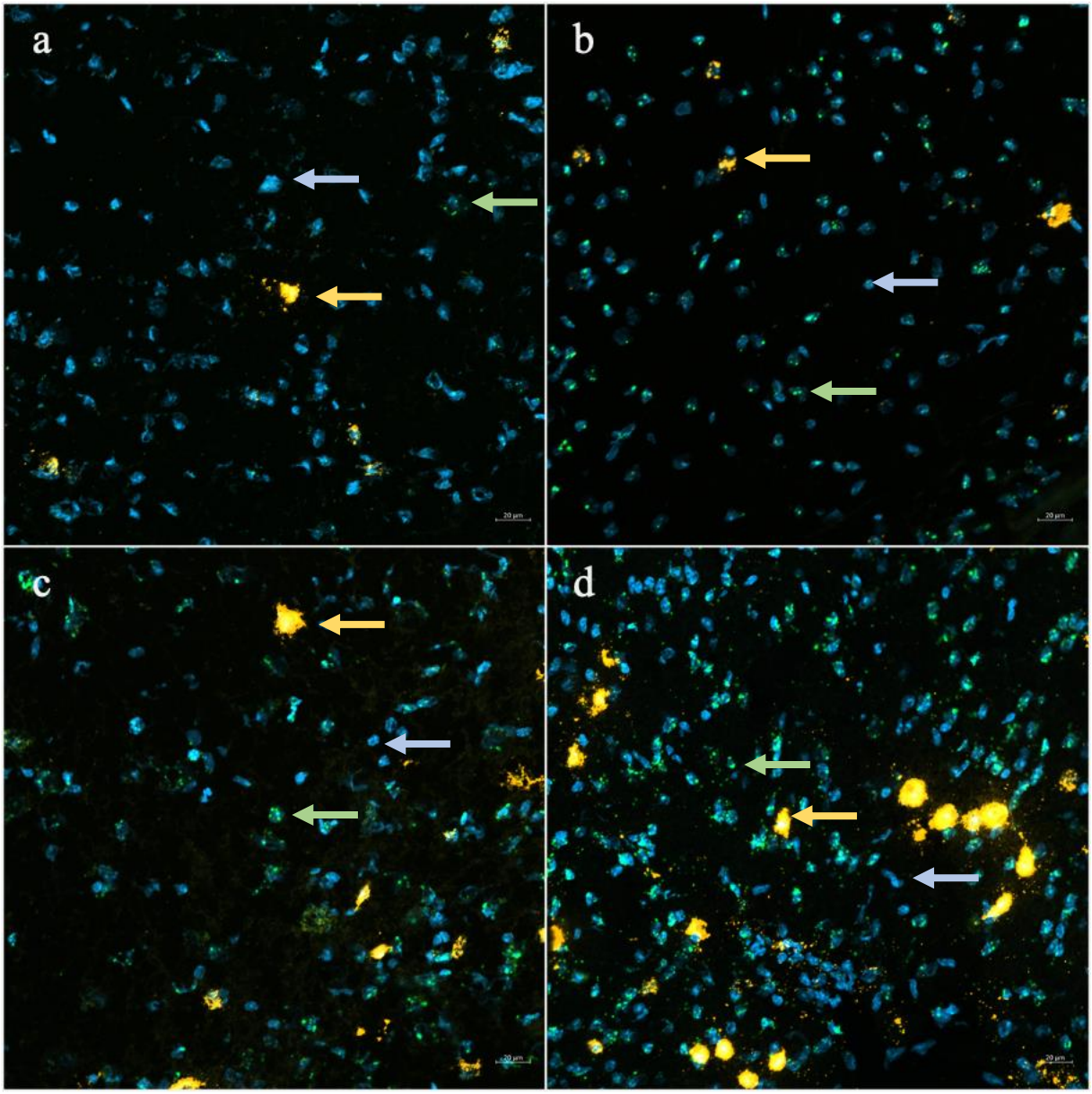

Figure 9. *Images of the mPFC-IL region.* In alphabetical order: a) CTR Male, b) LT-UCMS Male, c) CTR Female, and d) LT-UCMS Female. The images qualitatively show an increase in SK3C mRNA density in both LT-UCMS Male and Female when compared to their respective control counterparts. Interestingly, LT-UCMS Female demonstrate a higher level of SST mRNA in general when compared to the other groups. Images shown are at x20 magnification. SST mRNA = yellow arrow colour, SK3C = green arrow, nuclei = light-blue arrow.

3.9 LT-UCMS significantly increased co-expression of SK3C-PV mRNA in the NAcc region but not in other brain regions

The detrimental effects of stress exposure on PV-IN has been well-characterized (Reviewed in Woodward & Coutellier., 2021) commanding special attention, as indeed, such effects could be potentiated through overexpression of SK3C mRNA within this specific GABAergic interneuron. Our current results demonstrate that in fact, LT-UCMS generally increases the co-expression level of SK3C-PV mRNA across our ROIs. Conducting 2x2 ANOVAs showed a marginally significant interaction ($F_{(1,10)} = 6.75$, $p = .078$, $\eta^2 = 0.17$) and a significant main effect of Treatment ($F_{(1,10)} = 6.96$, $p = .025$, $\eta^2 = 0.31$), but no significant main effect of Sex in the DRN region. Similarly, only a significant main effect of Treatment ($F_{(1,12)} = 10.51$, $p = .007$, $\eta^2 = 0.44$) was observed for the NAcc region. For the mPFC, CA1, CA3, and DG regions, no significant main effects and no significant interaction were reported.

Independent samples *t* tests were conducted to determine if a significant difference was present between CTR and LT-UCMS animals (sex-pooled data) across the areas of interest (Figure 10). For the NAcc region, a significant difference (Student's *t* test, $p = .005$, Cohen's $d = -1.86$, 95% CI [-3.29, -0.35]) was observed, with CTR animals ($M = 28.59\%$, $SE = 3.69\%$) having considerably lower level of SK3C-PV mRNA co-expression compared to their LT-UCMS counterparts ($M = 47.67\%$, $SE = 4.07\%$). For the following regions of interest, a marginally significant difference was observed: 1) DRN (Student's *t* test, $p = .055$, Cohen's $d = -1.13$, 95% CI [-2.32, 0.12], CTR [$M = 28.77\%$, $SE = 5.79\%$], LT-UCMS [$M = 42.18\%$, $SE = 6.84\%$]), 2) CA3 (Student's *t* test, $p = .067$, Cohen's $d = -1.03$, 95% CI [-2.17, 0.16], CTR [$M = 28.77\%$, $SE = 3.45\%$], LT-UCMS [$M = 36.01\%$, $SE = 4.62\%$]), and 3) DG (Welch's *t* test, $p = .054$, Cohen's $d = -1.26$, 95% CI [-2.49, 0.03], CTR [$M = 45.28\%$, $SE = 0.91\%$], LT-UCMS [$M = 58.03\%$, $SE = 5.32\%$]). For the mPFC and CA1 regions, no significant differences were reported.

A summary of the results is reported in Table 6. For the NAcc regions, there was a significant difference (p_{Tukey} = .041, Cohen's d = -2.18, 95% CI [-4.00, -0.36]) between CTR Females (M = 19.74%, SE = 8.98%) and LT-UCMS Females (M = 50.76%, SE =9.93%). For the DRN, a marginal significant difference (p_{Tukey} = .051, Cohen's d = -2.48, 95% CI [-4.69, -0.28]) was observed between CTR Males (M = 25.02%, SE = 10.97%) and LT-UCMS Males (M = 61.63%, SE = 0.48%). Additionally, CTR Females (M = 31.58%, SE = 7.14%) and LT-UCMS Males also had a marginally significant difference (p_{Tukey} = .092, Cohen's d = -2.04, 95% CI [-4.02, -0.06]). For the mPFC, CA1, CA3, and DG, no groups significantly differed from the others and no marginal significance was reported.

Figure 10

LT-UCMS effects on the overall co-expression level of SK3C-PV mRNA

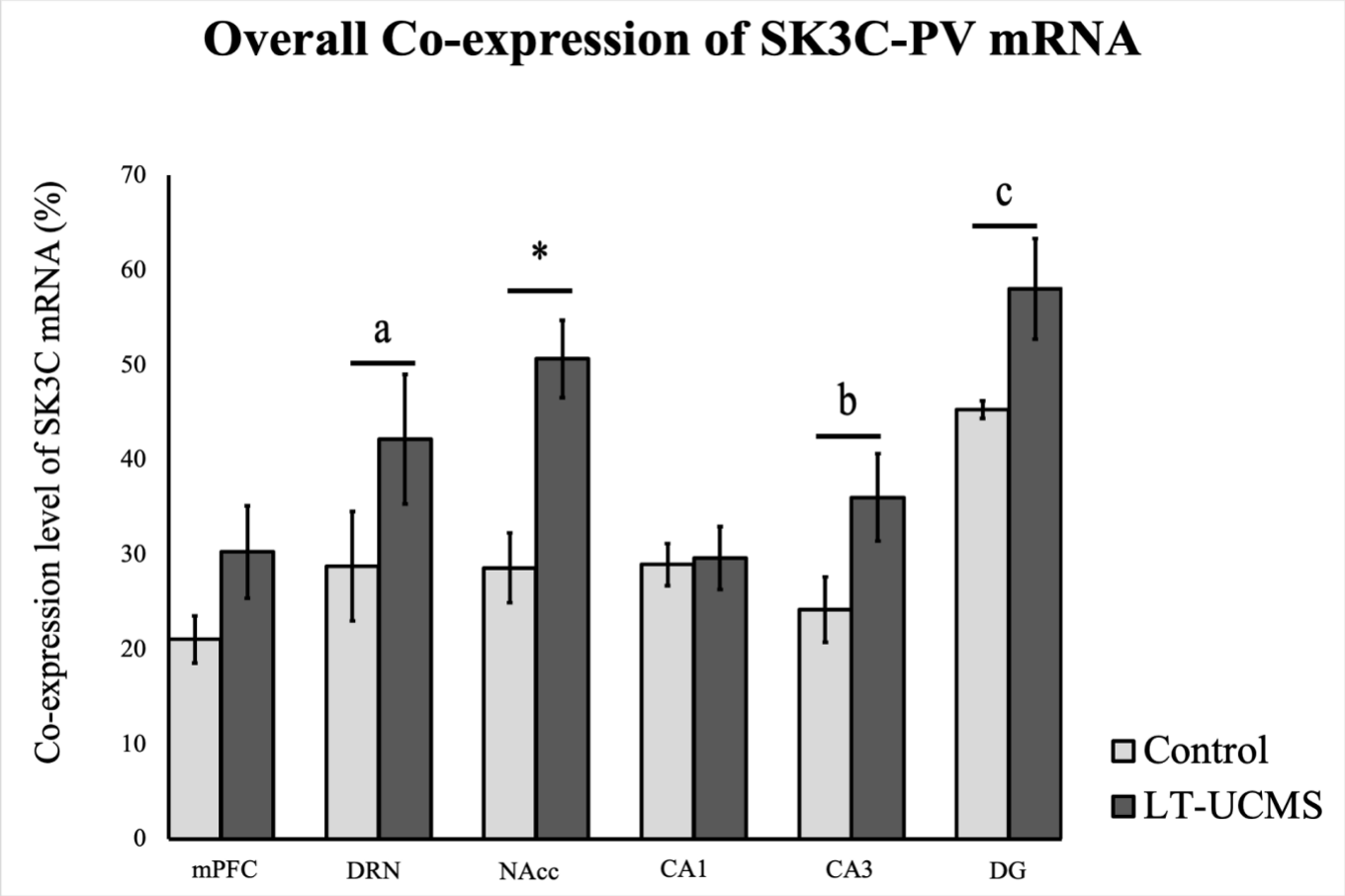

Figure 10. *Overall co-expression of SK3C-PV mRNA across different brain regions after LT-UCMS exposure*. The figure compares the difference in co-expression of SK3C-PV mRNA in the mPFC (CTR: n = 7; LT-UCMS: n = 7), DRN (CTR: n = 7; LT-UCMS: n = 7), NAcc (CTR: n = 7; LT-UCMS: n = 7), CA1 (CTR: n = 8; LT-UCMS: n = 8), CA3 (CTR: n = 7; LT-UCMS: n = 8), and DG (CTR: n = 7; LT-UCMS: n = 7) between controls and long-term stressed animals. LT-UCMS animals generally demonstrate an increase in SK3C-PV co-expression across all brain regions, but the increase was significant only in NAcc. For the DRN, CA3, and DG, the increase was marginally significant. Data were sex-pooled. Student's *t* test: $*p < .01$, $^{a}p = .055$, $^{b}p = .067$, Welch's *t* test: $^{c}p = .054$

Table 6

Post-hoc Tukey test Results for Co-Expression for SK3C-PV mRNA

ROI	♂		♀		p_{Tukey}
	CTR	LT-UCMS	CTR	LT-UCMS	
DRN	25.02±10.97%	61.63±0.48%			.051
	25.02±10.97%		31.58±7.14%		.092
NAcc			19.74±8.98%	50.76±9.93%	.041

Table 6. *Summary of post-hoc Tukey test for the overall co-expression level of SK3C-PV mRNA after LT-UCMS exposure*. Only the NAcc reported a significant difference between CTR Females (n = 4) and LT-UCMS Females (n = 4), with stressed females having a higher level of co-expression than non-stressed females. For the DRN, a marginal significant difference was observed between CTR Males (n = 3) and LT-UCMS Males (n = 3), and CTR Males and CTR Females (n = 4). An expression level of 0% indicate that no neurons expressed SK3C mRNA in this ROI, whereas an expression level of 100% indicate that all neurons expressed SK3C mRNA. The p_{Tukey} value of the comparison is reported in the right-end column titled "p_{Tukey}". Only comparisons which are significant or marginally significant are shown. Cells filled in grey indicate that no significant difference was observed with these comparisons.

Figure 11

Co-expression of SK3C-PV mRNA in the NAcc region of LT-UCMS animals

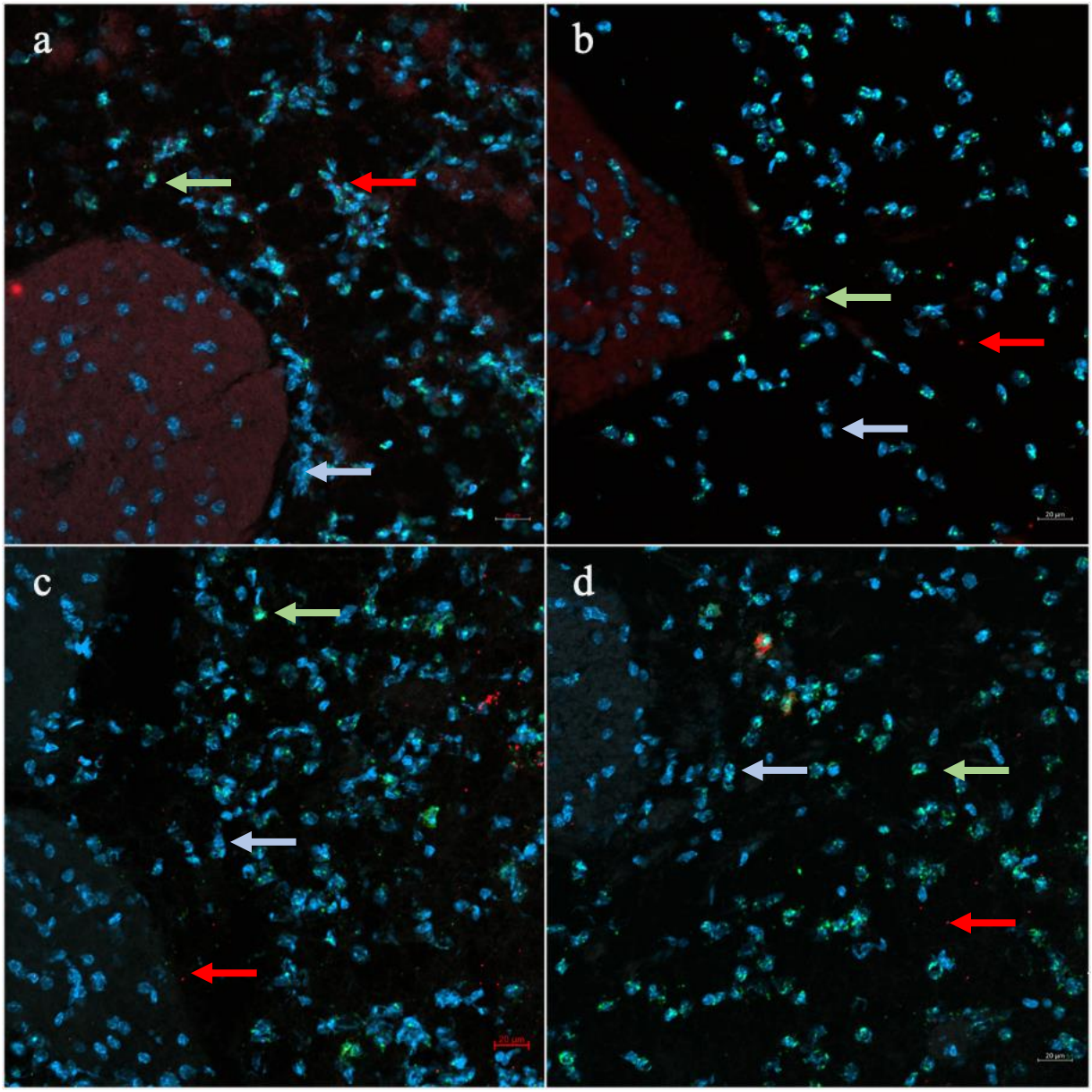

Figure 11. *Images of the NAcc region.* In alphabetical order: a) CTR Male, b) LT-UCMS Male, c) CTR Female, and d) LT-UCMS Female. The images qualitatively show an increase in SK3C mRNA density in both LT-UCMS Male and Female when compared to their respective control counterparts. Interestingly, LT-UCMS Female demonstrate a lower level of PV mRNA in general when compared to CTR Females. Images shown are at x20 magnification. PV mRNA = far-red arrow, SK3C = green arrow, nuclei = light-blue arrow

3.10 LT-UCMS generally increases the expression level of SST mRNA across several brain regions in a sex-dependent manner

After determining the effects of LT-UCMS on the co-expression level of SK3C-SST mRNA, we next sought to establish if such outcomes would impact the overall SST mRNA density across our ROIs. Considering that SST is an essential neurotransmitter, and its deficiency has been reported in several neuropsychiatric disorders (Reviewed in Fee et al., 2017; Song et al., 2021), we posited on whether SK3C overexpression due to LT-UCMS could be affecting the production of the neuropeptide, and possibly the general neuronal activity of SST-IN. Our results demonstrate that there is a general increase in SST mRNA density across the mPFC, DRN, NAcc, and CA3, while the CA1 and DG regions displayed a reduction (Figure 12), which is similar to the findings for the ST-UCMS cohort. 2x2 ANOVAs were conducted for each ROI and they show that for the mPFC, there is a significant interaction ($F_{(1,12)} = 25.58$, $p < .001$, $\eta^2 = 0.56$). For the DRN, no significant interaction and no significant main effect of Treatment were reported, but a significant main effect of Sex ($F_{(1,12)} = 16.57$, $p = .002$, $\eta^2 = 0.55$) was observed. Regarding the NAcc and CA1 regions, the ANOVAs results showed a significant interaction for both cases (NAcc: $F_{(1,13)} = 7.65$, $p = .016$, $\eta^2 = 0.35$; CA1: $F_{(1,13)} = 8.11$, $p = .014$, $\eta^2 = 0.33$), but no significant main effects were reported. On the other hand, for the CA3 and DG regions, ANOVA results yielded no significant main effects nor interaction for both.

Independent samples *t* tests were conducted to determine if LT-UCMS exposure would significantly alter the density of SST mRNA of stressed animals compared to their control counterparts. For the mPFC, DRN, NAcc, and CA1 regions, no significant differences were determined, however, for the CA3 (Student's *t* test: $p = .081$, Cohen's $d = -0.94$, 95% CI [-2.01, -0.18] and DG (Student's *t* test: $p = .099$, Cohen's $d = 0.86$, 95% CI [-0.20, 1.87] regions, a marginally significant difference was observed in each case. For the CA3, LT-UCMS animals

(*M* = 21.38%, *SE* = 3.22%) had higher density of SST mRNA compared to their controls (*M* = 14.06%, *SE* = 2.17%), while the opposite was observed for the DG, whereby the LT-UCMS animals (*M* = 9.93%, *SE* = 1.62%) exhibited lower SST mRNA density than the controls (*M* = 15.47%, *SE* = 2.59%).

For the mPFC, CTR Females (*M* = 13.64%, *SE* = 3.10%) significantly differed from LT-UCMS Females (*M* = 32.65%, *SE* = 2.26%), with CTR Females having lower level of SST mRNA compared to their stressed homologues (p_{Tukey} = .002, Cohen's *d*= -3.16, 95% CI [-5.18, -1.13]). Similarly, a significant difference between LT-UCMS Males (*M* = 9.27%, *SE* = 0.82%) and LT-UCMS Females was also reported (p_{Tukey} = .001, Cohen's *d*= -3.88, 95% CI [-6.28, -1.48]). For the comparison between CTR Males (*M* = 21.24%, *SE* = 3.61%) and LT-UCMS Males, a marginally significant difference was observed (p_{Tukey} = .094, Cohen's *d*= 1.99, 95% CI [0.10, 3.87]), and a similar result was reported between CTR Males and LT-UCMS Females, with stressed females having a marginally higher SST mRNA density than non-stressed males (p_{Tukey} = .082, Cohen's *d*= -1.89, 95% CI [-3.65, -0.14]). For the DRN, a significant difference was observed between CTR Males (*M* = 6.55%, *SE* = 2.23%) and LT-UCMS Females (*M* = 37.08%, *SE* = 7.74%), with stressed females having higher SST mRNA level than stress-naive males (p_{Tukey} = .014, Cohen's *d*= -2.69, 95% CI [-4.68, -0.10]). For the comparison between LT-UCMS Males (*M* = 14.43%, *SE* = 2.44%) and LT-UCMS Females, a marginally significant difference was observed (p_{Tukey} = .050, Cohen's *d*= -2.00, 95% CI [-3.71, -0.29]), and similar results were reported for the comparison between CTR Males and CTR Females (*M* = 30.88%, *SE* = 4.53%), with non-stressed females having a marginally higher SST mRNA level than their male homologues (p_{Tukey} = .066, Cohen's *d*= -2.14, 95% CI [-4.06, -0.23]). Concerning the NAcc regions, only the comparison between CTR Females (*M* = 9.52%, *SE* = 3.52%) and LT-UCMS

Females (M = 26.40%, SE = 4.79%) showed a marginally significant difference (p_{Tukey} = .069, Cohen's d= -1.85, 95% CI [-3.50, -0.20]), while other comparisons were not significant, nor marginally significant. For the CA1 region, a significant difference was observed between CTR Males (M = 11.17%, SE =2.27%) and CTR Females (M = 25.40%, SE = 2.50%), with the females having a significantly higher level of SST mRNA (p_{Tukey} = .025, Cohen's d= -2.22, 95% CI [-3.95, -0.49]) compared to the males. A marginally significant difference (p_{Tukey} = .074, Cohen's d= -1.82, 95% CI [0.18, 3.46]) was also observed between CTR Females and LT-UCMS Females (M = 13.75%, SE = 1.47%) for the CA1 region. Finally, for both the CA3 and DG regions, no comparisons were significant nor marginally significant when conducting post-hoc Tukey tests. A summary of the results was reported in Table 7.

Figure 12

LT-UCMS effects on the overall expression of SST mRNA

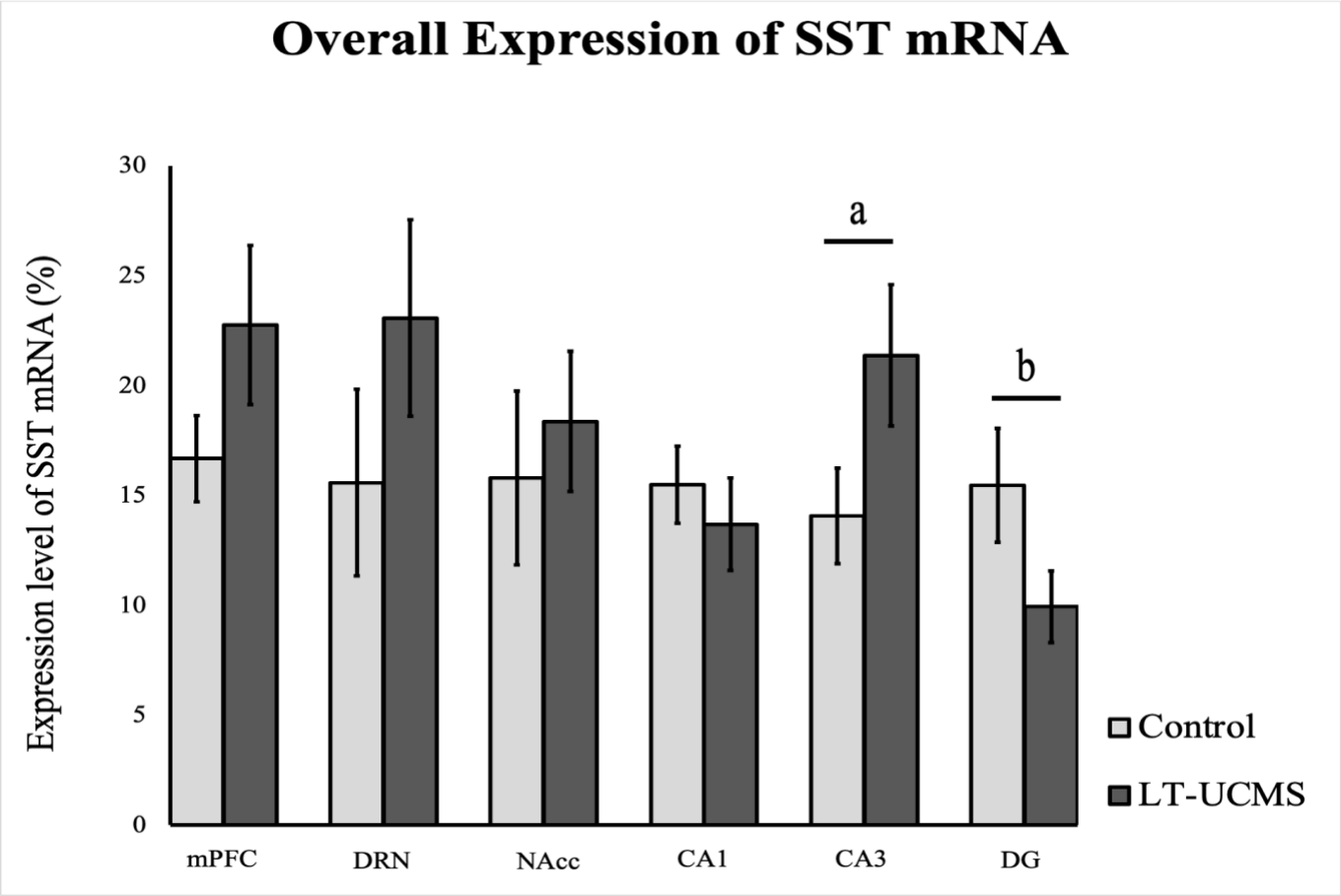

Figure 12. *Overall expression of SST mRNA across different brain regions after LT-UCMS exposure.* The figure compares the difference in overall expression level of SST mRNA in the mPFC (CTR: n = 9; LT-UCMS: n = 9), DRN (CTR: n = 8; LT-UCMS: n = 8), NAcc (CTR: n = 8; LT-UCMS: n = 8), CA1 (CTR: n = 8; LT-UCMS: n = 7), CA3 (CTR: n = 8; LT-UCMS: n = 8), and DG (CTR: n = 9; LT-UCMS: n = 8) regions between CTR and LT-UCMS animals. Interestingly, LT-UCMS increases the expression of SST mRNA in general although no comparisons were significant. The comparisons for CA3 and DG regions were marginally significant. Data were sex pooled. Student's *t* test: ^{a}p = .081, ^{b}p =.099.

Table 7

Summary of Post-hoc Tukey test for Overall Expression of SST mRNA

ROI	♂		♀		p_{Tukey}
	CTR	LT-UCMS	CTR	LT-UCMS	
mPFC			13.64±3.10%	32.65±2.63%	.002
		9.27±0.82%		32.65±2.63%	.001
	21.24±3.61%	9.27±0.82%			.094
	21.24±3.61%			32.65±2.63%	.082
DRN	6.55±2.23%			37.08±7.74%	.014
		14.43±2.44%		37.08±7.74%	.050
	6.55±2.23%		30.88±4.53%		.066
NAcc			9.52±3.52%	26.40±4.79%	.069
CA1	11.17±2.27%		25.40±2.50%		.025
			25.40±2.50%	13.75±1.47%	.074

Table 7. *Summary of post-hoc Tukey test for the overall expression level of SST mRNA after LT-UCMS exposure*. For the mPFC: CTR Males (n = 4), LT-UCMS Males (n = 3), CTR Females (n = 5), and LT-UCMS Females (n = 4). For the DRN: CTR Males (n = 3), LT-UCMS Males (n = 4), CTR Females (n = 4), and LT-UCMS Females (n = 5). For NAcc: CTR Females (n = 4) and LT-UCMS Females (n = 5). For the CA1: CTR Males (n = 4), CTR Females (n = 5), and LT-UCMS Females (n = 4). An expression level of 0% indicate that no neurons expressed SST mRNA in this ROI, whereas an expression level of 100% indicate that all neurons expressed SST mRNA. The p_{Tukey} value of the comparison is reported in the right-end column titled "p_{Tukey}". Only comparisons which are significant or marginally significant are shown. Cells filled in grey indicate no significant nor marginally significant comparisons were observed

3.11 LT-UCMS significantly decreases the expression level of PV mRNA across several brain regions

Considering the general increasing trend in SK3C mRNA co-expression with PV mRNA, we then sought to determine if LT-UCMS exposure would impact the transcription of PV mRNA in general. 2x2 ANOVAs were conducted and the results showed that for the NAcc region, a significant interaction were reported ($F_{(1,12)} = 14.16$, $p = .003$, $\eta^2 = 0.31$). Similarly, a significant interaction was also reported for the CA1 region ($F_{(1,13)} = 8.11$, $p = .014$, $\eta^2 = 0.33$), whereas for the DG region, the results demonstrated a a marginally significant interaction ($F_{(1,12)} = 16.57$, $p = .092$, $\eta^2 = 0.14$) and significant main effect of Treatment ($F_{(1,12)} = 16.57$, $p = .016$, $\eta^2 = 0.34$). Regarding the mPFC, DRN, and CA3 regions, no significant main effects and interactions were reported.

Independent samples *t* tests were conducted to determine if exposure to LT-UCMS significantly altered the density of PV mRNA compared to stress-naïve animals (Figure 13). The results obtained for the LT-UCMS cohort mirrored those observed for the ST-UCMS cohort, with the only noticeable exception being the DRN region. Indeed, stress exposure significantly reduced PV mRNA density in the DRN (CTR: $M = 45.03\%$, $SE = 4.45\%$, LT-UCMS: $M = 27.45\%$, $SE = 4.54\%$, Student's *t* test: $p = .017$, Cohen's $d = 1.42$, 95% CI [0.10, 2.67], while in ST-UCMS, it was increased. For the NAcc (CTR: $M = 19.10\%$, $SE = 3.44\%$, LT-UCMS: $M = 7.43\%$, $SE = 1.35\%$, Welch's *t* test: $p = .014$, Cohen's $d = 1.67$, 95% CI [0.29, 3.07]), the CA1 (CTR: $M = 20.42\%$, $SE = 2.21\%$, LT-UCMS: $M = 11.90\%$, $SE = 2.42\%$, Student's *t* test: $p = .021$, Cohen's $d = 1.30$, 95% CI [0.08, 2.45]), and DG (CTR: $M = 16.11\%$, $SE = 1.22\%$, LT-UCMS: $M = 9.61\%$, $SE = 0.86\%$, Student's *t* test: $p < .001$, Cohen's $d = 2.30$, 95% CI [0.64, 3.90]). For the CA3 region, a marginally significant decrease in PV mRNA (Student's *t* test: $p = .051$, Cohen's $d = 1.07$, 95% CI [-0.08, 2.16]) was observed between CTR ($M = 27.04\%$, $SE =$

3.23%) and LT-UCMS (*M* = 18.43%, *SE* = 2.43%) animals. No significant difference was reported for the mPFC region.

For the NAcc region, a significant difference was observed ($p_{Tukey} < .001$, Cohen's *d*= 3.87, 95% CI [1.56, 6.18]) between CTR Males (*M* = 26.85%, *SE* = 2.45%) and LT-UCMS Males (*M* = 5.01%, *SE* = 1.83%), between CTR Males and CTR Females (*M* = 10.48%, *SE* = 4.61%; $p_{Tukey} = .007$, Cohen's *d*= 2.90, 95% CI [0.89, 4.91]), and between CTR Males and LT-UCMS Females (*M* = 9.85%, *SE* = 1.11%; ($p_{Tukey} = .005$, Cohen's *d*= 3.01, 95% CI [0.97, 5.06]). Regarding the CA1 region, a significant decrease in PV mRNA density was observed ($p_{Tukey} = .036$, Cohen's *d*= 2.09, 95% CI [0.39, 3.79]) between CTR Females (*M* = 20.34%, *SE* = 3.91%) and LT-UCMS Females (*M* = 7.87%, *SE* = 0.98%), while a marginally significant difference was reported ($p_{Tukey} = .087$, Cohen's *d*= 1.85, 95% CI [0.14, 3.57]) between LT-UCMS Males (*M* = 18.83%, *SE* = 3.34%) and LT-UCMS Females. Additionally, for the DG region, a significant difference was observed ($p_{Tukey} = .019$, Cohen's *d* = 2.36, 95% CI [0.56, 4.15]) between CTR Females (*M* = 21.97%, *SE* = 5.87%) and LT-UCMS Females (*M* = 6.99%, *SE* = 1.47%). For the mPFC, DRN, and CA3 regions, post-hoc Tukey tests revealed no significant nor marginally significant comparisons. The significant and marginally significant comparisons are summarized in Table 8.

Figure 13

LT-UCMS effects on overall expression of PV mRNA

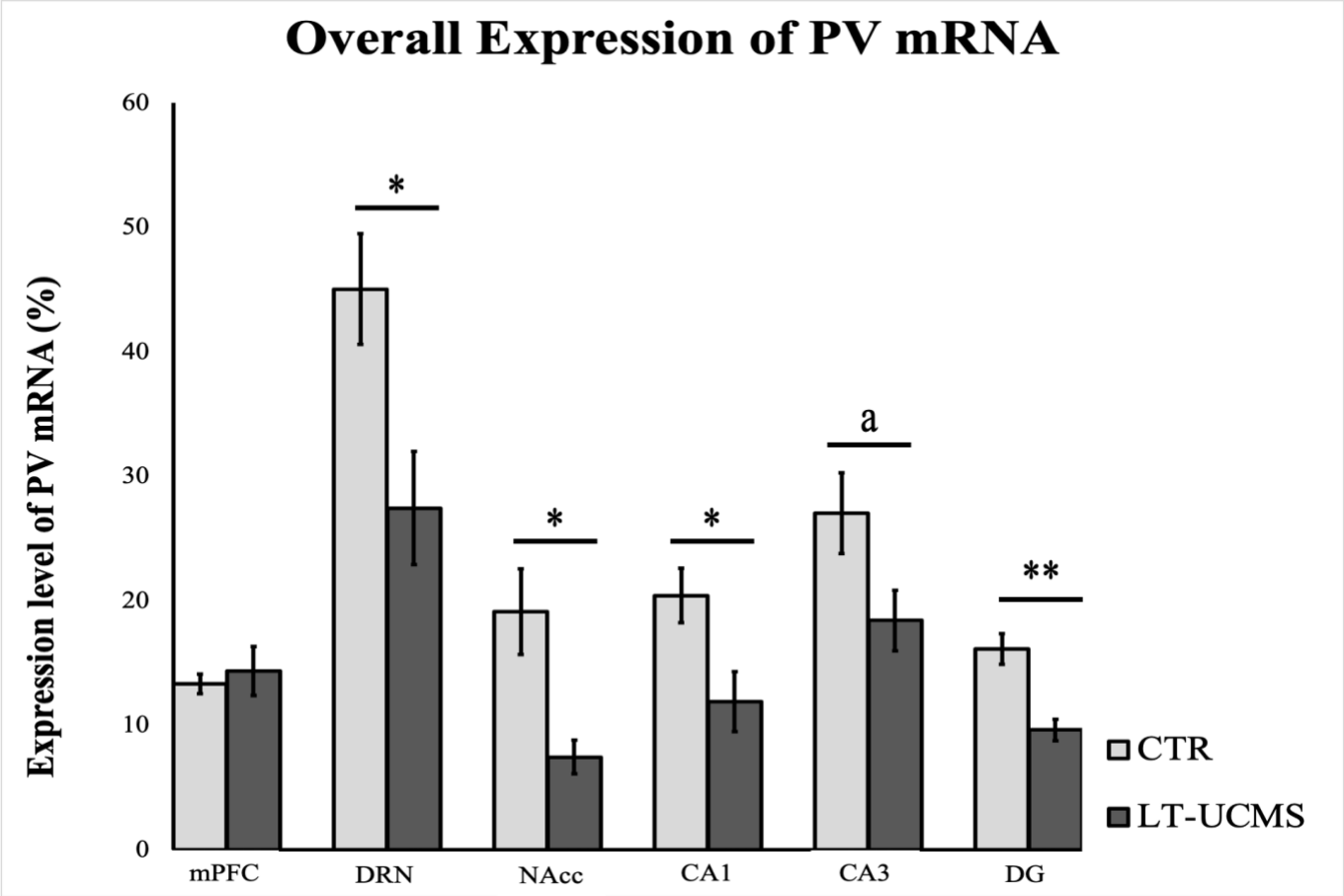

Figure 13. *Overall expression of PV mRNA across different brain regions after LT-UCMS exposure.* The figure compares the difference in overall expression level of PV mRNA in the mPFC (CTR: n = 7; LT-UCMS: n = 7), DRN (CTR: n = 7; LT-UCMS: n = 8), NAcc (CTR: n = 7; LT-UCMS: n = 8), CA1 (CTR: n = 8; LT-UCMS: n = 8), CA3 (CTR: n = 8; LT-UCMS: n = 8), and DG (CTR: n = 7; LT-UCMS: n = 8) regions between CTR and LT-UCMS animals. In general, LT-UCMS decreases the expression of PV mRNA across the DRN, NAcc, CA1, CA3, and DG. Data were sex pooled. For the DRN, CA1, and DG, Student's *t* test was significant: $*p < .05$, $**p < .001$. For the NAcc, Welch's *t* test was significant: $*p < .05$. For the CA3, Student's *t* test was marginally significant: $^{a}p = .051$.

Table 8

Summary of Post-hoc Tukey test for Overall Expression of PV mRNA

ROI	♂		♀		p_{Tukey}
	CTR	LT-UCMS	CTR	LT-UCMS	
NAcc	26.85±2.45%	5.01±1.83%			< .001
	26.85±2.45%		10.48±4.61%		.007
	26.85±2.45%			9.85±1.11%	.005
CA1			20.34±3.91%	7.87±0.98%	.036
		18.93±3.34%		7.87±0.98%	.087
DG			21.97±5.87%	6.99±1.47%	.019

Table 8. *Summary of post-hoc Tukey test for the overall expression level of PV mRNA after LT-UCMS exposure*. For the NAcc: CTR Males (n = 4), LT-UCMS Males (n = 4), CTR Females (n = 4), and LT-UCMS Females (n = 4). For the CA1: LT-UCMS Males (n = 4), CTR Females (n = 5), and LT-UMCS Females (n = 4). For the DG: CTR Females (n = 4) and LT-UCMS Females (n = 5). An expression level of 0% indicate that no neurons expressed PV mRNA in this ROI, whereas an expression level of 100% indicate that all neurons expressed PV mRNA. The p_{Tukey} value of the comparison is reported in the right-end column titled "p_{Tukey}". Only comparisons which are significant or marginally significant are shown. Cells filled in grey indicate that no significant nor marginally significant comparisons were observed.

4.0 Discussion

In the present study, we investigated the effects of both ST-UCMS and LT-UCMS exposure on the onset of depressive-like symptoms and cognitive impairments, using a battery of behavioural tests. Following behavioural testing, the RNAscope™ procedure was implemented to identify, visualize, and quantify the density levels of the SST mRNA, PV mRNA, in addition to the co-expression levels of SK3C-SST mRNA and SK3C-PV mRNA. The transcriptomic investigation was conducted across different brain regions, notably the mPFC and NAcc, involved with depressive-like symptoms. The research objectives of the current thesis were: 1) to determine if stress exposure results in overexpression of SK3C mRNA in specific brain areas, and 2) if the overexpression levels of SK3C mRNA would differ between short-term and long-term stress. As such, we hypothesized the following: 1) both short-term and long-term stress exposure would result in higher expression levels of SK3C within both SST-IN and PV-IN, and 2) both short-term and long-term stress exposure would result in lower overall density of SST and PV mRNA. Given the present results, only our first hypothesis was confirmed. Indeed, we can observe that both ST- and LT-UCMS induced a higher co-expression level of both SK3C-SST and SK3C-PV, which is in accordance with our first hypothesis. However, contrary to our initial expectation, both ST- and LT-UCMS resulted in an increase in SST mRNA density, contradicting our second hypothesis.

4.1 LT-UCMS induced a differential behavioural phenotypic profile as compared to ST-UCMS

As expected, administration of different UCMS paradigm durations resulted in distinct behavioural outcomes characterized and presented in the current study. Indeed, animals exposed to the LT-UCMS regimen demonstrated more pronounced depressive-like outcomes as compared

to their ST-UCMS counterparts. For instance, the SPT showed a significant reduction in sucrose consumption in stressed animals at eight weeks of UCMS exposure. On the other hand, at two weeks of UCMS, the stressed animals demonstrated no significant change in sucrose consumption. The SPT is a well-established behavioral test which is used to characterize anhedonia-like reactivity in animal models and recapitulating one of the two cardinal features of depression in humans, the other one being depressed mood (Z. Chen et al., 2021; Golding & Lipton, 1990).

Interestingly, our study demonstrated that LT-UCMS caused anhedonia-like reactivity in stressed animals, which was not reported in ST-UCMS animals, inferring that the duration of stressful events play a pivotal role in the pathogenesis of MDD. In fact, such finding could reflect the slow, insidious onset of stress-dependent depression. Further confirming the gradual, time-dependent impact of stress exposure on MDD's development, we also reported a significant difference in the latency to reach food in the NSFT-Novel cage phase for LT-UCMS animals only. Indeed, LT-UCMS animals took significantly more time to reach and eat the food as compared to their control counterparts, which is indicative of depressive-like behaviors, as the stressed animals have lower food-motivation and greater novelty-induced anxiety-like behaviours. Such observation was not reported in the ST-UCMS cohort. Interestingly, it can be observed in the ST-UCMS cohort that the controls expressed a high latency to reach the food, almost at the same level as the ST-UCMS animals. Considering that the purpose of the NSFT-Novel cage phase is to introduce an anxiogenic stimulus, that is, the presence of the novel environment, it is expected to yield a higher latency in the controls. However, regarding the LT-UCMS cohort's controls, the low latency could be attributed to the fact that these controls have been exposed to more manipulation due to the nature of the LT-UCMS duration. Hence, these

animals potentially developed a certain level of resilience or habituation to mildly anxiogenic situations, but since their LT-UCMS counterparts were primed to respond to stress exposure due to the UCMS paradigm, they demonstrated a significantly higher latency, explaining the disparity in the observed results.

The advanced explanation is further confirmed when investigating the reported results for the NSFT-Home cage phase. Indeed, in the home cage phase, the animals were tested in a familiar and safe environment, removing the anxiety-inducing novelty attribute. In this condition, it can be observed that for both LT-UCMS and ST-UCMS animals, a significant effect of stress exposure was reported, implying that in a neutral environment, both UCMS duration exerted a depressive-like symptom. To be noted, in the LT-UCMS regimen, LT-UCMS Females expressed a distinctly higher latency to reach the food as compared to their control counterparts, while this was not observed in LT-UCMS Males and in the ST-UCMS cohort. Furthermore, in the LT-UCMS regimen, the stressed animals expressed a lower latency when compared to their counterparts in the ST-UCMS regimen, indicating a possible underlying coping mechanism.

In the SIT-Spontaneous sociability phase, it is interesting to note that a significant main effect of UCMS exposure was observed in the LT-UCMS regimen only, whereas in the ST-UCMS regimen, only a marginal effect of Sex was observed. These findings further indicate that LT-UCMS exposure result in more distinct depressive-like outcomes since the stressed animals demonstrated a lower index of time spent with a conspecific subject. Furthermore, LT-UCMS Females had a significantly lower sociability index compared to their CTRs, whereas for LT-UCMS Males, only a marginal difference was reported. Moreover, the LT-UCMS Females also showed a lower sociability score than LT-UCMS Males, although the difference was not significant. Such observations were not found in the ST-UCMS cohort. Interestingly, when

observing grooming behaviours, only the ST-UMCS group demonstrated a significant main effect of Sex, while the LT-UCMS group reported no significance. Additionally, ST-UMCS Females had a significantly higher latency for grooming as compared to their respective CTR Male and such difference was not reported in the LT-UCMS cohort. Furthermore, when comparing the LT-UCMS and ST-UCMS Females, we observed that with longer stress duration, the animals expressed a reduced latency in grooming, indicating an improvement in depressive-like condition. Our observation could infer a possible sex-specific adaptive mechanism regarding grooming tendencies. Taken together, the current data clearly demonstrate that LT-UCMS exposure induced depressive-like symptoms to a greater extent when compared to ST-UCMS regimen, outlining a distinct depressive profile that differs depending on stress exposure duration.

As opposed to what was initially expected, we reported an increase in cognitive ability in the LT-UCMS cohort, while in the ST-UCMS group, such observation was not found. In fact, both the NORT and SIT-Social discrimination phase in the LT-UCMS regimen showed only a significant main effect of Sex. Furthermore, for both tests at baseline and after stress exposure, females demonstrated higher cognitive abilities compared to their male counterparts. Interestingly, for the ST-UCMS regimen, we can also observe in the NORT that at baseline, females express higher cognitive performance, but after exposure to ST-UCMS, males experienced a slight increase in cognitive score while females demonstrated a decrease, although only the difference between the ST-UCMS Females and CTR Females was marginally significant. The disparity in cognitive performance between males and females could potentially be explained by the intrinsic sex-specific physiological differences. For example, Resciniti et al (2023) demonstrated that men display a lower cognitive score as compared to women, which is

due to sex-specific frailty. Frailty is a physical condition that predisposes an individual to future health risks, such as hospitalization, physical and/or mental impairments, or mortality. Therefore, a natural, sex-specific difference in frailty between males and females could explain the observed disparity in the current results. In the ST-UCMS cohort, a significant interaction between Sex and stress duration was observed in the NORT, which could indicate that at this level of UCMS exposure, stress and sex have a coupling effect which would result in the differential outcomes observed between males and females.

4.2 Both LT-UCMS and ST-UCMS resulted in increased co-expression level of SK3C-SST mRNA and SK3C-PV mRNA in the mPFC and NAcc respectively.

Data analysis for the ST-UCMS cohort is still ongoing. As such no conclusive statements can be made in light of the current data. Nevertheless, it is interesting to note that both ST-UCMS and LT-UCMS resulted in an increased co-expression density of SK3C-SST mRNA in the mPFC. More importantly, the increase in co-expression is more pronounced in the LT-UCMS cohort (reaching significant levels) than in the ST-UCMS group. Such finding indicates that under stressful conditions, SST-INs produce more SK3C protein in the mPFC region. Our result shows that stress exposure leads to higher density of SK3C mRNA and thus, SK3C protein. This is in line with the similar findings reported by other members of our laboratory (Bambico et al., 2020). In fact, the authors demonstrated that UCMS exposure resulted in depressive-like behaviours in rats, which was reversed after a single-dose administration of scopolamine, a muscarinic acetylcholine receptor antagonist. They further proposed that the action of scopolamine was mediated through the inhibition of the M1 receptor-SKC pathway. Thus, from their study, it can be inferred that UCMS exposure results in elevated SKC level, particularly SK3C, in the mPFC, consequently leading to a depressive-like state. Impairments in

the prefrontal cortex (PFC) region have garnered critical attention in the past decades (Reviewed in Price & Drevets, 2010). Notably, the PFC is involved in the perception and evaluation of controllability over stressful events, behavioural changes, and goal-directed tasks (Amat et al., 2005; Granon et al., 2000; Varela et al., 2012). Depressed patients demonstrate reduced cortical volume and signs of neurodegeneration in almost every subregion of the PFC, including the mPFC, which is reflected by diverse abnormal alterations in glucose levels in the orbito-anterior cingulate area, and dorsomedial and anterolateral regions (similar to the infralimbic and prelimbic region of rodents' mPFC, respectively). However, such changes in glucose metabolism are not observed in treated patients (Reviewed in Price & Drevets, 2010). These localized disruptions in glucose metabolism could indicate potential mechanisms controlling neuronal signalling which are impaired through stress-induced overexpression of SK3C in the mPFC regions. Moreover, the mPFC is a crucial component of the DMN (Buckner et al., 2008) and as such, an upregulation of SK3C levels in cortical SST-INs due to stress exposure could indicate a general inhibition of this interneuron subtype. Considering that SST-INs are known to preferentially synapse on the dendritic region of pyramidal cells and primarily act as a gatekeeper for incoming information through the recruitment of dendritic pyramidal alpha5-$GABA_A$ receptors (Schulz et al., 2018), it is interesting to observe that stress exposure results in overexpression of SK3C mRNA within the SST-INs. This could subsequently lead to an hyper-inhibition of GABAergic neurons, since a higher level of SK3C is present and would cause a hyperpolarizing effect, as SKCs are involved with the mAHP of action potentials (Adelman et al., 2012). Additionally, since the co-expression levels of SK3C-SST mRNA differ between ST-UCMS and LT-UCMS groups, with the ST-UCMS having a lower co-expression density than LT-UCMS, this could potentially explain the conflicting hyper- and hypoactive DMN results

reported in MDD patients. In fact, it is possible that the increase in SK3C level within SST-INs has not yet reached a pathological level following ST-UCMS, but the onset of stress-dependent depression could potentially be already triggered due to the presence of stressors. However, during LT-UCMS, the co-expression level eventually reaches the pathological threshold and would cause a general hyperactivity of the mPFC, and thus the DMN, because the SST-IN are being inhibited, thus removing the filtering effect on the pyramidal neurons. Consequently, this hyperactivity of the DMN could be involved in rumination, a hallmark of depression (Abela & Hankin, 2011; Zhou et al., 2020), and other symptoms associated with a depressive state.

Regarding the co-expression level of SK3C-PV mRNA, only the NAcc region displayed a significant difference between the controls and LT-UCMS animals. Interestingly, the co-expression density for both ST-UCMS and LT-UCMS groups within the NAcc was similar, indicating that no differences between the two UCMS regimens could be observed at this level. PV-INs are essential components of the overall neuronal inhibitory circuitry, and their dysfunction has been reported in numerous neuropsychiatric disorders (Reviewed in Ruden et al., 2020). Therefore, observing a distinct increase in SK3C mRNA within the PV-INs of the NAcc could indicate a specific mechanism through which stress impacts the functionality of this particular brain area. In fact, the NAcc is associated with the reward pathway, which is involved in the sex drive, appetitive behaviours and addiction (Castro & Bruchas, 2019; Dai et al., 2022). Thus, abnormal activity within this region could be associated with anhedonia, depression, and potentially substance abuse which is highly prevalent in depressive disorders (Compton et al., 2006; Cornelius et al., 2004; Grant et al., 2004). Interestingly, a reduction in functional connectivity from the NAcc to the ventromedial PFC (vmPFC) has been associated with a decrease in appetite and was observed in female patients suffering from MDD (Kroemer et al.,

2022). Such findings reflect our current results for the NAcc region. Indeed, the NAcc is mostly composed of GABAergic neurons, some of which express PV (R. Chen et al., 2021). Thus, the increase in SK3C-PV mRNA observed in our current results could indicate that these accumbal GABAergic neurons are being severely inhibited in the context of LT-UCMS exposure due to the overexpression of SK3C. Subsequently, such inhibition would result in reduced activity from the NAcc and ultimately, decreased functional connectivity to the vmPFC, which in turn could result in decreased appetitive and reward-related behaviours. This scenario of events involving over-expression of SK3C within PV-IN of the NAcc due to stress exposure, and the subsequent reduction in functional connectivity, could possibly explain the significantly prolonged feeding latency observed in the LT-UCMS Females. Considering that Kroemer et al. (2022) showed a reduced functional connectivity of the NAcc to the vmPFC in MDD female patients only, the effects of LT-UCMS condition on the NAcc activity through overexpression of SK3C within PV-positive GABAergic neurons could provide a feasible explanation for the different depressive phenotypic profile between males and females. Indeed, female MDD patients usually report higher somatic symptoms, including reduced appetite, low energy level, and insomnia (Angst et al., 2002; Silverstein et al., 2013; Vetter et al., 2021). Therefore, taken together, our current results provide a potential mechanism involving SK3C overexpression in specific brain regions through which LT-UCMS exposure could induce depressive-like symptoms.

4.3 Both ST-UCMS and LT-UCMS resulted in increased SST mRNA production

Regarding the overall production of SST mRNA, present results unexpectedly showed that exposure to both ST- and LT-UCMS caused a general increase in density of the mRNA across several ROIs. Interestingly, after the LT-UCMS regimen, LT-UCMS Females expressed

significantly higher levels of SST mRNA in the mPFC region as compared to both CTR Females and LT-UCMS Males, and a similar trend was observed in the DRN. In a recent study, SST-IN have been observed to increase mRNA translation through the inhibition of phosphorylated Eukaryotic Initiation Factor 2-alpha (p-eIF2-alpha) following fear conditioning (Sharma et al., 2020). Fear conditioning is a learning paradigm that models fear and anxiety in rodents. In the paradigm, an animal learns to associate an aversive stimulus to a certain condition (Reviewed in Acevedo-Triana et al., 2020). In the context of our LT-UCMS paradigm, it is possible that the stressed animals inadvertently experienced an enhancement of fear and anxiety, especially with a prolonged stress exposure. This was also evinced by the anxiety-like reactivity observed in the NFST. Such explanation could potentially account for the unexpected increase in SST mRNA density. Indeed, upregulated translational factors could possibly result in increased transcriptional processes, thus producing more mRNAs. However, it is important to note that the same study used only male mice, while in the current research, the increase in SST mRNA is mainly observed in LT-UCMS Females. Yet, LT-UCMS Males expressed more SK3C mRNA in the SST-INs as opposed to LT-UCMS Females in the mPFC region. This discrepancy in our results and those of others can potentially be explained through the action of sex hormones, and specifically estrogen. In fact, estradiol benzoate, an estrogen-based medication, was found to increase the expression of SST proteins after a five-day administration regimen in ovariectomized guinea pigs (Dufourny & Warembourg, 1999). Therefore, the following scenario could explain the current findings: 1) upon exposure to LT-UCMS, the stressed animals were inadvertently conditioned to express enhanced fear and anxiety, which are themselves prevalent in depression, 2) this led to an increase in SK3C mRNA synthesis and translation (the increase is observed in both LT-UCMS Males and Females), 3) the effect of LT-UCMS eventually reduced

SST mRNA density in LT-UCMS Males but not LT-UCMS Females, since the females experienced the beneficial neuroprotective effects of estrogen, promoting the production of SST mRNA and its protein. Indeed, this potential scenario is plausible since a significant interaction between Sex and stress duration was observed in the mPFC for the SST mRNA analysis, indicating that there is a synergistic mechanism that involves both stress exposure and sex. The RNAscope™ findings could also explain the differences observed in terms of cognitive performance between males and females, and why LT-UCMS Females tend to express better cognitive performance compared to their male or control female counterparts. Furthermore, the sex-specific increase in SST mRNA levels due to longer stressors administration could be the reason behind the grooming behaviours disparity between LT-UCMS and ST-UCMS Females, and their male counterparts.

4.4 Both ST-UCMS and LT-UCMS resulted in a general decrease in PV mRNA

Regarding the overall PV mRNA density, the effect of stress exposure follows what was initially expected. Indeed, in both the ST- and LT-UCMS paradigms, a decrease in PV mRNA density was observed across multiple ROIs. The NAcc deserves a particular attention since it was the only region which co-expressed a significantly higher density of SK3C-PV mRNA following LT-UCMS exposure, and a similar trend can also be observed in the ST-UCMS animals for both co-expression of SK3C-PV mRNA and expression of PV mRNA only. Therefore, the NAcc could be a prime target for the effects of stress exposure through the over-expression of SK3C within PV-positive GABAergic neurons. PV is an important calcium-binding protein and thus its presence help in rapidly sequestrating the influx of Ca^{2+} following an action potential (Reviewed in Ruden et al., 2021). This in turn reduces or prevents the activation

of calcium-dependent potassium channels, such as SK3C, thus attenuating the mAHP period, allowing the neurons to fire again quicker. Therefore, a reduction of PV mRNA density could translate to a decrease in PV protein levels, and ultimately, a dysregulated sequestration of Ca^{2+}. Such situation would have the following impacts: 1) SK3C, and other calcium-dependent inhibitory channels, would become overactivated, resulting in a general hyper-inhibition of the neurons, and 2) the increased $[CA^{2+}]_{in}$ could lead to cell apoptosis. Indeed, higher $[CA^{2+}]_{in}$ would result in an overburdened mitochondrial system, which is one of the major intracellular storages of excess Ca^{2+} (Reviewed in Schrank et al., 2020). However, with increasing excessive $CA^{2+}]_{in}$, mitochondrial overload would eventually take place, resulting in mitochondrial degeneration and the release of several cytotoxic components such as free radicals (Sas et al., 2018; Verma et al., 2022) and ultimately cell death. Therefore, the ROIs which presented a significant reduction in PV mRNA density due to LT-UCMS exposure (DRN, NAcc, CA1, and DG) could potentially be experiencing the cascade of events previously described, thus resulting in the depressive-like outcomes observed.

4.5 Proposed mechanistic pathway through which stress exposure result in depressive outcomes

Given our current results, we propose the following possible mechanistic route through which LT-UCMS, but not ST-UCMS exposure, could induce specific depressive outcomes, such as rumination and anhedonia, which are characteristics of MDD. First, upon exposure to a stressor, the brain starts to upregulate the production of SK3C within the SST-INs of the cortical regions, and more precisely the mPFC. However, upon prolonged stressful condition (i.e., LT-UCMS), SK3C production within the SST-INs reaches a pathological threshold and starts to significantly inhibit the neurons, preventing them from firing and acting as a filter to the

incoming excitatory signals onto the dendritic areas of the pyramidal neurons. The unsorted signals eventually summate and cause an increase in firing rate of pyramidal cells, which in turn excessively release glutamate reaching a pathological level, eventually causing glutamatergic excitotoxicity. Since the mPFC connects directly to the NAcc, the excessive excitatory inputs due to unregulated glutamate release causes an overactivation of the PV-positive GABAergic neurons present in the NAcc. Initially, the increased in SK3C levels in the PV-positive neurons of the NAcc due to LT-UCMS is potentially a coping mechanism to help prevent the hyper-activity of the neurons. However, due to the reduced PV levels, the influx of Ca^{2+} caused by excessive excitatory inputs from the mPFC cannot be controlled, ultimately resulting in cellular apoptosis due to mitochondrial overload. The loss of PV neurons would then cause the NAcc to gradually become inactive, leading to reduced functional connectivity to the vmPFC, and thus possibly inducing the anhedonia symptoms of MDD.

Simultaneously, the DRN, CA1, and DG might also be experiencing the same excitotoxic events due to a reduction in PV mRNA, but probably at a different rate since no upregulation of SK3C was observed in the current study. Given that the CA3 demonstrated a marginal significant decrease in the PV mRNA level, it is possible that this brain region is also impacted to the same extent as the others. Considering that the hippocampus is essential in the processing of memory and cognition, having a reduction in PV levels, and thus a reduced inhibitory mechanism, the initial overexcitation due to LT-UCMS could potentially explain the observed results in the NORT and SIT-Social Discrimination phase. However, we expect that if the LT-UCMS paradigm was extended further, such observation would be reversed since with time, the overexcitation would eventually become detrimental. Furthermore, the possible hyperactivity of the hippocampal formation and DG due to reduced PV levels could potentially explain the

rumination aspect of MDD. Indeed, the hippocampal region also forms part of the DMN and is often associated with the constant remembering of past events (Reviewed in Kaefer et al., 2022).

The effects of stress exposure on the pathological development of MDD are also sex-dependent, since females had a higher level of SST mRNA following LT-UCMS exposure compared to males. The present results reflect the sex-specific transcriptomic profiles previously reported (Labonté et al., 2017), but also the stress-induced transcriptional pathway alterations related specifically to SST-INs specifically (Girgenti et al., 2019). The SST protein helps in cortical processing and is beneficial in preventing the development of neuropsychiatric disorder (Reviewed in Song et al., 2021; Fee et al., 2017). Furthermore, SST is known to modulate glutamatergic release potentially in a presynaptic manner (Reviewed in Pittaluga et al., 2021). Taken together, this suggests that females could potentially have a transient protective mechanism against stress-related neuronal deficits through the overexpression of SST mRNA, and thus SST proteins. However, this protective mechanism would have to be limited to the mPFC only since it was the only region in which we observed such an effect. Furthermore, only LT-UCMS Females demonstrated a significant increase in SK3C density within PV-positive neurons in the NAcc. As mentioned earlier, this upregulation of SK3C level would result in a hypo-activity of the PV-positive neuron, coupled with glutamatergic excitotoxicity caused by LT-UCMS exposure. The combined effects would lead to a severe inhibition of the NAcc, which in turn would potentially induce the appetitive symptoms of MDD characteristics in female patients.

Taken together, the current results allow us to propose a potential mechanism through which stress exposure contributes to the pathogenesis of MDD. Our model advances that the duration of stress exposure could provide tentative explanations regarding the differential and

conflicting DMN activity reported in MDD patients: long-term stress would result in heightened activity due to the overexpression of SK3C proteins within the SST-IN, while in short-term stress, no differences would be observed. Moreover, our model also proposes novel insights, possibly explaining the differences in phenotypic profile between depressed males and females. Indeed, depressed males tend to have lower cognitive performance, whereas depressed females tend to demonstrate higher somatic symptoms. These sex-specific effects could possibly be explained by the differences in the effects of long-term stress exposure on the mPFC (through the overproduction of SST mRNA in females) and the NAcc (stressed females showed higher co-expression levels of SK3C-PV mRNA). Although the ST-UCMS cohort analysis has to be completed, the current results obtained from the LT-UCMS cohort still allows us to infer some valuable observations which could be helpful for future studies.

4.6 Limitations and future directions

Despite the novelty of the reported results and their potential usefulness towards the understanding of stress-induced depression, we recognize that the current thesis has limitations which should be noted. Firstly, the sample size for the RNAscope™ of the ST-UCMS cohort was limited to one brain per group, which severely restricted our ability to obtain conclusive results. Secondly, the season during which the ST-UCMS cohort was experimented on could be a contributing factor to the observed results. Indeed, the cohort was tested during the transition period between fall and winter, implying a reduction in daylight, decreasing temperature, and other change in environmental cues. It is possible that the animals were exposed to these external environmental factors during transfers for behavioural testing. Even though necessary steps were taken to prevent such situation, for instance, behavioral tests were conducted at the same time

and room temperature was maintained constant through the room thermostat, we could not anticipate and control the innate biological system of the animals. In fact, mice experiencing shorter daylight, for example during winter, demonstrate lower hippocampal neurogenesis compared to those experiencing longer daylight (Taniguchi et al., 2021), possibly accounting for our observed results. Considering the limitations of the current study, for future experiments or replications, the following could be implemented: 1) increasing the sample size for the RNAscope™ procedures of the ST-UCMS cohort, 2) repeating the RNAscope™ procedures for both the ST- and LT-UCMS cohorts, and 3) conducting all behavioral tests during the summer or fall. For future potential studies, we intend to combine both the RNAscope™ and immunohistochemistry techniques, such that to determine the full impact of stress exposure on protein synthesis, from transcription to translation. Moreover, pharmacological interventions will also be investigated to further determine the pathological contributions of SK3C in the onset of stress-dependent depression, and the transition from ST-UCMS to LT-UCMS.

4.7 Conclusion

In conclusion, the current study showed that LT-UCMS caused a sex-dependent increase in co-expression levels of SK3C-SST and SK3C-PV mRNAs in the mPFC and NAcc respectively, a general increase in SST mRNA, but a general decrease in PV mRNA. We also showed that ST-UCMS and LT-UCMS resulted in differential phenotypic profiles of depressive-like symptoms, which could be linked to differential mRNA levels. Moreover, we showed that mPFC SK3C is potential key player in the etiology of stress-dependent depression and as such, could be a future target for pharmacological intervention. The present thesis also described a potential mechanism that involves the interplay among different brain regions in the onset of

MDD. Therefore, the insights provided by our study are beneficial in the quest for further understanding depression pathophysiology and for identifying more effective treatments for depression.

References

Abela, J. R. Z., & Hankin, B. L. (2011). Rumination as a vulnerability factor to depression during the transition from early to middle adolescence: A multiwave longitudinal study. *Journal of Abnormal Psychology*, *120*(2), 259–271. https://doi.org/10.1037/a0022796

Acevedo-Triana, C., Rico, J. L., Ortega, L. A., Cardenas, M. A. N., Cardenas, F. P., Rojas, M. J., Forigua-Vargas, J. C., Cifuentes, J., & Hurtado-Parrado, C. (2020). Fear Incubation Using an Extended Fear-Conditioning Protocol for Rats. *Journal of Visualized Experiments*, *162*, 60537. https://doi.org/10.3791/60537

Adelman, J. P., Maylie, J., & Sah, P. (2012). Small-Conductance Ca^{2+} -Activated K^{+} Channels: Form and Function. *Annual Review of Physiology*, *74*(1), 245–269. https://doi.org/10.1146/annurev-physiol-020911-153336

Alix, P., Venkatesan, K., Scuvée-Moreau, J., Massotte, L., Nguyen Trung, M.-L., Cornil, C. A., & Seutin, V. (2014). Mechanism of the medium-duration afterhyperpolarization in rat serotonergic neurons. *European Journal of Neuroscience*, *39*(2), 186–196. https://doi.org/10.1111/ejn.12408

Alqurashi, G. K., Hindi, E. A., Zayed, M. A., Abd El-Aziz, G. S., Alturkistani, H. A., Ibrahim, R. F., Al-thepyani, M. A., Bakhlgi, R., Alzahrani, N. A., Ashraf, G. M., & Alghamdi, B. S. (2022). The Impact of Chronic Unpredictable Mild Stress-Induced Depression on Spatial, Recognition and Reference Memory Tasks in Mice: Behavioral and Histological Study. *Behavioral Sciences*, *12*(6), 166. https://doi.org/10.3390/bs12060166

Amat, J., Baratta, M. V., Paul, E., Bland, S. T., Watkins, L. R., & Maier, S. F. (2005). Medial prefrontal cortex determines how stressor controllability affects behavior and dorsal raphe nucleus. *Nature Neuroscience*, *8*(3), 365–371. https://doi.org/10.1038/nn1399

Andrews-Hanna, J. R., Smallwood, J., & Spreng, R. N. (2014). The default network and self-generated thought: Component processes, dynamic control, and clinical relevance: The brain's default network. *Annals of the New York Academy of Sciences*, *1316*(1), 29–52. https://doi.org/10.1111/nyas.12360

Angst, J., Gamma, A., Gastpar, M., L�pine, J.-P., Mendlewicz, J., & Tylee, A. (2002). Gender differences in depression. *European Archives of Psychiatry and Clinical Neuroscience*, *252*(5), 201–209. https://doi.org/10.1007/s00406-002-0381-6

Antonoudiou, P., Tan, Y. L., Kontou, G., Upton, A. L., & Mann, E. O. (2020). Parvalbumin and Somatostatin Interneurons Contribute to the Generation of Hippocampal Gamma Oscillations. *The Journal of Neuroscience*, *40*(40), 7668–7687. https://doi.org/10.1523/JNEUROSCI.0261-20.2020

Augustinavicius, J. L. S., Zanjani, A., Zakzanis, K. K., & Shapiro, C. M. (2014). Polysomnographic features of early-onset depression: A meta-analysis. *Journal of Affective Disorders*, *158*, 11–18. https://doi.org/10.1016/j.jad.2013.12.009

Avenevoli, S., Swendsen, J., He, J.-P., Burstein, M., & Merikangas, K. R. (2015). Major Depression in the National Comorbidity Survey–Adolescent Supplement: Prevalence, Correlates, and Treatment. *Journal of the American Academy of Child & Adolescent Psychiatry*, *54*(1), 37-44.e2. https://doi.org/10.1016/j.jaac.2014.10.010

Ballesteros-Merino, C., Watanabe, M., Shigemoto, R., Fukazawa, Y., Adelman, J. P., & Luján, R. (2014). Differential subcellular localization of SK3-containing channels in the hippocampus. *European Journal of Neuroscience*, *39*(6), 883–892. https://doi.org/10.1111/ejn.12474

Bambico, F. R., Li, Z., Creed, M., De Gregorio, D., Diwan, M., Li, J., McNeill, S., Gobbi, G., Raymond, R., & Nobrega, J. N. (2020). A Key Role for Prefrontocortical Small Conductance Calcium-Activated Potassium Channels in Stress Adaptation and Rapid Antidepressant Response. *Cerebral Cortex*, *30*(3), 1559–1572. https://doi.org/10.1093/cercor/bhz187

Bambico, F. R., Nguyen, N.-T., & Gobbi, G. (2009). Decline in serotonergic firing activity and desensitization of 5-HT1A autoreceptors after chronic unpredictable stress. *European Neuropsychopharmacology*, *19*(3), 215–228. https://doi.org/10.1016/j.euroneuro.2008.11.005

Borges, M. K., Aprahamian, I., Romanini, C. V., Oliveira, F. M., Mingardi, S. V. B., Lima, N. A., Cecato, J. F., Petrella, M., & Oude Voshaar, R. C. (2021). Depression as a determinant of frailty in late life. *Aging & Mental Health*, *25*(12), 2279–2285. https://doi.org/10.1080/13607863.2020.1857689

Brown, B. M., Shim, H., Christophersen, P., & Wulff, H. (2020). Pharmacology of Small- and Intermediate-Conductance Calcium-Activated Potassium Channels. *Annual Review of Pharmacology and Toxicology*, *60*(1), 219–240. https://doi.org/10.1146/annurev-pharmtox-010919-023420

Buckner, R. L., Andrews-Hanna, J. R., & Schacter, D. L. (2008). *The Brain's Default Network*: *Anatomy, Function, and Relevance to Disease*. *Annals of the New York Academy of Sciences*, *1124*(1), 1–38. https://doi.org/10.1196/annals.1440.011

Burstein, O., & Doron, R. (2018). The Unpredictable Chronic Mild Stress Protocol for Inducing Anhedonia in Mice. *Journal of Visualized Experiments*, *140*, 58184. https://doi.org/10.3791/58184

Cai, H., Jin, Y., Liu, S., Zhang, Q., Zhang, L., Cheung, T., Balbuena, L., & Xiang, Y.-T. (2021). Prevalence of suicidal ideation and planning in patients with major depressive disorder: A meta-analysis of observation studies. *Journal of Affective Disorders*, *293*, 148–158. https://doi.org/10.1016/j.jad.2021.05.115

Castro, D. C., & Bruchas, M. R. (2019). A Motivational and Neuropeptidergic Hub: Anatomical and Functional Diversity within the Nucleus Accumbens Shell. *Neuron*, *102*(3), 529–552. https://doi.org/10.1016/j.neuron.2019.03.003

Ceruso, A., Martínez-Cengotitabengoa, M., Peters-Corbett, A., Diaz-Gutierrez, M. J., & Martínez-Cengotitabengoa, M. (2020). Alterations of the HPA Axis Observed in Patients with Major Depressive Disorder and Their Relation to Early Life Stress: A Systematic Review. *Neuropsychobiology*, *79*(6), 417–427. https://doi.org/10.1159/000506484

Chen, R., Blosser, T. R., Djekidel, M. N., Hao, J., Bhattacherjee, A., Chen, W., Tuesta, L. M., Zhuang, X., & Zhang, Y. (2021). Decoding molecular and cellular heterogeneity of mouse nucleus accumbens. *Nature Neuroscience*, *24*(12), 1757–1771. https://doi.org/10.1038/s41593-021-00938-x

Chen, Z., Tao, S., Zhu, R., Tian, S., Sun, Y., Wang, H., Yan, R., Shao, J., Zhang, Y., Zhang, J., Yao, Z., & Lu, Q. (2021). Aberrant functional connectivity between the suprachiasmatic nucleus and the superior temporal gyrus: Bridging RORA gene polymorphism with diurnal mood variation in major depressive disorder. *Journal of Psychiatric Research*, *132*, 123–130. https://doi.org/10.1016/j.jpsychires.2020.09.037

Compton, W. M., Conway, K. P., Stinson, F. S., & Grant, B. F. (2006). Changes in the Prevalence of Major Depression and Comorbid Substance Use Disorders in the United States Between 1991–1992 and 2001–2002. *Am J Psychiatry*.

Cornelius, J. R., Maisto, S. A., Martin, C. S., Bukstein, O. G., Salloum, I. M., Daley, D. C., Scott Wood, D., & Clark, D. B. (2004). Major depression associated with earlier alcohol relapse in treated teens with AUD. *Addictive Behaviors*, *29*(5), 1035–1038. https://doi.org/10.1016/j.addbeh.2004.02.056

Dai, B., Sun, F., Tong, X., Ding, Y., Kuang, A., Osakada, T., Li, Y., & Lin, D. (2022). Responses and functions of dopamine in nucleus accumbens core during social behaviors. *Cell Reports*, *40*(8), 111246. https://doi.org/10.1016/j.celrep.2022.111246

Dang, R., Wang, M., Li, X., Wang, H., Liu, L., Wu, Q., Zhao, J., Ji, P., Zhong, L., Licinio, J., & Xie, P. (2022). Edaravone ameliorates depressive and anxiety-like behaviors via Sirt1/Nrf2/HO-1/Gpx4 pathway. *Journal of Neuroinflammation*, *19*(1), 41. https://doi.org/10.1186/s12974-022-02400-6

Descalzo, V. F., Nowak, L. G., Brumberg, J. C., McCormick, D. A., & Sanchez-Vives, M. V. (2005). Slow Adaptation in Fast-Spiking Neurons of Visual Cortex. *Journal of Neurophysiology*, *93*(2), 1111–1118. https://doi.org/10.1152/jn.00658.2004

Diamond, D. M., Park, C. R., Campbell, A. M., & Woodson, J. C. (2005). Competitive interactions between endogenous LTD and LTP in the hippocampus underlie the storage of emotional memories and stress-induced amnesia. *Hippocampus*, *15*(8), 1006–1025. https://doi.org/10.1002/hipo.20107

Dufourny, L., & Warembourg, M. (1999). Estrogen modulation of neuropeptides: Somatostatin, neurotensin and substance P, in the ventrolateral and arcuate nuclei of the female guinea pig. *Neuroscience Research*, *33*(3), 223–228. https://doi.org/10.1016/S0168-0102(99)00009-7

Ebert, D. D., Buntrock, C., Mortier, P., Auerbach, R., Weisel, K. K., Kessler, R. C., Cuijpers, P., Green, J. G., Kiekens, G., Nock, M. K., Demyttenaere, K., & Bruffaerts, R. (2019). Prediction of major depressive disorder onset in college students. *Depression and Anxiety*, *36*(4), 294–304. https://doi.org/10.1002/da.22867

Egorova, P. A., Karelina, T. V., Vlasova, O. L., Antonov, S. M., & Bezprozvanny, I. B. (2014). The effect of SK channel modulators on the simple spike firing frequency in discharge of cerebellar Purkinje cells in laboratory mice. *Journal of Evolutionary Biochemistry and Physiology*, *50*(2), 114–120. https://doi.org/10.1134/S0022093014020045

Eliwa, H., Brizard, B., Le Guisquet, A.-M., Hen, R., Belzung, C., & Surget, A. (2021). Adult neurogenesis augmentation attenuates anhedonia and HPA axis dysregulation in a mouse model of chronic stress and depression. *Psychoneuroendocrinology*, *124*, 105097. https://doi.org/10.1016/j.psyneuen.2020.105097

Etchepare, L., Gréa, H., Durand, P., Bouchet, D., & Groc, L. (2021). NMDA receptor membrane dynamics tunes the firing pattern of midbrain dopaminergic neurons. *The Journal of Physiology*, *599*(11), 2933–2951. https://doi.org/10.1113/JP281104

Fee, C., Banasr, M., & Sibille, E. (2017). Somatostatin-Positive Gamma-Aminobutyric Acid Interneuron Deficits in Depression: Cortical Microcircuit and Therapeutic Perspectives. *Biological Psychiatry*, *82*(8), 549–559. https://doi.org/10.1016/j.biopsych.2017.05.024

Figueroa, C. A., Mocking, R. J. T., Van Wingen, G., Martens, S., Ruhé, H. G., & Schene, A. H. (2017). Aberrant default-mode network-hippocampus connectivity after sad memory-recall in remitted-depression. *Social Cognitive and Affective Neuroscience*, *12*(11), 1803–1813. https://doi.org/10.1093/scan/nsx108

Fiksdal, A., Hanlin, L., Kuras, Y., Gianferante, D., Chen, X., Thoma, M. V., & Rohleder, N. (2019). Associations between symptoms of depression and anxiety and cortisol responses to and recovery from acute stress. *Psychoneuroendocrinology*, *102*, 44–52. https://doi.org/10.1016/j.psyneuen.2018.11.035

Fonte, A., & Coutinho, B. (2021). Seasonal sensitivity and psychiatric morbidity: Study about seasonal affective disorder. *BMC Psychiatry*, *21*(1), 317. https://doi.org/10.1186/s12888-021-03313-z

Girgenti, M. J., Wohleb, E. S., Mehta, S., Ghosal, S., Fogaca, M. V., & Duman, R. S. (2019). Prefrontal cortex interneurons display dynamic sex-specific stress-induced transcriptomes. *Translational Psychiatry*, *9*(1), 292. https://doi.org/10.1038/s41398-019-0642-z

Godfrey, K. E. M., Gardner, A. C., Kwon, S., Chea, W., & Muthukumaraswamy, S. D. (2018). Differences in excitatory and inhibitory neurotransmitter levels between depressed patients and healthy controls: A systematic review and meta-analysis. *Journal of Psychiatric Research*, *105*, 33–44. https://doi.org/10.1016/j.jpsychires.2018.08.015

Golding, J. M., & Lipton, R. I. (1990). Depressed mood and major depressive disorder in two ethnic groups. *Journal of Psychiatric Research*, *24*(1), 65–82. https://doi.org/10.1016/0022-3956(90)90025-L

Golitabari, N., Mohammadian, F., Salari, A.-A., & Amani, M. (2022). Neonatal NMDA blockade alters the LTP, LTD and cognitive functions in male and female Wistar rats. *Neuropharmacology*, *205*, 108896. https://doi.org/10.1016/j.neuropharm.2021.108896

Gonchar, Y. (2008). Multiple distinct subtypes of GABAergic neurons in mouse visual cortex identified by triple immunostaining. *Frontiers in Neuroanatomy*, *1*. https://doi.org/10.3389/neuro.05.003.2007

Granon, S., Passetti, F., Thomas, K. L., Dalley, J. W., Everitt, B. J., & Robbins, T. W. (2000). Enhanced and Impaired Attentional Performance After Infusion of D1 Dopaminergic Receptor Agents into Rat Prefrontal Cortex. *The Journal of Neuroscience*, *20*(3), 1208–1215. https://doi.org/10.1523/JNEUROSCI.20-03-01208.2000

Grant, B. F., Stinson, F. S., Dawson, D. A., Chou, S. P., Dufour, M. C., Compton, W., Pickering, R. P., & Kaplan, K. (2004). Prevalence and Co-occurrence of Substance Use Disorders and IndependentMood and Anxiety Disorders: Results From the National Epidemiologic Survey on Alcohol and RelatedConditions. *ARCH GEN PSYCHIATRY*, *61*, 807–816.

Greenberg, P. E., Fournier, A.-A., Sisitsky, T., Simes, M., Berman, R., Koenigsberg, S. H., & Kessler, R. C. (2021). The Economic Burden of Adults with Major Depressive Disorder in the United States (2010 and 2018). *PharmacoEconomics*, *39*(6), 653–665. https://doi.org/10.1007/s40273-021-01019-4

Høifødt, R. S., Waterloo, K., Wang, C. E. A., Eisemann, M., Figenschau, Y., & Halvorsen, M. (2019). Cortisol levels and cognitive profile in major depression: A comparison of currently and previously depressed patients. *Psychoneuroendocrinology*, *99*, 57–65. https://doi.org/10.1016/j.psyneuen.2018.08.024

Jones, S. L., & Stuart, G. J. (2013). Different Calcium Sources Control Somatic versus Dendritic SK Channel Activation during Action Potentials. *The Journal of Neuroscience*, *33*(50), 19396–19405. https://doi.org/10.1523/JNEUROSCI.2073-13.2013

Jones, S. L., To, M.-S., & Stuart, G. J. (2017). Dendritic small conductance calcium-activated potassium channels activated by action potentials suppress EPSPs and gate spike-timing dependent synaptic plasticity. *ELife*, *6*, e30333. https://doi.org/10.7554/eLife.30333

Kaefer, K., Stella, F., McNaughton, B. L., & Battaglia, F. P. (2022). Replay, the default mode network and the cascaded memory systems model. *Nature Reviews Neuroscience*, *23*(10), 628–640. https://doi.org/10.1038/s41583-022-00620-6

Kalueff, A. V., Stewart, A. M., Song, C., Berridge, K. C., Graybiel, A. M., & Fentress, J. C. (2016). Neurobiology of rodent self-grooming and its value for translational neuroscience. *Nature Reviews Neuroscience*, *17*(1), 45–59. https://doi.org/10.1038/nrn.2015.8

Kantrowitz, J. T., Dong, Z., Milak, M. S., Rashid, R., Kegeles, L. S., Javitt, D. C., Lieberman, J. A., & John Mann, J. (2021). Ventromedial prefrontal cortex/anterior cingulate cortex Glx, glutamate, and GABA levels in medication-free major depressive disorder. *Translational Psychiatry*, *11*(1), 419. https://doi.org/10.1038/s41398-021-01541-1

Kavuran Buran, İ., Onalan Etem, E., & Tektemur, A. (2022). Inhibition of TRPC1, TRPM4 and CHRNA6 ion channels ameliorates depression-like behavior in rats. *Behavioural Brain Research*, *423*, 113765. https://doi.org/10.1016/j.bbr.2022.113765

Kinlein, S. A., Phillips, D. J., Keller, C. R., & Karatsoreos, I. N. (2019). Role of corticosterone in altered neurobehavioral responses to acute stress in a model of compromised hypothalamic-pituitary-adrenal axis function. *Psychoneuroendocrinology*, *102*, 248–255. https://doi.org/10.1016/j.psyneuen.2018.12.010

Köhler, M., Hirschberg, B., Bond, C. T., Kinzie, J. M., Marrion, N. V., Maylie, J., & Adelman, J. P. (1996). Small-Conductance, Calcium-Activated Potassium Channels from Mammalian Brain. *Science*, *273*(5282), 1709–1714. https://doi.org/10.1126/science.273.5282.1709

Kroemer, N. B., Opel, N., Teckentrup, V., Li, M., Grotegerd, D., Meinert, S., Lemke, H., Kircher, T., Nenadić, I., Krug, A., Jansen, A., Sommer, J., Steinsträter, O., Small, D. M., Dannlowski, U., & Walter, M. (2022). Functional Connectivity of the Nucleus Accumbens and Changes in Appetite in Patients With Depression. *JAMA Psychiatry*, *79*(10), 993. https://doi.org/10.1001/jamapsychiatry.2022.2464

Kverno, K. S., & Mangano, E. (2021). Treatment-Resistant Depression: Approaches to Treatment. *Journal of Psychosocial Nursing and Mental Health Services*, *59*(9), 7–11. https://doi.org/10.3928/02793695-20210816-01

Labonté, B., Engmann, O., Purushothaman, I., Menard, C., Wang, J., Tan, C., Scarpa, J. R., Moy, G., Loh, Y.-H. E., Cahill, M., Lorsch, Z. S., Hamilton, P. J., Calipari, E. S., Hodes, G. E., Issler, O., Kronman, H., Pfau, M., Obradovic, A. L. J., Dong, Y., … Nestler, E. J. (2017). Sex-specific transcriptional signatures in human depression. *Nature Medicine*, *23*(9), 1102–1111. https://doi.org/10.1038/nm.4386

Li, Q. S., Shabalin, A. A., DiBlasi, E., Gopal, S., Canuso, C. M., FinnGen, International Suicide Genetics Consortium, Palotie, A., Drevets, W. C., Docherty, A. R., & Coon, H. (2023). Genome-wide association study meta-analysis of suicide death and suicidal behavior. *Molecular Psychiatry*, *28*(2), 891–900. https://doi.org/10.1038/s41380-022-01828-9

Li, Q., Zhao, Y., Chen, Z., Long, J., Dai, J., Huang, X., Lui, S., Radua, J., Vieta, E., Kemp, G. J., Sweeney, J. A., Li, F., & Gong, Q. (2020). Meta-analysis of cortical thickness

abnormalities in medication-free patients with major depressive disorder. *Neuropsychopharmacology*, *45*(4), 703–712. https://doi.org/10.1038/s41386-019-0563-9

Li, Q.-Q., Chen, J., Hu, P., Jia, M., Sun, J.-H., Feng, H.-Y., Qiao, F.-C., Zang, Y.-Y., Shi, Y.-Y., Chen, G., Sheng, N., Xu, Y., Yang, J.-J., Xu, Z., & Shi, Y. S. (2022). Enhancing GluN2A-type NMDA receptors impairs long-term synaptic plasticity and learning and memory. *Molecular Psychiatry*, *27*(8), 3468–3478. https://doi.org/10.1038/s41380-022-01579-7

Liang, S., Deng, W., Li, X., Greenshaw, A. J., Wang, Q., Li, M., Ma, X., Bai, T.-J., Bo, Q.-J., Cao, J., Chen, G.-M., Chen, W., Cheng, C., Cheng, Y.-Q., Cui, X.-L., Duan, J., Fang, Y.-R., Gong, Q.-Y., Guo, W.-B., … Li, T. (2020). Biotypes of major depressive disorder: Neuroimaging evidence from resting-state default mode network patterns. *NeuroImage: Clinical*, *28*, 102514. https://doi.org/10.1016/j.nicl.2020.102514

Liu, M.-Y., Yin, C.-Y., Zhu, L.-J., Zhu, X.-H., Xu, C., Luo, C.-X., Chen, H., Zhu, D.-Y., & Zhou, Q.-G. (2018). Sucrose preference test for measurement of stress-induced anhedonia in mice. *Nature Protocols*, *13*(7), 1686–1698. https://doi.org/10.1038/s41596-018-0011-z

Liu, T.-Y., Hsieh, J.-C., Chen, Y.-S., Tu, P.-C., Su, T.-P., & Chen, L.-F. (2012). Different patterns of abnormal gamma oscillatory activity in unipolar and bipolar disorder patients during an implicit emotion task. *Neuropsychologia*, *50*(7), 1514–1520. https://doi.org/10.1016/j.neuropsychologia.2012.03.004

Liu, X., Liu, S., Li, M., Su, F., Chen, S., Ke, Y., & Ming, D. (2022). Altered gamma oscillations and beta–gamma coupling in drug-naive first-episode major depressive disorder: Association with sleep and cognitive disturbance. *Journal of Affective Disorders*, *316*, 99–108. https://doi.org/10.1016/j.jad.2022.08.022

Marrion, N. V., & Tavalin, S. J. (1998). Selective activation of Ca2+-activated K+ channels by co-localized Ca2+ channels in hippocampal neurons. *Nature*, *395*(6705), 900–905. https://doi.org/10.1038/27674

Martin, S., Lazzarini, M., Dullin, C., Balakrishnan, S., Gomes, F. V., Ninkovic, M., El Hady, A., Pardo, L. A., Stühmer, W., & Del-Bel, E. (2017). SK3 Channel Overexpression in Mice Causes Hippocampal Shrinkage Associated with Cognitive Impairments. *Molecular Neurobiology*, *54*(2), 1078–1091. https://doi.org/10.1007/s12035-015-9680-6

Mayer, S. E., Lopez-Duran, N. L., Sen, S., & Abelson, J. L. (2018). Chronic stress, hair cortisol and depression: A prospective and longitudinal study of medical internship. *Psychoneuroendocrinology*, *92*, 57–65. https://doi.org/10.1016/j.psyneuen.2018.03.020

Moreno-Agostino, D., Wu, Y.-T., Daskalopoulou, C., Hasan, M. T., Huisman, M., & Prina, M. (2021). Global trends in the prevalence and incidence of depression:a systematic review and meta-analysis. *Journal of Affective Disorders*, *281*, 235–243. https://doi.org/10.1016/j.jad.2020.12.035

Nashed, M. G., Waye, S., Hasan, S. M. N., Nguyen, D., Wiseman, M., Zhang, J., Lau, H., Dinesh, O. C., Raymond, R., Greig, I. R., Bambico, F. R., & Nobrega, J. N. (2022). Antidepressant activity of pharmacological and genetic deactivation of the small-conductance calcium-activated potassium channel subtype-3. *Psychopharmacology*, *239*(1), 253–266. https://doi.org/10.1007/s00213-021-06045-w

Obermair, G. J., Kaufmann, W. A., Knaus, H.-G., & Flucher, B. E. (2003). The small conductance Ca^{2+} -activated K^{+} channel SK3 is localized in nerve terminals of excitatory synapses of cultured mouse hippocampal neurons: Presynaptic localization of

SK3. *European Journal of Neuroscience*, *17*(4), 721–731. https://doi.org/10.1046/j.1460-9568.2003.02488.x

Page, C. E., Shepard, R., Heslin, K., & Coutellier, L. (2019). Prefrontal parvalbumin cells are sensitive to stress and mediate anxiety-related behaviors in female mice. *Scientific Reports*, *9*(1), 19772. https://doi.org/10.1038/s41598-019-56424-9

Payne, J. L., & Maguire, J. (2019). Pathophysiological mechanisms implicated in postpartum depression. *Frontiers in Neuroendocrinology*, *52*, 165–180. https://doi.org/10.1016/j.yfrne.2018.12.001

Pesarico, A. P., Carceller, H., Guirado, R., Coviello, S., & Nacher, J. (2022). Long term effects of 24-h-restraint stress on the connectivity and structure of interneurons in the basolateral amygdala. *Progress in Neuro-Psychopharmacology and Biological Psychiatry*, *115*, 110512. https://doi.org/10.1016/j.pnpbp.2022.110512

Pittaluga, A., Roggeri, A., Vallarino, G., & Olivero, G. (2021). Somatostatin, a Presynaptic Modulator of Glutamatergic Signal in the Central Nervous System. *International Journal of Molecular Sciences*, *22*(11), 5864. https://doi.org/10.3390/ijms22115864

Price, J. L., & Drevets, W. C. (2010). Neurocircuitry of Mood Disorders. *Neuropsychopharmacology*, *35*(1), 192–216. https://doi.org/10.1038/npp.2009.104

Resciniti, N. V., Farina, M. P., Merchant, A. T., & Lohman, M. C. (2023). Depressive Symptoms Partially Mediate the Association of Frailty Phenotype Symptoms and Cognition for Females but Not Males. *Journal of Aging and Health*, *35*(1–2), 42–49. https://doi.org/10.1177/08982643221100688

Riedemann, T. (2019). Diversity and Function of Somatostatin-Expressing Interneurons in the Cerebral Cortex. *International Journal of Molecular Sciences*, *20*(12), 2952. https://doi.org/10.3390/ijms20122952

Ruden, J. B., Dugan, L. L., & Konradi, C. (2021). Parvalbumin interneuron vulnerability and brain disorders. *Neuropsychopharmacology*, *46*(2), 279–287. https://doi.org/10.1038/s41386-020-0778-9

Sailer, C. A., Kaufmann, W. A., Marksteiner, J., & Knaus, H.-G. (2004). Comparative immunohistochemical distribution of three small-conductance Ca2+-activated potassium channel subunits, SK1, SK2, and SK3 in mouse brain. *Molecular and Cellular Neuroscience*, *26*(3), 458–469. https://doi.org/10.1016/j.mcn.2004.03.002

Sargin, D., Oliver, D. K., & Lambe, E. K. (2016). Chronic social isolation reduces 5-HT neuronal activity via upregulated SK3 calcium-activated potassium channels. *ELife*, *5*, e21416. https://doi.org/10.7554/eLife.21416

Saris, I. M. J., Penninx, B. W. J. H., Dinga, R., Van Tol, M.-J., Veltman, D. J., Van Der Wee, N. J. A., & Aghajani, M. (2020). Default Mode Network Connectivity and Social Dysfunction in Major Depressive Disorder. *Scientific Reports*, *10*(1), 194. https://doi.org/10.1038/s41598-019-57033-2

Sas, K., Szabó, E., & Vécsei, L. (2018). Mitochondria, Oxidative Stress and the Kynurenine System, with a Focus on Ageing and Neuroprotection. *Molecules*, *23*(1), 191. https://doi.org/10.3390/molecules23010191

Schrank, S., Barrington, N., & Stutzmann, G. E. (2020). Calcium-Handling Defects and Neurodegenerative Disease. *Cold Spring Harbor Perspectives in Biology*, *12*(7), a035212. https://doi.org/10.1101/cshperspect.a035212

Schulz, J. M., Knoflach, F., Hernandez, M.-C., & Bischofberger, J. (2018). Dendrite-targeting interneurons control synaptic NMDA-receptor activation via nonlinear α5-GABAA receptors. *Nature Communications*, *9*(1), 3576. https://doi.org/10.1038/s41467-018-06004-8

Sharma, V., Sood, R., Khlaifia, A., Eslamizade, M. J., Hung, T.-Y., Lou, D., Asgarihafshejani, A., Lalzar, M., Kiniry, S. J., Stokes, M. P., Cohen, N., Nelson, A. J., Abell, K., Possemato, A. P., Gal-Ben-Ari, S., Truong, V. T., Wang, P., Yiannakas, A., Saffarzadeh, F., … Sonenberg, N. (2020). EIF2α controls memory consolidation via excitatory and somatostatin neurons. *Nature*, *586*(7829), 412–416. https://doi.org/10.1038/s41586-020-2805-8

Silverstein, B., Edwards, T., Gamma, A., Ajdacic-Gross, V., Rossler, W., & Angst, J. (2013). The role played by depression associated with somatic symptomatology in accounting for the gender difference in the prevalence of depression. *Social Psychiatry and Psychiatric Epidemiology*, *48*(2), 257–263. https://doi.org/10.1007/s00127-012-0540-7

Smolin, B., Karry, R., Gal-Ben-Ari, S., & Ben-Shachar, D. (2012). Differential expression of genes encoding neuronal ion-channel subunits in major depression, bipolar disorder and schizophrenia: Implications for pathophysiology. *The International Journal of Neuropsychopharmacology*, *15*(07), 869–882. https://doi.org/10.1017/S1461145711001428

Song, Y., Shen, X., Mu, X., Mao, N., & Wang, B. (2020). A study on BOLD fMRI of the brain basic activities of MDD and the first-degree relatives. *International Journal of Psychiatry in Clinical Practice*, *24*(3), 236–244. https://doi.org/10.1080/13651501.2020.1744663

Song, Y.-H., Yoon, J., & Lee, S.-H. (2021). The role of neuropeptide somatostatin in the brain and its application in treating neurological disorders. *Experimental & Molecular Medicine*, *53*(3), 328–338. https://doi.org/10.1038/s12276-021-00580-4

Spijker, S., Koskinen, M.-K., & Riga, D. (2020). Incubation of depression: ECM assembly and parvalbumin interneurons after stress. *Neuroscience & Biobehavioral Reviews*, *118*, 65–79. https://doi.org/10.1016/j.neubiorev.2020.07.015

Subramanian, S., Haroutounian, S., Palanca, B. J. A., & Lenze, E. J. (2022). Ketamine as a therapeutic agent for depression and pain: Mechanisms and evidence. *Journal of the Neurological Sciences*, *434*, 120152. https://doi.org/10.1016/j.jns.2022.120152

Swaab, D. F., Bao, A.-M., & Lucassen, P. J. (2005). The stress system in the human brain in depression and neurodegeneration. *Ageing Research Reviews*, *4*(2), 141–194. https://doi.org/10.1016/j.arr.2005.03.003

Taniguchi, E., Tashiro, A., Hattori, A., Furuse, M., & Yasuo, S. (2021). Photoperiodic changes in hippocampal neurogenesis and plasma metabolomic profiles in relation to depression-like behavior in mice. *Behavioural Brain Research*, *403*, 113136. https://doi.org/10.1016/j.bbr.2021.113136

Thalamuthu, A., Mills, N. T., Berger, K., Minnerup, H., Grotegerd, D., Dannlowski, U., Meinert, S., Opel, N., Repple, J., Gruber, M., Nenadić, I., Stein, F., Brosch, K., Meller, T., Pfarr, J.-K., Forstner, A. J., Hoffmann, P., Nöthen, M. M., Witt, S., … Baune, B. T. (2022). Genome-wide interaction study with major depression identifies novel variants associated with cognitive function. *Molecular Psychiatry*, *27*(2), 1111–1119. https://doi.org/10.1038/s41380-021-01379-5

Udakis, M., Pedrosa, V., Chamberlain, S. E. L., Clopath, C., & Mellor, J. R. (2020). Interneuron-specific plasticity at parvalbumin and somatostatin inhibitory synapses onto CA1 pyramidal neurons shapes hippocampal output. *Nature Communications*, *11*(1), 4395. https://doi.org/10.1038/s41467-020-18074-8

Van Brederode, J. F. M., Mulligan, K. A., & Hendrickson, A. E. (1990). Calcium-binding proteins as markers for subpopulations of GABAergic neurons in monkey striate cortex. *The Journal of Comparative Neurology*, *298*(1), 1–22. https://doi.org/10.1002/cne.902980102

Vance, A., & Winther, J. (2021). Irritability, Depressed Mood, Inattention and Spatial Working Memory in Children and Adolescents with Major Depressive Disorder With/Without Persistent Depressive Disorder. *Child Psychiatry & Human Development*, *52*(5), 800–807. https://doi.org/10.1007/s10578-020-01061-x

Varela, J. A., Wang, J., Christianson, J. P., Maier, S. F., & Cooper, D. C. (2012). Control over Stress, But Not Stress Per Se Increases Prefrontal Cortical Pyramidal Neuron Excitability. *The Journal of Neuroscience*, *32*(37), 12848–12853. https://doi.org/10.1523/JNEUROSCI.2669-12.2012

Verma, M., Lizama, B. N., & Chu, C. T. (2022). Excitotoxicity, calcium and mitochondria: A triad in synaptic neurodegeneration. *Translational Neurodegeneration*, *11*(1), 3. https://doi.org/10.1186/s40035-021-00278-7

Vetter, J. S., Spiller, T. R., Cathomas, F., Robinaugh, D., Brühl, A., Boeker, H., Seifritz, E., & Kleim, B. (2021). Sex differences in depressive symptoms and their networks in a treatment-seeking population – a cross-sectional study. *Journal of Affective Disorders*, *278*, 357–364. https://doi.org/10.1016/j.jad.2020.08.074

Wang, S., Deng, Z., Wang, J., Zhang, W., Liu, F., Xu, J., & Ma, Y. (2021). Decreased GABAergic signaling, fewer parvalbumin-, somatostatin- and calretinin-positive neurons in brain of a rat model of simulated transport stress. *Research in Veterinary Science*, *134*, 86–95. https://doi.org/10.1016/j.rvsc.2020.12.005

Willner, P. (2005). Chronic Mild Stress (CMS) Revisited: Consistency and Behavioural-Neurobiological Concordance in the Effects of CMS. *Neuropsychobiology*, *52*(2), 90–110. https://doi.org/10.1159/000087097

Woodward, E. M., & Coutellier, L. (2021). Age- and sex-specific effects of stress on parvalbumin interneurons in preclinical models: Relevance to sex differences in clinical neuropsychiatric and neurodevelopmental disorders. *Neuroscience & Biobehavioral Reviews*, *131*, 1228–1242. https://doi.org/10.1016/j.neubiorev.2021.10.031

Xu, X., Roby, K. D., & Callaway, E. M. (2010). Immunochemical characterization of inhibitory mouse cortical neurons: Three chemically distinct classes of inhibitory cells. *The Journal of Comparative Neurology*, *518*(3), 389–404. https://doi.org/10.1002/cne.22229

Yamamoto, J., Suh, J., Takeuchi, D., & Tonegawa, S. (2014). Successful Execution of Working Memory Linked to Synchronized High-Frequency Gamma Oscillations. *Cell*, *157*(4), 845–857. https://doi.org/10.1016/j.cell.2014.04.009

Zajkowska, Z., Walsh, A., Zonca, V., Gullett, N., Pedersen, G. A., Kieling, C., Swartz, J. R., Karmacharya, R., Fisher, H. L., Kohrt, B. A., & Mondelli, V. (2021). A systematic review of the association between biological markers and environmental stress risk factors for adolescent depression. *Journal of Psychiatric Research*, *138*, 163–175. https://doi.org/10.1016/j.jpsychires.2021.04.003

Zhang, S., Chen, J., Kuang, L., Cao, J., Zhang, H., Ai, M., Wang, W., Zhang, S., Wang, S., Liu, S., & Fang, W. (2016). Association between abnormal default mode network activity and suicidality in depressed adolescents. *BMC Psychiatry*, *16*(1), 337. https://doi.org/10.1186/s12888-016-1047-7

Zhou, H.-X., Chen, X., Shen, Y.-Q., Li, L., Chen, N.-X., Zhu, Z.-C., Castellanos, F. X., & Yan, C.-G. (2020). Rumination and the default mode network: Meta-analysis of brain imaging studies and implications for depression. *NeuroImage*, *206*, 116287. https://doi.org/10.1016/j.neuroimage.2019.116287

Appendix

Appendix 1

Example of the schedule used for the UCMS paradigm

Stress Paradigm Schedule				
Week	**Days and date**	**Morning (8:00 to 10:00)**	**Afternoon (12:00 to 2:00 pm)**	**Overnight (6:00 pm to 8:00 am)**
Week 1	Monday	Cage tilt (duration: 2 hrs- starts around **8.30**)	Predator odor (duration: 2hrs -starts around **1.30 pm**)	Stroboscope (duration: overnight- starts around **6.30 pm**)
	Tuesday	High-frequency sounds (duration: 30min- starts around **9 am**)	Difficult food and water access (duration: 2hrs- starts around **12 pm**)	No bedding (duration: overnight- starts around **6 pm**)
	Wednesday	Predator odor (duration: 2 hrs- starts around **8.30 am**)	Cage tilt (duration: 2 hrs- starts around **12.30 pm**)	Overnight illumination (duration: overnight- starts around **7 pm**)
	Thursday	Cage tilt (duration: 2 hrs- starts around **9.30 am**)	High-frequency sounds (duration: 30 min- starts around **12 pm**)	Difficult food and water access (duration: overnight- starts around **6.30 pm**)*
	Friday	NO STRESSORS ADMINISTRATION		
	Saturday	High-frequency sounds (duration: 30min- starts around **9 am**)	No bedding (duration: 2 hrs- starts around **12.30 pm**)	Water in cage+ overnight illumination (duration: overnight- starts around **6 pm**)
	Sunday	NO STRESSORS ADMINISTRATION		
Week 2	Monday	Cage tilt (duration: 2 hrs- starts around **8.30 am**)	Predator odor (duration: 2hrs- starts around **12 pm**)	Stroboscope (duration: overnight- starts around **6.30 pm**)
	Tuesday	High-frequency sounds (duration: 30min- starts around **9 am**)	Difficult food and water access (duration: 2hrs-starts around **12.30 pm**)	No bedding (duration: overnight- starts around **6 pm**)
	Wednesday	NO STRESSORS ADMINISTRATION		
	Thursday	Water in cage (duration: 2 hrs- starts around **9 am**)	High-frequency sounds (duration: 30 min- starts around **12.30 pm**)	Difficult food and water access+ overnight illumination (duration: overnight-starts around **6 pm**)*
	Friday	NO STRESSORS ADMINISTRATION		
	Saturday	High-frequency sounds (duration: 30min- starts around **9.30 am**)	Shaking (duration: 30 min- starts around **1.30 pm**)	Water in cage+ overnight illumination (duration: overnight- starts around **6 pm**)
	Sunday	Cage tilt (duration: 2 hrs- starts around **9.30 am**)	Predator odor (duration: 2 hrs- starts around **1 pm**)	Stroboscope (duration: overnight- starts around **7 pm**)
Week 3	Monday	Shaking (duration: **45 min- starts around 8.30 am**)	Predator odor (duration: 2hrs- starts around **12 pm**)	Water in cage + stroboscope (duration: overnight- starts around **6 pm**)
	Tuesday	High-frequency sounds (duration: **45min- starts around 9 am**)	Water in cage (duration: 2hrs- starts around **1 pm**)	No bedding (duration: overnight- starts around **6.30 pm**)
	Wednesday	Predator odor+ cage tilt (duration: 2 hrs- starts around **9.30 am**)	Shaking (duration: **45 min- starts around 1.30 pm**)	Cage tilt + Overnight illumination (duration: overnight- starts around **6.30 pm**)*
	Thursday	NO STRESSORS ADMINISTRATION		
	Friday			
	Saturday	Shaking (duration: **45 min- starts around 9:00 am**)	No bedding (2 hrs- starts around **1 pm**)	Water in cage+ overnight illumination (duration: overnight- starts around **6 pm**)
	Sunday	Cage tilt (duration: 2 hrs- starts around **9.30 am**)	Predator odor (duration: 2 hrs- starts around **1 pm**)	No bedding + stroboscope (duration: overnight- starts around **6 pm**)

Appendix 1. *A detailed example of the schedule used for the UCMS paradigm*. The figure shows the schedule used for the ST-UCMS cohort. The animals were exposed to three weeks of stressors administration, at three different time points per day, denoted as morning, afternoon, and overnight. The time range in brackets indicate that a stressor should be initiated within this range to be considered a morning, afternoon, or overnight stressor. A week was considered to start on Monday and finish on Sunday. Two days per week were randomly chosen as rest days (denoted with the labeling "NO STRESSORS ADMINISTRATION" in red bold, in the cells filled with gray). The duration and recommended time for stressor initiation are given in brackets by the side of each stressor. For the LT-UCMS group, a similar schedule was used but was extended for eight to nine weeks.

Appendix 2a

Results for the OFT

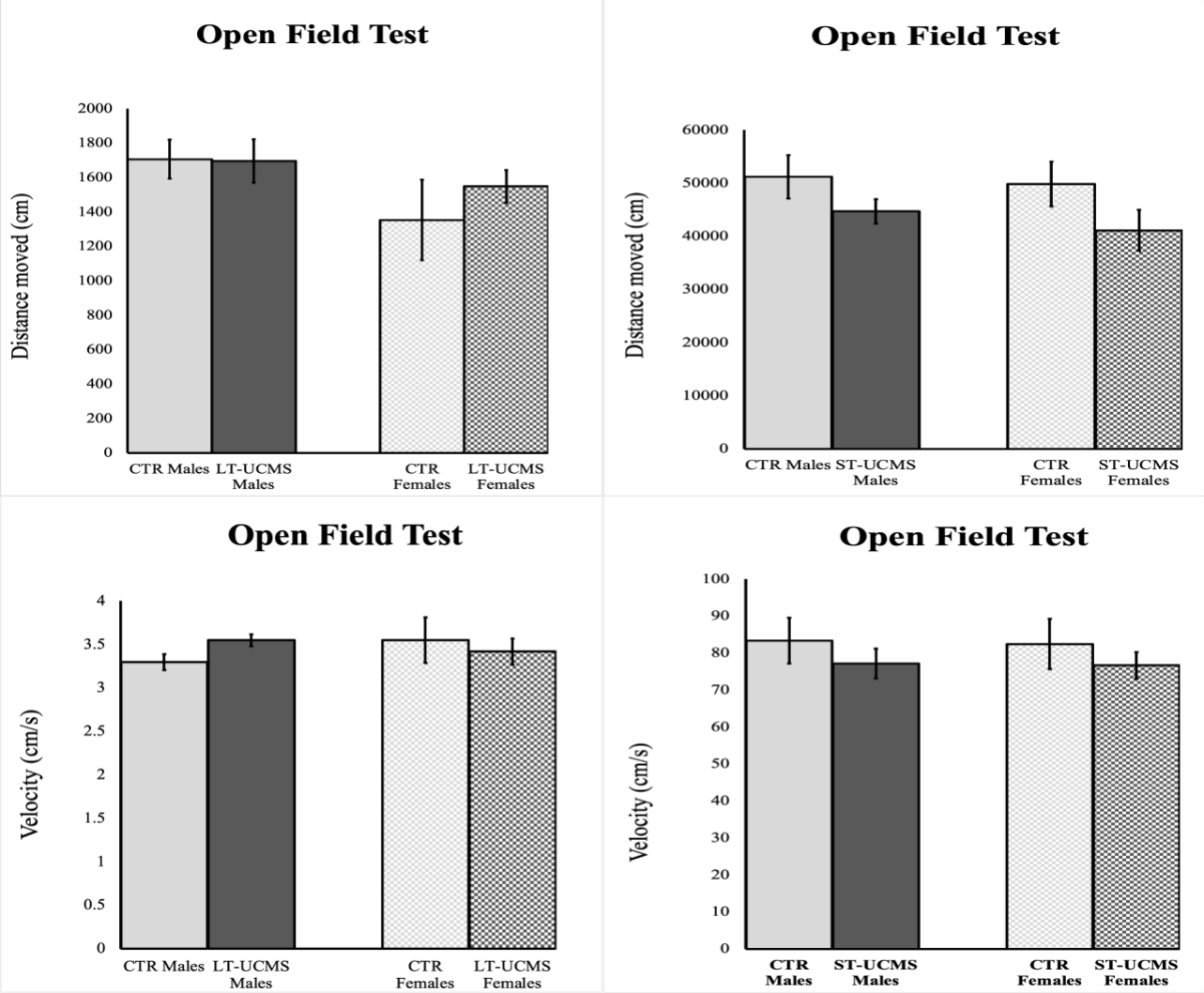

Appendix 2a. *Results of the OFT for both ST-UCMS and LT-UCMS groups*. The figure shows the results obtained for locomotor activity. The two upper panels report the overall distance moved by the subjects, while the two lower panels indicate the overall velocity. It is interesting to note that ST-UCMS groups demonstrated higher distance travelled and velocity than the LT-UCMS cohort. This could potentially be due to manipulation or analysis error, or the ST-UCMS group are more active. No significant interactions nor main effects were found for both the ST-UCMS and LT-UCMS groups.

Appendix 2b

Results for the FST

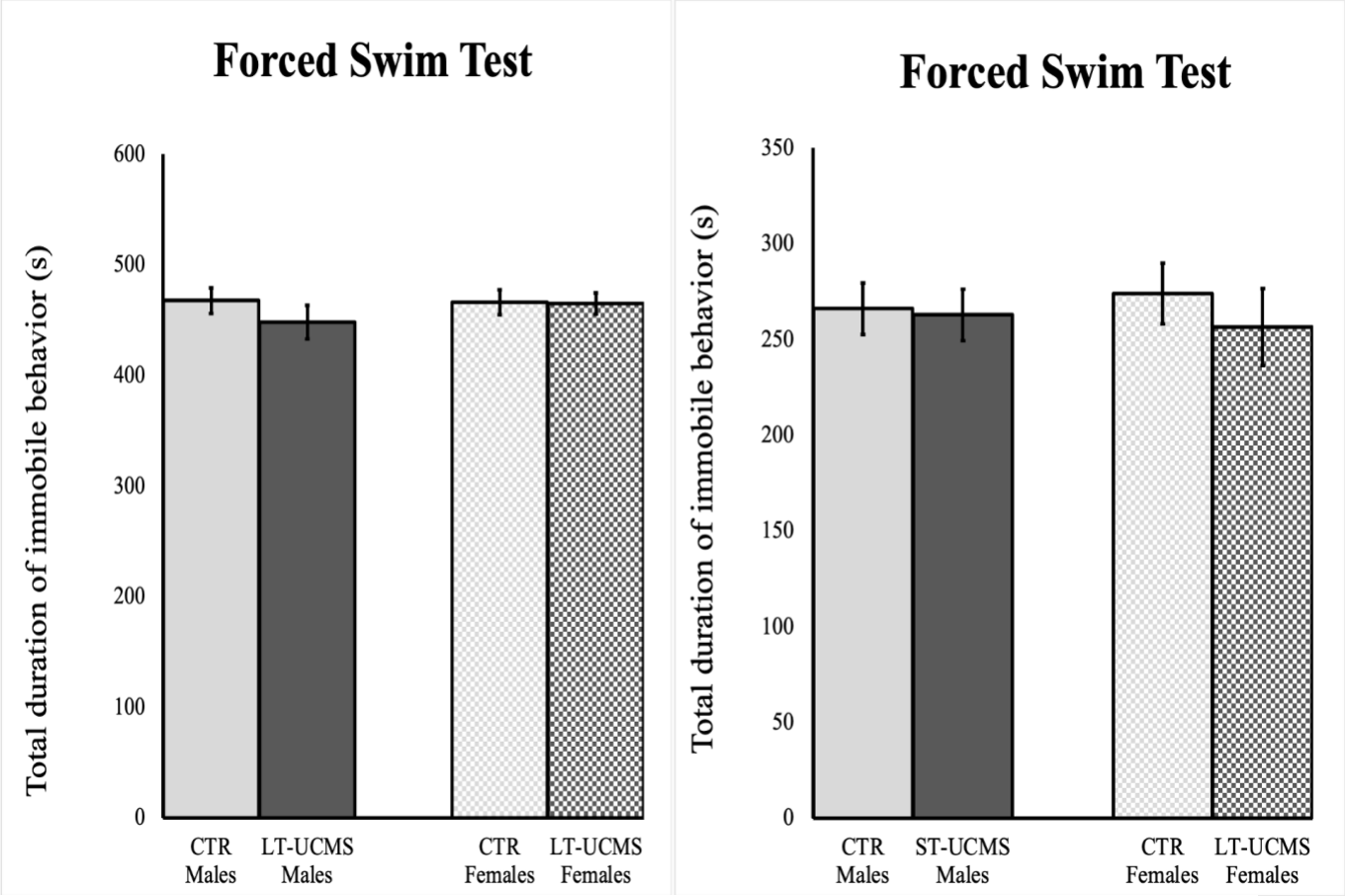

Appendix 2b. *Results of the FST for both ST-UCMS and LT-UCMS groups*. The figure shows the results obtained for immobility duration. It is interesting to note that ST-UCMS groups demonstrated immobility time than the LT-UCMS cohort. However, the controls for both groups demonstrate varied immobility time, with the ST-UCMS group's controls having lower freezing behaviour than the LT-UCMS group counterparts. This difference could be accounted with the fact that the LT-UCMS group's controls experienced were by nature manipulated more than the ST-UCMS groups because LT-UCMS lasted longer. Considering that FST is a sensitive test, this discrepancy could result in the observed differences between the two control groups. No significant interactions nor main effects were found for both the ST-UCMS and LT-UCMS

Appendix 3

Positive and negative controls for RNAscope™ procedure

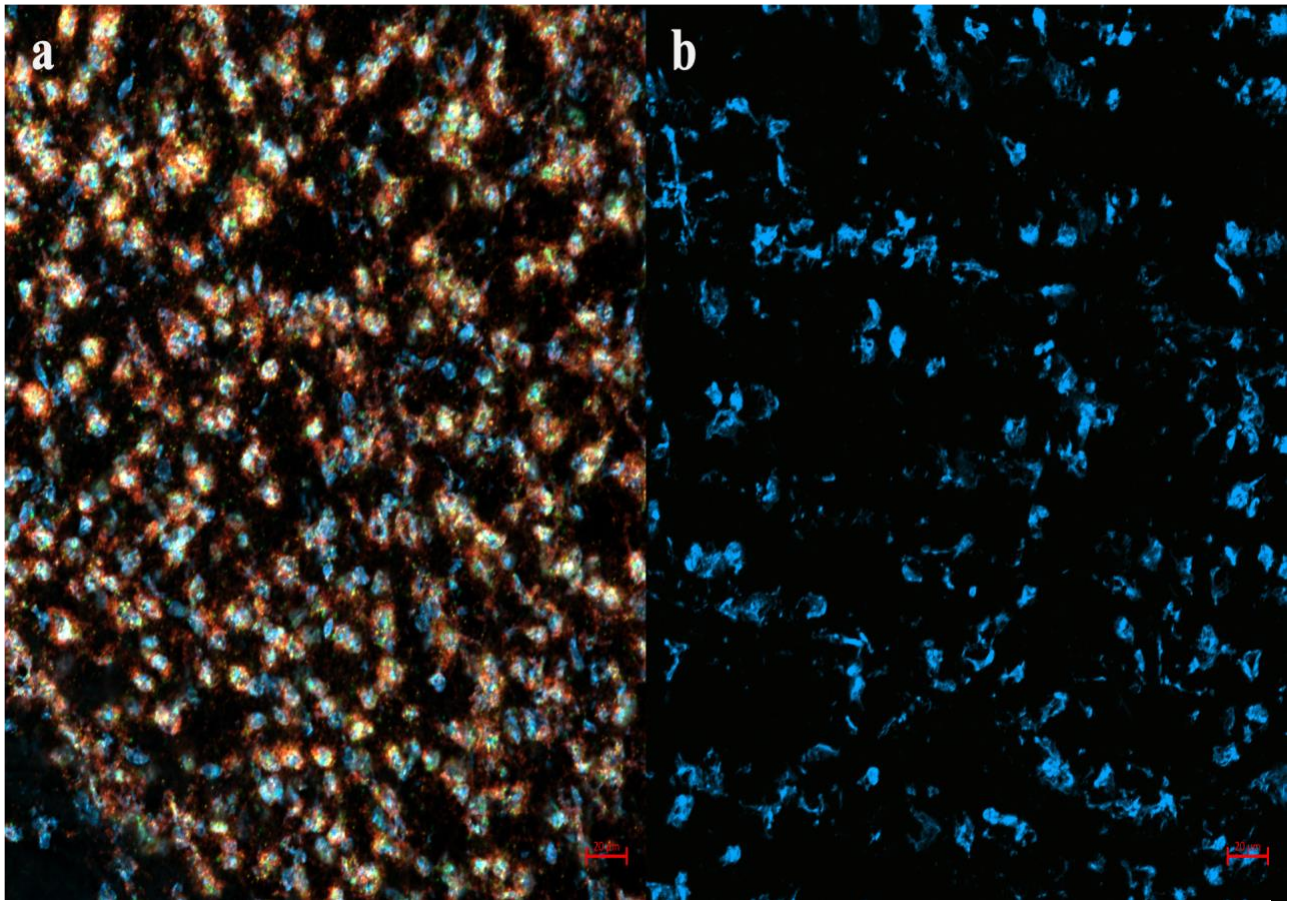

Appendix 3. *Qualitative images for the positive and negative controls of the RNAscope™ procedure*. Panel a represents a positive control used to test the quality of our RNAscope™ procedure. For the positive control, specific probes that target housekeeping genes were used. The genes are as follows: *POLR2A* in channel C1, *PPIB* in channel C2, and *UBC* in channel C3. Panel b represents a negative control used in our procedure. The negative control probe targets a specific bacterial gene, *dapB*, which are absent in mouse. The gene was associated with all three channels, from C1 to C3. The images were collected from the mPFC region of a control male. Positive and negative controls were conducted on the other ROIs. Nuclei are in blue and are denoted with the light-blue arrow. The images were taken at x20 magnification.